# The future of fracture management

## Feasibility of in-house design, production and implementation of 3D printed wrist casts for the treatment of distal radius fractures

Master Thesis Technical Medicine
Imaging & Intervention


C.D.Y. Mooij, BSc

Prof. Dr. Ir. J. Harlaar
Dr. J. Zhou

Dr. J.M.M. Heyligers
Drs. M. Bemelman
Drs. L. Brouwers

# The future of fracture management

## Feasibility of in-house design, production and implementation of 3D printed wrist casts for the treatment of distal radius fractures

- official frontpage -


Charlotte Désirée Yvonne Mooij
Student number : 4377508

28th May 2021

Thesis in partial fulfilment of the requirements for the joint degree of Master of Science in
*Technical Medicine*
Leiden University ; Delft University of Technology ; Erasmus University Rotterdam

Master thesis project (TM30004 ; 35 ECTS)
Dept. of Biomechanical Engineering, TUDELFT
December 2020 – May 2021
Supervisor(s):
Dr. J.M.M. Heyligers, ETZ
Dr. J. Zhou, TU Delft
Drs. M. Bemelman, ETZ
Drs. L. Brouwers, ETZ

Thesis committee members:
Prof. dr. ir. J. Harlaar, TU Delft (chair)
Dr. J.M.M. Heyligers, ETZ (medical supervisor)
Dr. J. Zhou, TU Delft (technical supervisor)
Drs. M. Bemelman, ETZ (medical supervisor)

# Acknowledgements

One year ago, after a three month Corona break, I finally got to start the last part of my Technical Medicine Master adventure in Tilburg. This thesis is the product of a year of hard work and challenges that I could not have done without  the help and support of a great number of people.

First of all, I would like to thank Mike Bemelman, Jan Heyligers and Lars Brouwers for the continuous support, nice discussions and for giving me the chance to learn new things. You really challenged me this year. I value all of your input and I am grateful that I was given the chance to contribute to the amazing 3D lab of the ETZ.

Also, I would like to thank the staff, support and residents from the surgery department, as well as the plaster technicians for the nice collaborations, interesting conversations and help during my project. Myrthe and Marco, thanks for your help and contributions during the patient studies.

At the TU Delft, I would like to thank Jie Zhou for his technical input, time and support throughout this thesis.

A big thank you to all the people that have contributed to this thesis by taking part in the comfort study, dad for helping me create the really cool phantom arm and mom for being a literary genius.

Thanks to my fellow students of the 3D lab, Annabel and Vito, for the nice coffee and chai latte breaks, laughter, secret random dancing and uplifting conversations.

Moreover I would like to thank my family and friends for their support during the past year. Sometimes, it was hard to persist, but thanks to all of your support I made it. Especially, I would like to thank my parents, André and Irma, for always being there for me whenever I need you, even when I think I don't.

Lastly, I would like to give my most special thanks to my boyfriend. Thanks for listening to my complaints, for sometimes giving me a kick in the butt or a cuddle when I needed it, but most of all for endlessly having my back. I love you.

It was an intense year, but as I have learned: "*Science is like a street lamp: long, cold, hard and grey, but at the end you will find a point of light.*" – M. Bemelman.

Enjoy reading!

All the best,

Charlotte Mooij

## Summary

**INTRODUCTION** Distal radius fractures are traditionally treated with plaster casts. Although this has been the gold standard for treatment for years, it also comes with disadvantages. These are the weight, not being water-resistant and a lack of ventilation, leading to skin problems, itching and compromised hygiene. Furthermore, plaster has no possibility for visual inspection of the skin, while up to 30% of all treatments with plaster casting lead to, mainly skin related, problems. With 3D printing, a lightweight, waterproof, open latticed and personalized cast can be created to overcome the issues with plaster casting. Multiple start-ups, researchers and other individuals already created these 3D printed casts, however, there is no consensus about the materials and design that should be used. Also, implementation of these 3D printed wrist casts into clinical practice stays out. The main research goal is to investigate the feasibility of in-house design, production and implementation of 3D printed wrist casts for the treatment of distal radius fractures.

**METHODS** To answer the main research question, multiple sub studies were performed. First, design requirements were formulated in consultation with clinicians. Then, material tests were performed, followed by creating a design workflow. Subsequently, the optimal design pattern and validation of the stabilization requirements were investigated during a mechanical phantom study. Also, to affirm adequate ease of use and comfort, a comfort study was carried out. The final step was a pilot study, in which the necessary alterations in the workflow were investigated, as well as clinical outcomes and patient experiences.

**RESULTS** The material tests showed that color resin, printed with an SLA printer is most suitable for the production of 3D printed wrist casts. A semi-automated design workflow was created in which a 3D printed wrist cast can be produced within 24 hours. A 3D printed cast with a Voronoi design pattern is most successful for adequate wrist immobilization, achieving similar stabilization abilities as a plaster cast. Furthermore, the comfort study showed that the 3D printed wrist casts ensure adequate comfort, with a mean score of 8.1 out of 10.0 and sufficient ease of use. During the pilot study, two children with greenstick or buckle/torus fractures were successfully treated with the wrist casts. To implement the treatment of distal radius fractures with 3D printed wrist casts into the current workflow, a workflow as used for traditional treatment during the evenings and weekends is required.

**CONCLUSION** A customized, lightweight, water-resistant and ventilated wrist cast can successfully be designed, with adequate stabilization abilities. This cast can be produced within 24 hours, with the use of a semi-automated design algorithm that creates a wrist cast with ventilation holes based on a Voronoi pattern. The 3D printing should be performed with an SLA printer, with the use of color resin. The produced wrist casts ensure adequate comfort and ease of use and can be implemented clinically for successful treatment of children with greenstick and buckle/torus fractures. Only small alterations are necessary in the current workflow to allow for the production of the 3D printed wrist casts. No extra hospital visits are required and the new workflow is comparable to the weekend workflow. Further research is necessary to tackle the unfavorable cost-effectiveness and the adaption of the casts to swelling. For the future, treatment with 3D printed casts should be extrapolated to unstable fractures, other body parts and the field of orthotics.

# Table of contents

*Acknowledgements* 3

*Summary* 4

INTRODUCTION 4

METHODS 4

RESULTS 4

CONCLUSION 4

*Table of contents* 5

*Background and general information* 8

Wrist joint and biomechanics 8

Distal radius fractures in children 9

Treatment of distal radius fractures 10

Additive manufacturing technologies 11

3D printing in the medical field 15

*Literature study (systematic literature review)* 17

3D printed wrist casts for the treatment of distal radius fractures in children: challenges and perspectives 17

Introduction 17

Methods 17

Results 18

Discussion 25

Conclusion 26

*Research goal and thesis outline* 27

Clinical problem 27

Research goal 27

Thesis outline 27

*Design requirements* 28

Requirements with clinical input 28

Stabilization abilities similar to plaster casting 28

Solid design 28

Personalized fit 28

Open-latticed pattern for ventilation and visual inspection 28

Water resistance 28

Lightweight 28

Closing system 29

Smooth surface finish 29

Biocompatibility 29

Semi-automated design 29

*Printing technique and material selection* 30

Introduction 30

Materials and methods 30

Materials 30

Test samples 31
Data collection 32
Calculations 34
Statistical analysis 35

**Results 35**
Test samples 35
Data collection 37
Statistical analysis 37

**Conclusion 39**

***Design 40***

**3D scanning of the limb 40**

**Design algorithm 40**
Preparation of the arm model 40
Cast creation algorithm 41
Addition of the closing mechanism 44

**3D printing 44**

**Workflow 45**

***Mechanical phantom study 46***

**Introduction 46**

**Materials and methods 46**
Phantom design 46
Wrist casts printing and plastering 47
Test set-up 47
Data collection 48
Statistical analysis 49

**Results 49**
Wrist casts printing and plastering 49
Data collection 49
Statistical analysis 50

**Conclusion 51**

***Comfort study 52***

**Introduction 52**

**Methods 52**
Protocol 52
Questionnaire 52
Analysis of the results 52

**Results 53**
Produced wrist casts 53
Questionnaire 53

**Conclusion 56**

***Pilot study 57***

**Introduction 57**

**Methods 58**
Inclusion 58
Workflow 58

Questionnaire ______ 58

**Results** ______ **59**

Included patients ______ 59

**Conclusion** ______ **60**

***Patient case: orthosis for wrist arthrosis*** ______ ***61***

**Patient case** ______ **61**

**Prototypes** ______ **61**

**Conclusion** ______ **62**

***Discussion*** ______ ***63***

**Limitations** ______ **63**

Printing technique and material selection ______ 63

Design ______ 63

Mechanical phantom study ______ 64

Comfort study ______ 64

Pilot study ______ 64

General limitations ______ 64

**Future perspectives** ______ **65**

Extrapolation to unstable fracture ______ 65

Clinical implementation ______ 65

Extrapolation to other body parts ______ 65

Orthotics ______ 66

**Medical Device Regulation (MDR)** ______ **66**

***Conclusion*** ______ ***67***

***References*** ______ ***68***

***Appendix I: Stress-Strain curves for flexural testing*** ______ ***73***

***Appendix II: Stress-Strain curves for tensile testing*** ______ ***76***

***Appendix III: Angular displacement under loading*** ______ ***79***

***Appendix IV: Information letter comfort study*** ______ ***81***

***Appendix V: Questionnaire comfort study*** ______ ***82***

***Appendix VII: Information letter pilot study*** ______ ***85***

***Appendix VII: Questionnaire pilot study - child*** ______ ***86***

***Appendix VIII: Questionnaire pilot study - parents*** ______ ***89***

# Background and general information

## Wrist joint and biomechanics

The wrist is considered to be one of the most complex joints of the body [1]. With 15 bones and various supporting structures, such as a complex composition of muscles, tendons and ligaments, a nerve system and vascularization, the wrist joint forms the basis of complex movements of the hand [1]. The radius is one of the two bones in the forearm. Together with the ulna, carpal bones and base of the metacarpals, the radius forms the wrist joint [1, 2]. The wrist joint is actually a combination of three joints: the radiocarpal joint (RCJ), ulnocarpal joint (UCJ) and distal radioulnar joint (DRUJ) [1, 2, 3]. These joints together form an ellipsoid joint, which produces four main movements: (palmar) flexion, (dorsal) extension, radial deviation/abduction and ulnar deviation/adduction. A combination of these motions can produce circumduction of the hand [2]. Also, the radius and ulna form a rolling joint together, which can produce pronation and supination of the hand [4]. The normative values for the range of motion (ROM) of the wrist are stated in Table 1 and the wrist movements are shown in Figure 1. The bony anatomy of the wrist bones is shown in Figure 2.

***Table 1**: Normative ROM values for the wrist joint [1, 5].*

| Movement | Degrees ROM (°) |
|---|---|
| Flexion (palmar) | 80-90 |
| Extension (dorsal) | 60-70 |
| Radial deviation/Abduction | 15-20 |
| Ulnar deviation/Adduction | 30-40 |

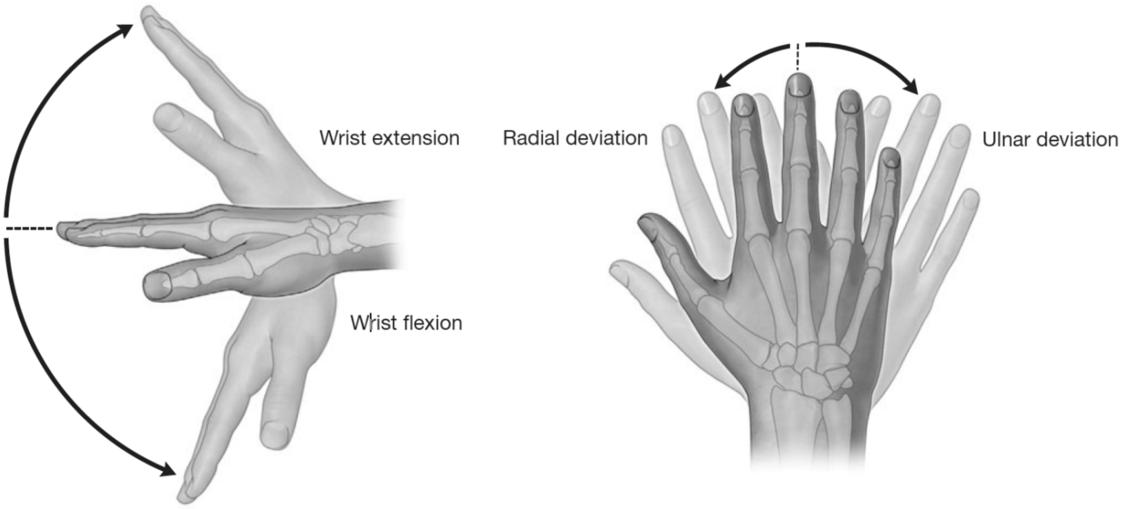


***Figure 1**: Movements of the wrist joint [5].*

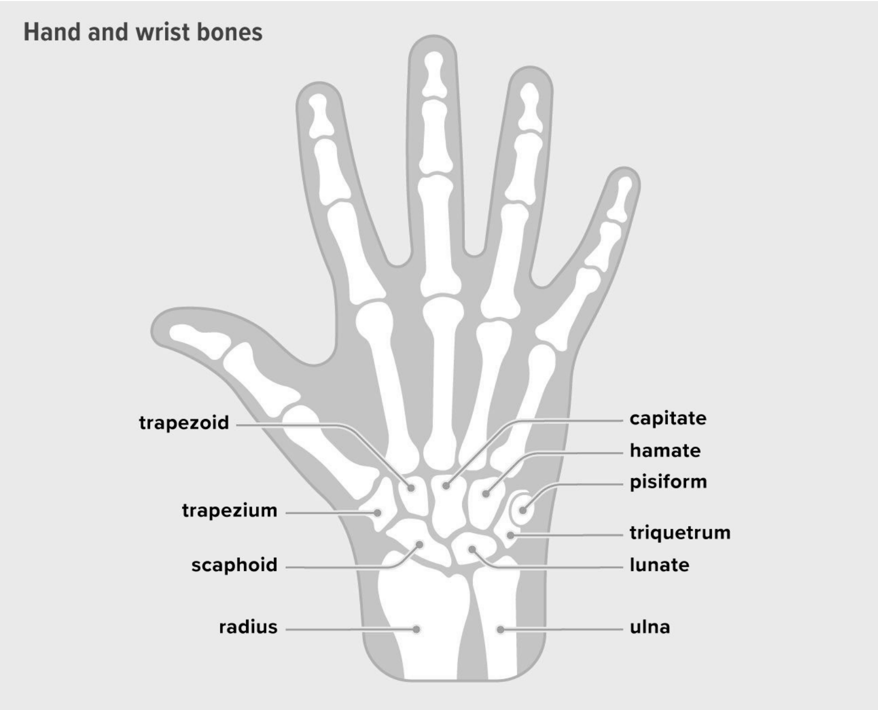

***Figure 2**: Bony anatomy of the wrist and hand [3].*

## Distal radius fractures in children

Yearly, 0,4% of the total population in the Netherlands suffers from distal radius fractures [6]. Out of all the bones in the human body, the radius is the one that is most often fractured [7]. In children especially, distal radius fractures are the most common type of fractures. Between 0-15 years of age, 30-35% of all registered fractures involve the distal radius [6, 8, 9]. Distal radius fractures are any fractures of the radius close to the wrist joint [10]. This includes, among others, Colles', Smith's, die-punch, Salter-Harris's, greenstick and buckle/torus fractures [10]. Every type of distal radius fracture (DRF) has a different presentation, mechanism of injury and indicated form of treatment [10]. The majority of DRFs in children consist of torus/buckle fractures and greenstick fractures. A typical aspect of these fractures is angular malalignment without shortening [8]. The higher compliance of pediatric bones causes bones to bend rather than to break in children. Therefore fractures are more often incomplete fractures, such as greenstick and buckle/torus fractures [10]. These fractures are relatively stable and not prone to displacement [11].

Both greenstick and buckle/torus fractures are most often caused by breaking of a fall on an outstretched hand/arm and therefore the fracture is most often angulated dorsally [10, 12, 14]. Buckle/Torus fractures are caused by axial loading forces and are characterized by buckling of the bone without radiographic fracture lines [10, 13]. The radius bends on the compressive side of the bone [8]. The cortex and periosteum buckle, showing a bump radiographically [10, 13]. Greenstick fractures are however caused by bending forces and are characterized by a radiographical gap at the apex of the fracture, but with an intact opposite side of the bone [8, 9, 10, 13]. The bending forces cause the surface of the convex/tension side to crack, while the surface of the concave/compressive side stays intact [9, 10]. Radiographically, a bending injury can be identified, with a fracture line that does not completely go through the bone [9]. Greenstick fractures are similar to the breaking of green twigs, hence the name [13]. The fracture patterns due to the different loading forces are shown schematically in Figure 3. Examples of X-ray images of a buckle/torus fracture and a greenstick fracture are shown in Figure 4.

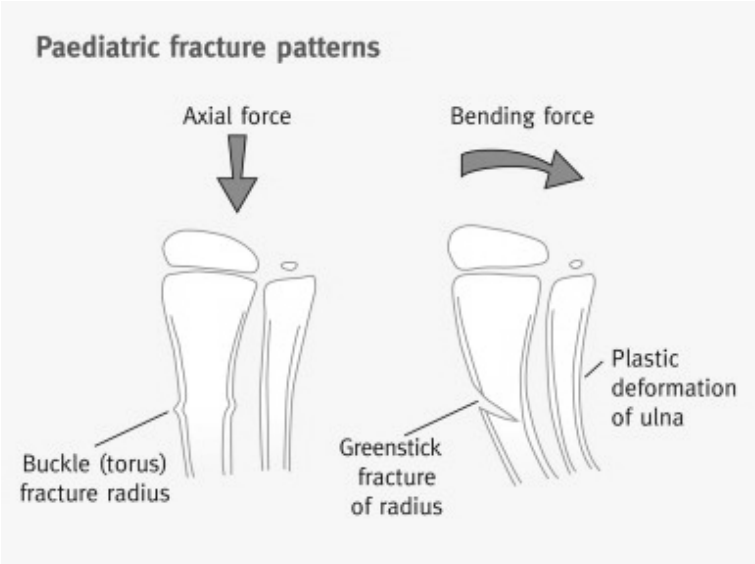


***Figure 3**: Fracture patterns of buckle/torus and greenstick fractures with impact forces [13].*

***Figure 4**: X-ray images of a buckle/torus (left) and greenstick (right) fracture [14].*

## Treatment of distal radius fractures

When a child comes to the emergency room (ER) with suspicion of a DRF, they often suffer from (pressure) pain, swelling and sometimes visible angular deviation [12, 14]. According to protocol of the Federation of Medical Specialists (FMS), first, an X-ray of the wrist is made from two perspectives: anterior-posterior (AP) and lateral [12, 15]. On the X-ray, a DRF can be confirmed or ruled out. Depending on the amount of angulation and the child's age, standard treatment of a distal radius fracture is repositioning, in case of angulation, and immobilization for approximately two weeks with a forearm cast [6, 12, 14, 15]. The younger the patient, the more angulation is allowed, since then there is more residual growth, allowing the child to outgrow the angulation. Traditionally, immobilization is established by plaster casting [16]. Although plaster casting is a relatively cheap and reliable solution, it also has its disadvantages.

For one, plaster is not waterproof, so bathing and swimming without special measures are out of questions during treatment [17]. The lack of bathing and also ventilation, complicates hygiene, increases sweating and can result in skin problems and itching [17, 18, 19, 20, 21]. With traditional casts, the skin is refrained from visual inspection, which also increases the risk of not detecting or late detection of, mainly skin related, complications [17, 22]. The weight of the arm cast can moreover cause pain in the neck or back and increase muscle loss [17]. The weight and poor hygiene are mostly disliked by patients [17, 18, 22]. Other complications associated with plaster casting are stiffness, pressure sores and compartment syndrome [21, 23]. Up to around 30% of all cases with cast immobilization result in complications or problems [19, 23].

Splinting or bandage therapy is an alternative that can be used in case of minimally angulated to affirm adequate ease of use and comfort and displaced fractures. A splint is often a slab of thermoplastic material or a soft brace that is fit to the arm with Velcro straps. Previous research has shown that for greenstick and buckle/torus fractures, splinting or bandage therapy is already sufficient for healing [18, 24]. Multiple studies show non-inferiority of splinting versus casting and some studies even show better clinical outcome when minimally angulated and displaced fractures are treated with splinting instead of traditional plaster casting [16, 18, 25, 26, 27, 28]. However, there is no consensus about the preferred treatment modality and duration [11, 26, 29, 30, 31]. Some physicians even state that immobilization of buckle fractures is unnecessary [29]. Previous studies show similar outcomes in joint function and comparable cost-effectiveness between casting and splinting, but with improved patient satisfaction, mainly in terms of weight and comfort [18, 32]. Splinting, however, is often accompanied with the same hygiene and inspectional issues as traditional plaster casting [17, 33]. The difference between a cast and splints is shown schematically in Figure 5.

***Figure 5****: Wrist splints (left and middle) and a plaster wrist cast (right) [34].*

## Additive manufacturing technologies

Additive manufacturing (AM) is a technique with which three-dimensional (3D) objects can be created by building up layers of a material on top of each other [35, 36, 37, 38]. The main principle is to turn a digital model into a physical object by building up one thin layer at a time [37, 38]. In this way, free form objects can easily be manufactured. AM is the total process of creating an object from 3D model data [39]. 3D printing, in this, is the most important step. According to the 52900 standard of the American Society for Testing and Materials (ASTM) F42 and International Organization for Standardization (ISO) TC 261, seven printing processes can be distinguished [37, 38, 40]. These technologies include material extrusion, vat photopolymerization, material jetting, binder jetting, powder bed fusion, direct energy deposition and sheet lamination [38, 40, 41]. An overview of the available AM technologies can be seen in Figure 6. A few of the most available 3D printing techniques are described below.

One of the most widely available 3D printing techniques is Fused Deposition Modelling (FDM). FDM is a form of material extrusion [38]. With FDM, filament from a spool is extruded continuously through a heated nozzle, so the material becomes fluid. By movement of the nozzle horizontally and vertical movement of the building plate, layers are built up until a 3D object is completed [38, 42]. FDM is a relatively cheap AM technique and often used to create medical models [43]. With FDM, objects can be made out of different materials, mainly (thermo)plastics and composites [3, 42]. Most FDM printers can use a maximum of two different materials in the same object, most of the time, one of these materials is used for (soluble) support. A FDM printer is shown schematically in Figure 7.

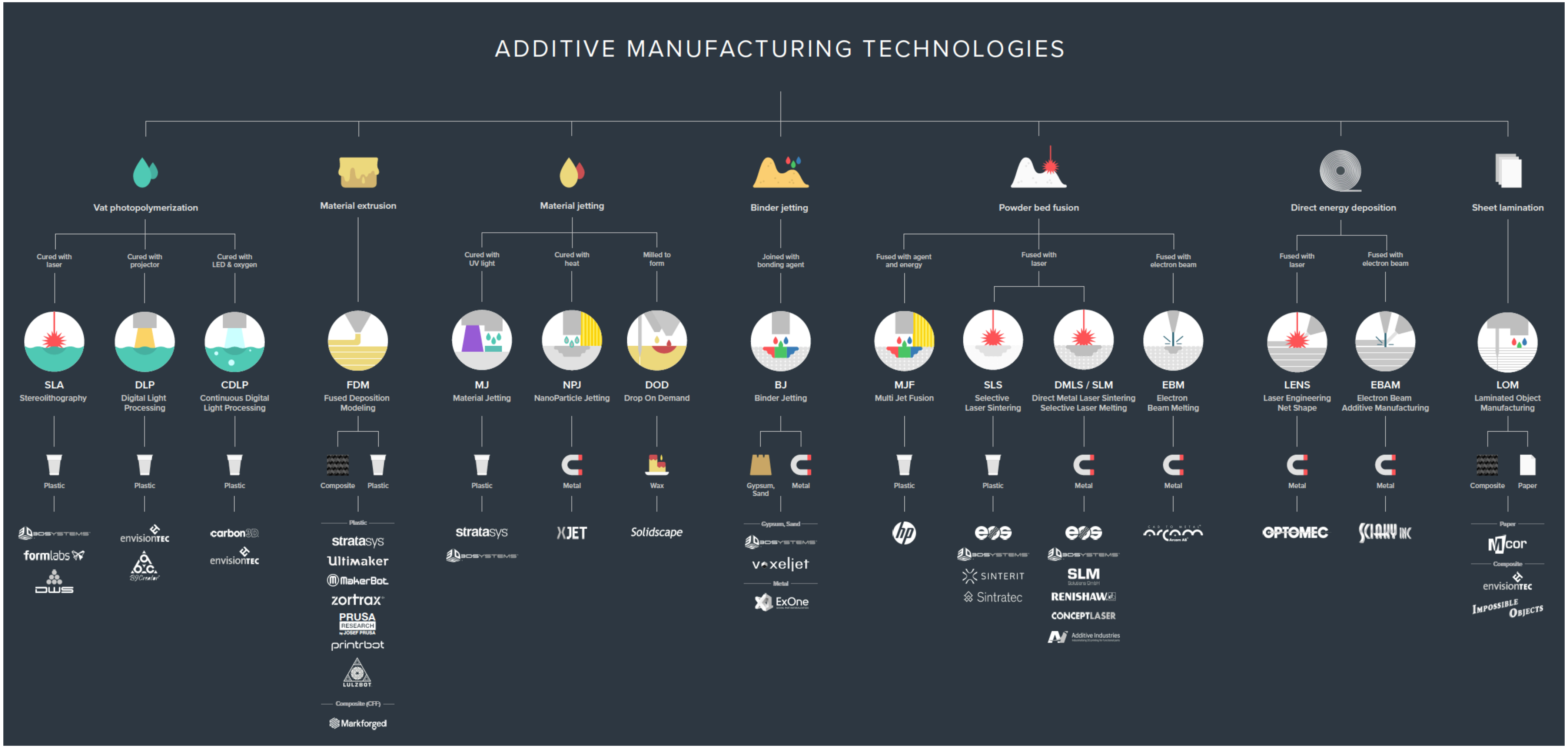


*Figure 6*: *Overview of AM technologies [38].*

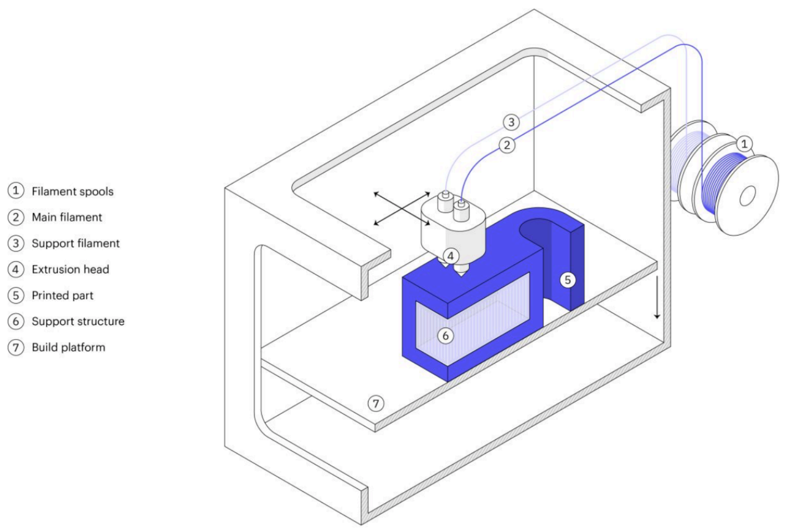


***Figure 7**: FDM printer [38].*

Two forms of vat polymerization are stereolithography (SLA) and digital light processing (DLP) [38]. SLA and DLP are very alike, since both processes are based on curing liquid resin in a vat by ultraviolet (UV) light. SLA produces a cured layer by moving a single laser through the resin. DLP, however, uses a digital light projector that creates a flash of a complete object layer to cure a complete layer of resin at once [38, 42]. Per layer, the build platform moves up a bit, until the 3D object is completed. After the build process, the object needs to be washed in isopropyl alcohol (IPA) to remove excess resin and cured again in an UV oven to strengthen the object [38, 42, 44]. A SLA printer is shown schematically in Figure 8.

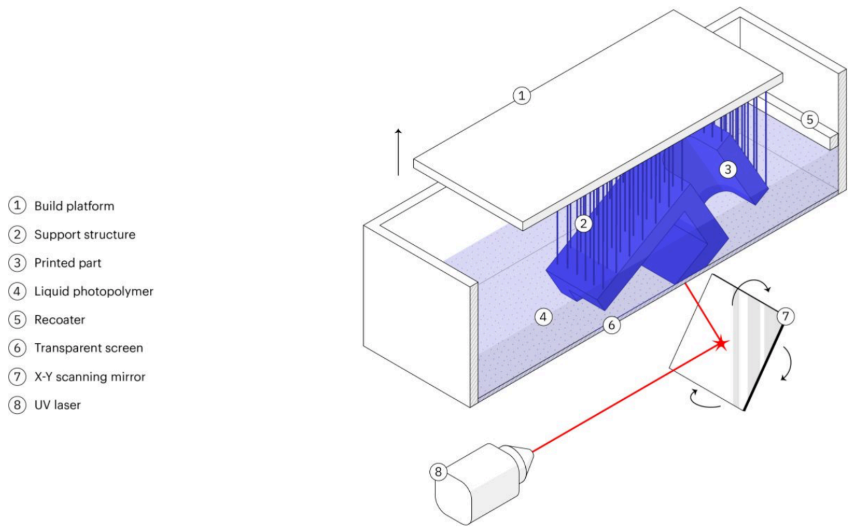


***Figure 8**: SLA printer. For a DLP printer, the laser is exchanged for a digital light projector [38].*

A form of powder bed fusion is selective laser sintering (SLS) [38]. With SLS, polymer powder in a bin is heated just below the melting point. A thin layer of this powder is deposited onto the build platform. Then, a $CO_2$ laser scans the surface and selectively sinters the particles that need to bind together to form an object layer. Subsequently, the build platform moves down a bit and the process repeats itself [38, 42]. After the sintering process, a solid part is surrounded by excess polymer powder. Post-processing, such as polishing can be applied after the powder bin is cooled down [38]. A variety of materials can be used in SLS, mostly nylon, potentially filled with carbon, graphite, metals, ceramics or glass [42]. A SLS printer is shown schematically in Figure 9.

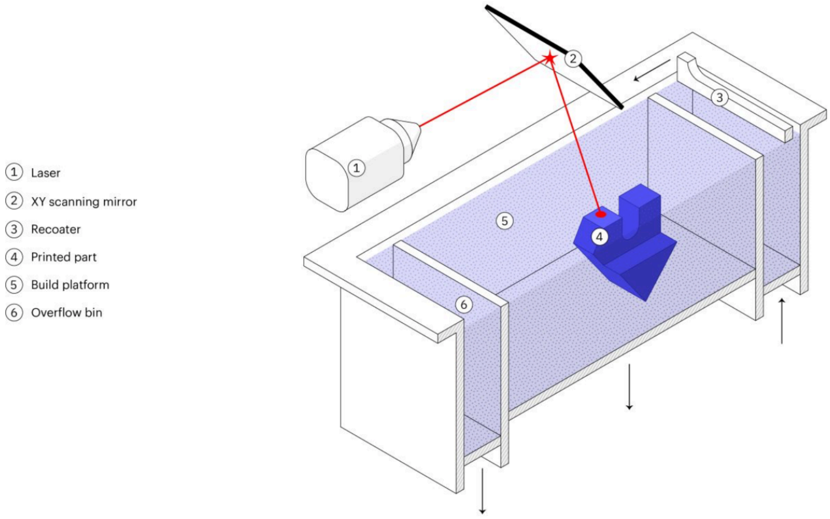


***Figure 9****: SLS printer [38].*

Similar to SLS are direct metal laser sintering (DMLS) and selective laser melting (SLM), both also forms of powder bed fusion [38]. In DMLS and SLM, a laser source partially or fully melts metal powder to create a solid object. In both technologies, a support structure is necessary because of the required high temperatures to melt the metal particles. A slight difference between DMLS and SLM is that in SLM full melt of the metal particles is required to fuse the powder, because single metals are used, while in DMLS the powder is only heated to reach a molecular fusion point to create parts from metal alloys [38, 42]. After the build process is completed, the support structure needs to be removed [38, 42]. A DMLS or SLM printer is shown schematically in Figure 10.

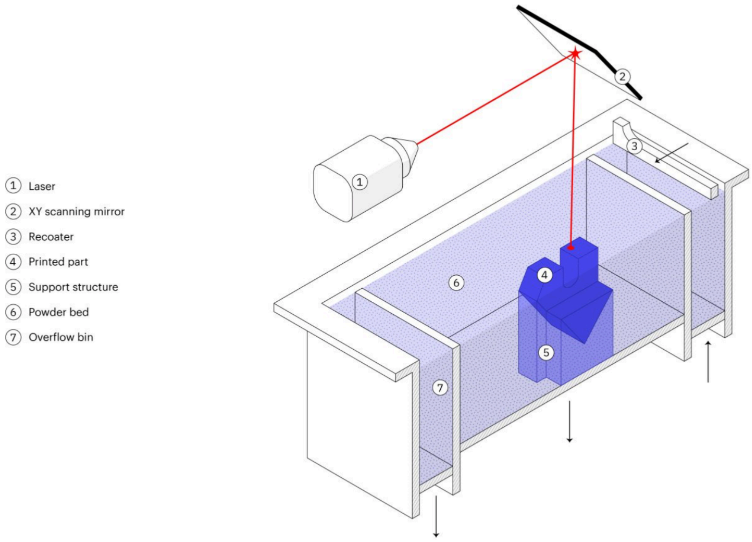


***Figure 10****: DMLS or SLM printer [38].*

Material jetting (MJ) is a 3D printing technique that is most similar to two-dimensional (2D) inkjet printing [38, 42]. Droplets of photopolymer are jetted onto a build platform by a printhead, that are solidified by UV light. After every layer, the build platform moves down a bit and a new layer is placed on top [38, 42]. Materials used in MJ are liquid acrylics [42]. Supports are needed in MJ, but for this purpose, water-soluble materials are available [38, 42]. MJ is one of the most precise but few printing techniques that can create an object out of multiple materials, in full-color and even has the ability to tune the glossiness of the end product [42]. A MJ printer is shown schematically in Figure 11.

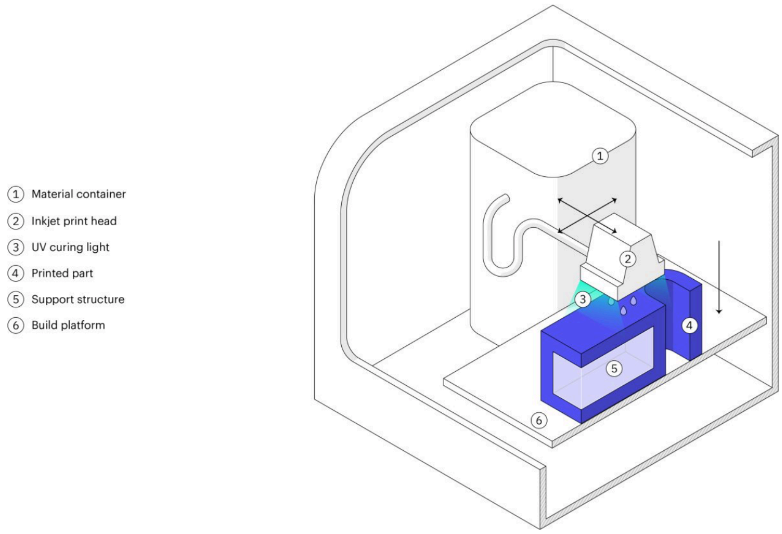


***Figure 11****: MJ printer [38].*

Finally, binder jetting (BJ) is one of the most diverse printing techniques [38]. BJ works with layers of powder particles that are placed onto a build platform. An adhesive binder is deposited selectively onto the powder, binding the particles and forming a layer of the object. The build platform moves down and the process is repeated until the part is completed [38, 42]. Cleaning and post-processing are necessary to complete the product, which can include sintering or infiltration of the product with metal or acrylic [38, 42]. BJ materials are most often metals or ceramics and BJ has the option of printing in full-color [42]. A MJ printer is shown schematically in Figure 12.

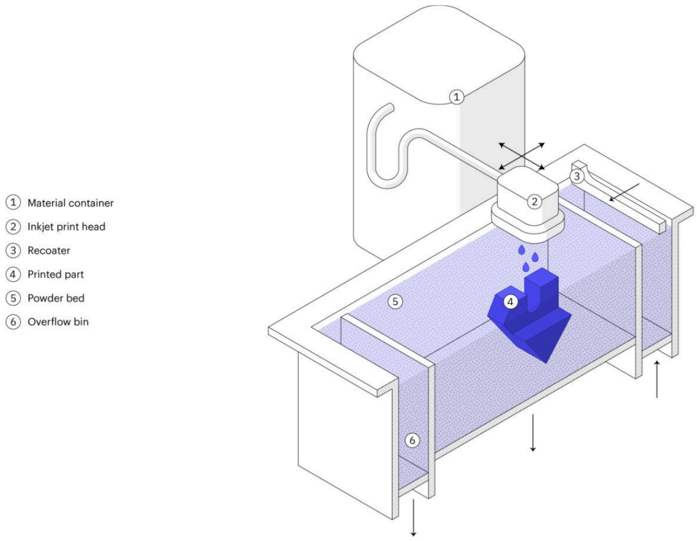


***Figure 12****: BJ printer [38].*

## 3D printing in the medical field

To produce a 3D object, different methodologies can be used. These methodologies include formative, subtractive and additive manufacturing [42]. Formative manufacturing works with molds, heat and pressure. Materials are melted and pressed into a mold, creating the desired object. On the other hand, subtractive manufacturing starts out with a solid block of material that is cut down with a tool or machine to create the object of interest. Finally, additive manufacturing builds layers of material on top of each other to form the object of demand [42]. These forms of manufacturing are visually represented in Figure 13. The different manufacturing technologies are cost-effectively and in terms of manageability suitable for different production processes. The more parts that need to be produced and the simpler the geometry, the better it is to use a standardized process, such as formative manufacturing. The trade-off between cost per part and the number of parts is simply shown in Figure 14. Since 3D objects in the medical field often need to be unique for a specific patient, AM is the best choice of manufacturing technique in this field [42].

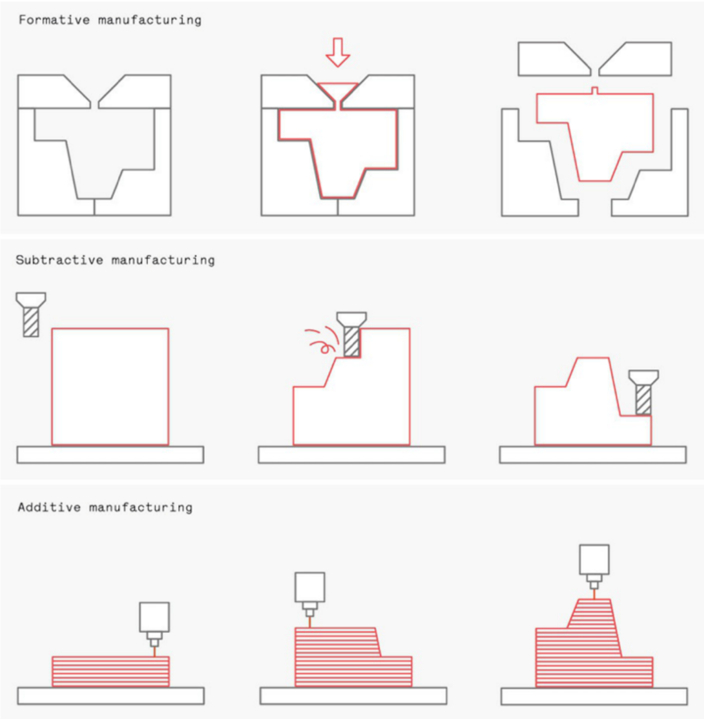


***Figure 13**: Manufacturing methodologies [42].*

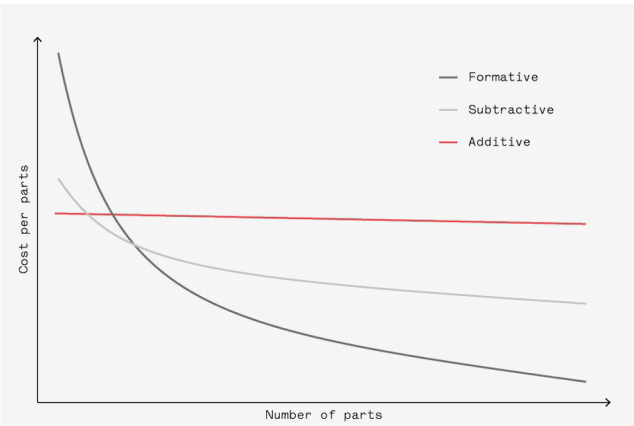


***Figure 14**: Trade-off between number of parts and costs per part for different manufacturing technologies [42].*

3D printing is thus a fast, affordable and widely available technique that is deployed in multiple industries, including the medical field [38, 45]. Medical applications that involve AM can mainly be found in orthopedics and surgery [46, 47]. Especially across the field of surgery, 3D printing is implemented in the clinical workflow more and more [48, 49]. More specifically, trauma and maxillofacial surgery, are well known to the use of 3D prints in their work [46, 48]. 3D printing in surgery is most often used for anatomical models, surgical instruments and implants or prostheses [46, 48, 50, 51, 52]. These products are used for surgical planning, training or education and personalized treatment [48, 52]. Since most produced objects are thus customized pieces of equipment or models, every produced element is unique, which plays into the importance of personalized medicine. Also, benefits such as reduction of operation time, lower costs and better understanding of the medical problem are associated with the use of 3D printing in surgery [46, 51].

# Literature study (systematic literature review)

## 3D printed wrist casts for the treatment of distal radius fractures in children: challenges and perspectives

### Introduction

*3D printed wrist casts*

To solve the issues associated with traditional plaster casting, 3D printing can be a good alternative with possibilities to create an open latticed, waterproof and lightweight cast. Multiple 3D printed cast or splint designs have emerged during the past few years [17, 22, 43, 53], but no clear design guidelines can be found. Previous work done at the Elisabeth-Tweesteden Hospital (ETZ) aimed to formulate general design guidelines, but was not specific in comparison of materials, printing techniques and different design patterns [54].

This systematic literature review aims to collect designs, materials and printing techniques from previous research on 3D printed wrist casts to form a foundation for a 3D printable wrist cast design that is implementable clinically. Best practices and reported challenges are formulated to take into account by creating a well-founded implementation plan for 3D printed wrist casts.

### Methods

*Literature search*

Both the PubMed and Scopus database were searched from the beginning of the database up to December 31st 2020. The specific search query for the PubMed database is presented in Figure 15 and for the Scopus database the query is shown in Figure 16.

| |
|---|
| *(((3D[Title] OR 3-dimensional [Title] OR three-dimensional [Title]) AND print* [Title]) OR (additive [Title] AND manufactur* [Title]))*<br>***AND***<br>*(device* [Title] OR cast* [Title] OR brac* [Title] OR orthos* [Title] OR splint* [Title])*<br>***AND***<br>*(patient-specific [Title/Abstract] OR wrist [Title/Abstract] OR orthop* [Title/Abstract] OR forearm [Title/Abstract] OR arm [Title/Abstract] OR (distal [Title/Abstract] AND radius [Title/Abstract]))* |

***Figure 15**: PubMed search query.*

| |
|---|
| *(TITLE (((3d OR 3-dimensional OR three-dimensional) AND print*) OR (additive AND manufactur*))*<br>***AND***<br>*(TITLE (device* OR cast* OR brac* OR orthos* OR splint*))*<br>***AND***<br>*(TITLE-ABS (patient-specific OR wrist OR orthop* OR forearm OR arm OR (distal AND radius)))* |

***Figure 16**: Scopus search query.*

*Selection of articles*

Articles that were found by the literature search in both databases were first screened on the presence of duplicates. Of the duplicates, one was removed from the search results. Articles were included if a cast, brace, splint, or orthosis was produced by 3D printing, if the application area was the forearm or wrist, if the device was used for immobilization purposes and if text was available in English. Moreover, a visual representation of the 3D printed product should be present and all steps of the production process (geometry digitalization, design and printing) should be described. Articles were excluded if the focus was on other body parts, such as the hand, heart, ankle or mandible, if the article was about a device with moveable parts or if the article was on mold casting. Also, reviews were excluded. Table 2 shows an overview of the in- and exclusion criteria. Firstly, the article titles were screened on the in- and exclusion criteria. Following that, the abstracts of the remaining articles were screened on the same in- and exclusion criteria. Finally, the full text articles were retrieved and screened on the in- and exclusion criteria. If the full text article was not available, the article was excluded.

***Table 2**: In- and exclusion criteria.*

| Inclusion criteria | Exclusion criteria |
|---|---|
| Cast, brace or splint is produced by 3D printing | Product is designed for other body parts than forearm or wrist |
| Forearm or wrist is the application area | Device has moveable parts |
| Device is used for immobilization purposes | Subject is mold casting |
| Text is available in English | Article is a review |
| Visual representation of the 3D printed product is present | Full text is not available |
| Production process (geometry digitization, design and printing) is described | |

### *Data extraction*

The relevant data was extracted manually from the included articles. This data includes general study characteristics as well as other information, such as the digitalization technique of the limb, printing technique, printing material, design program, and design pattern.

## Results

### *Literature selection*

The initial database search yielded 217 results. After removal of the duplicates, 147 articles remained. After reviewing the article titles, 47 articles were left. Subsequently, 13 articles were excluded based on abstract, so 34 articles were left to be screened on full text. Full text was unavailable for 2 articles and after applying the in- and exclusion criteria on the remaining full text articles, finally, 21 articles were included for data extraction. The literature selection process is presented in Figure 17. The study characteristics of the included articles are presented in Table 3.

### *Data extraction*

An overview of the extracted data (techniques for digitalization of the limb, printing techniques, printing material, design programs and design patterns) from the included articles is presented in Table 4.

### *Digitalization technique*

Considering the digitalization of the injured limb, two techniques can be distinguished. The first and most frequently used technique (18 out of 21 articles) is scanning the arm with a handheld 3D scanner. Different brands of scanners are described, but the principle of projecting a light source onto an object and generating a 3D point cloud out of the reflecting light is the key. The other technique is to perform routine clinical imaging. Thus, extracting the 3D model from a computed tomography (CT) scan or through magnetic resonance imaging (MRI). This causes exposure to radiation for the scanned person, in contrast to the 3D scanning technique. However, it is important to note that the articles that used this form of digitalization, already had access to these scans, due to the fact that these were needed in the clinical process of diagnosis and/or treatment [19, 20, 56].

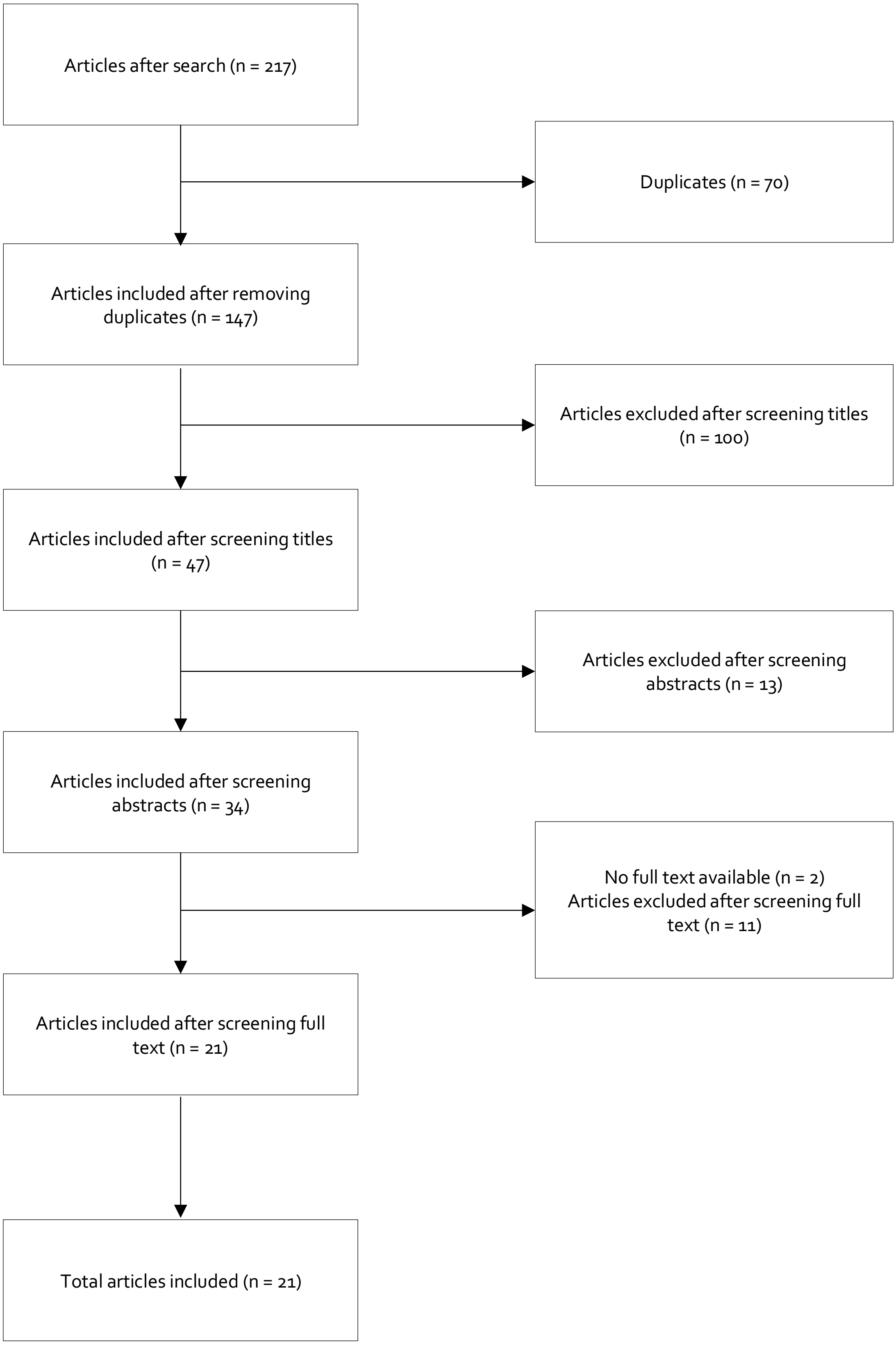


***Figure 17**: PRISMA flowchart literature selection.*

*Table 3: Study characteristics.*

| Authors | Year | Country | Journal (IF**) |
|---|---|---|---|
| Janzing et al. [55] | 2020 | The Netherlands | 3D Printing in Medicine (N/A*) |
| Chae et al. [56] | 2020 | Republic of Korea | Medicine (1.53) |
| Keller et al. [57] | 2020 | Switzerland | Hand Surgery and Rehabilitation (1.075) |
| Górski et al. [58] | 2020 | Poland | Materials (3.26) |
| Zheng et al. [59] | 2020 | China | Clinical Rehabilitation (2.737) |
| Górski et al. [60] | 2020 | Poland | Mechanisms and Machine Science (0.631) |
| Chen et al. [20] | 2020 | China | BioMed Research International (2.366) |
| Buonamici et al. [61] | 2020 | Italy | Visual Computer (1.948) |
| Hoogervorst et al. [43] | 2020 | Unites States of America | Hand (1.291) |
| Lee et al. [62] | 2019 | Republic of Korea | DISABILITY AND REHABILITATION: ASSISTIVE TECHNOLOGY (2.221) |
| Guida et al. [63] | 2019 | Italy | Journal of Pediatric Orthopaedics Part B (0.902) |
| Kim et al. [64] | 2018 | Republic of Korea | Prosthetics and Orthotics International (1.664) |
| Blaya et al. [17] | 2018 | Spain | Journal of Medical Systems (4.136) |
| Buonamici et al. [65] | 2018 | Italy | Computer-Aided Design and Applications (0.973) |
| Blaya et al. [66] | 2017 | Spain | TEEM 2017 (N/A*) |
| de Souza et al. [67] | 2017 | Brasil | Proceedings of the Annual International Conference of the IEEE Engineering in Medicine and Biology Society, EMBS (N/A*) |
| Chen et al. [19] | 2017 | China | 3D Printing in Medicine (N/A*) |
| Cazon et al. [68] | 2017 | United Kingdom | Proceedings of the Institution of Mechanical Engineers, Part H: Journal of Engineering in Medicine (1.603) |
| Paterson et al. [69] | 2015 | United Kingdom | Rapid Prototyping Journal (3.714) |
| Kim et al. [70] | 2015 | Republic of Korea | Journal of Mechanical Science and Technology (1.664) |
| Lin et al. [71] | 2015 | China | 3D Printing in Medicine (N/A*) |

* N/A = not available; ** IF = Impact factor, retrieved from Scimago journal ranking [72]

*Table 4: Design and printing techniques.*

| Authors | Digitalization technique | Printing technique | Printing material | Design program | Design pattern |
|---|---|---|---|---|---|
| Janzing et al. [55] | Structure optical 3D scanner (Occipital, Inc. San Francisco, US) | FDM (Wanhao duplicator I3, Wanhao, Zheiang, China) | PLA filament (Polymaker Polymax PLA, 1,7 mm, Polymaker, Utrecht, Netherlands) | Blender open source software | Round holes |
| Chae et al. [56] | CT images (1mm) imported into MIMICS Medical v17 (Materialize, Leuven, Belgium) | FDM (FINEBOT Z420 3D printer (TPC Mechatronics, Inc, Incheon, Korea)) | Thermoplastic polyurethane filament | Geomagic Freeform software (3D SYSTEM Corp, Santa Clara, USA) | Solid slab |
| Keller et al. [57] | Tablet (Apple iPad1 6th generation Apple Inc.™, Cupertino, California, USA) with an optical structure sensor (Mark I Structure Sensor1, Occipital Inc.™, Boulder, Colorado, USA) | Filament-based 3D printing (FDM)<br>DLP-technology | PP<br>Inmob A300 | Spentys© Point-of-Care Solution1 (Spentys SA/NV™, Brussels, Belgium) | Organic shaped holes |
| Górski et al. [58] | David SLS-3 optical scanner (David Vision Systems GmbH, Koblenz, Germany) | FDM (Raise 3D Pro machine (Raise 3D Technologies, Inc., Irvine, CA, USA)) | ABS<br>PLA<br>Nylon (PA12) (Spectrum Group, Pęcice, Poland)<br>High-impact polystyrene (HIPS) (MakerBot, New York, NY, USA) | Autodesk Inventor software (version 2019, Autodesk Company, San Rafael, CA, USA) | Diamond shaped openings |
| Zheng et al. [59] | Optical scanner (HCP; Creaform Co., Ltd, Canada) | SLA | Light-activated resin | Unigraphics NX 8.0 Software; Siemens, Germany | Round holes (fingers) and diamond openings (wrist/hand area) |
| Górski et al. [60] | GOM Atos Compact Scan 5 M blue light scanner | FDM (MakerBot Replicator 2X machine) | ABS material with HIPS material as a support | Autodesk Inventor 2018 | Irregular, spline-based shaped openings |
| Chen et al. [20] | CT imaging system (Aquillion 64, Toshiba, Japan)<br>MR (Achieva 1.5 or 3.0 T, Philips, Netherlands) | SLS (EOS P395 (Germany)) | Polyamide (PA2200) | Self-developed technique (Lin et al. [71]) | Round holes |

| | | | | | |
|---|---|---|---|---|---|
| Buonamici et al. [61] | SR300 (Intel RealSense) | FDM (Stratasys F370 FDM machine) | Stratasys ABS M30 | NXOpen Application Programming Interface (API) toolkit for NX 10 (Siemens) | Holes generated by topological optimization (TO) |
| Hoogervorst et al. [43] | Handheld 3D infrared scanner (Structure Sensor; Occipital, Inc., San Francisco, California) | MJF* (HP Multi Jet Fusion Printer (Palo Alto, California)) | HP PA12 Nylon | Standard Cyborg software (Standard Cyborg, San Francisco, California) | Droplet form holes |
| Lee et al. [62] | 3D optical scanner (Artec Eva, Artec Group, Luxembourg) | FDM (FB9600 printer (TPC Mechatronics Inc., Incheon, Korea)) | Thermoplastic polyurethane filament (eLastic (Shenzhen Esun Industrial Co. Ltd, Shenzhen, China)) | Geomagic Freeform software (3D SYSTEMS Corp., Rock Hill, SC) | Round holes |
| Guida et al. [63] | Laser scanner (3d Sense; 3D Systems Inc., Rock Hill, South Carolina, USA) | FDM | ABS (Z-UltraT; UltraT, Olsztyn, Poland) | Rhinoceros version 5.0 (Robert McNeel & Associates, Seattle, Washington, USA) | Large round holes |
| Kim et al. [64] | 3D scanner (Artec™ Eva, Artec Group) | FDM (FINEBOT Z420 3D printer (TPC Mechatronics Inc., Incheon, Korea)) | Thermoplastic polyurethane (TPU) filament | Geomagic Touch (3D SYSTEMS Corp., Rock Hill, SC, USA)<br>Geomagic Freeform software (3D SYSTEMS Corp.) | Solid slab |
| Blaya et al. [17] | Sense scanner | FDM (Prusa3iBQ Hephestos) | PLA | Geomagic® DesignX | Organic shaped holes |
| Buonamici et al. [65] | Intel RealSense SR300 | FDM (Stratasys F370 machine) | ABS-M30 material | Siemens NX modelling environment | Round holes |
| Blaya et al. [66] | 3D Systems Sense® scanner | FDM (Prusa 3i Hephestos BQ printer) | PLA | 3D Systems Geomatic Design X®<br>Rhinoceros 5 CAD program | Organic shaped holes |
| de Souza et al. [67] | REVScan (Creaform Ametek) | FDM (Graber i3) | PLA (polylactic acid) | Repetier | Honeycomb holes |
| Chen et al. [19] | CT imaging system (Aquillion CX 64, Toshiba, Japan)<br>MR (Achieva 1.5 T, Philips) imaging equipment | SLS (EOS P395 (Germany))<br>SLA (RS4500 (UnionTech, China)) | Polypropylene (PP)<br>Polyamide (PA2200) | Self-developed technique (Lin et al. [71]) | Round holes |

| | | | | | |
|---|---|---|---|---|---|
| Cazon et al. [68] | ZScanner 800 3D laser scanner (3D Systems, Rock Hill, SC, USA) | MJ (Objet Connex 500 (Stratasys Ltd., Minneapolis, MN, USA) PolyJet technology) | VeroWhitePlus (Fullcure 835) TangoBlackPlus (Fullcure 980) Fullcure 705 | Geomagic Studio 2013 (Geomagic, Morrisville, NC, USA) | Voronoi |
| Paterson et al. [69] | ZCorp Zscanner 800 hand-held 3D laser scanner (3D Systems, Rock Hill, SC, USA) | SLS (EOS P100 Formiga (EOS GmbH Electro Optical Systems, Krailling, Germany))<br>FDM (Stratasys Dimension SST1200es (Stratasys, Eden Prairie, MN, USA))<br>SLA (3D Systems 250 (3D Systems, Rock Hill, SC, USA))<br>MJ (PolyJet matrix Connex 500 (Stratasys, Eden Prairie, MN, USA)) | EOS PA2200 50:50 powder (EOS GmbH Electro Optical Systems, Krailling, Germany)<br>ABS (Stratasys, Eden Prairie, MN, USA)<br>Accura® Xtreme resin (3D Systems, Rock Hill, SC, USA) FullCure® 515 and FullCure®535 to generate RGD5160-DM (Stratasys, Eden Prairie, MN, USA) | Autodesk® Maya® 2011 (Autodesk, San Rafael, CA, USA)<br>Geomagic Studio 2012 (3D Systems, Rock Hill, SC, USA)<br>McNeel Rhinoceros® Version 4.0 with Grasshopper plugin (Robert McNeel & Associates, Seattle, WA, USA)<br>PTC Pro/Engineer Wildfire 5.0 (PTC, Needham, MA, USA)<br>FreeForm Modelling Plus (3D Systems, Rock Hill, SC, USA) | Voronoi, swirl |
| Kim et al. [70] | Photometric 3D scanner, REXCAN4 (Solutionix, Korea) | MJ (Objet500 Connex of Stratasys Inc. polyjet technology) | ABS plastic material | CAD software | Orthogonal |
| Lin et al. [71] | Photometric scanner (Artec Eva and Artec Space Spider (Luxembourg)) | SLA (RS6000 3D printer (UnionTech, China)) | Polypropylene (PP) | Visualization Toolkit (VTK Kitware) | Round holes |

*MJF = Multi Jet Fusion (powder bed fusion technology)

### *Printing techniques and materials*

FDM is the 3D printing technique that is deployed in more than half of the analyzed articles (13 out of 21). In most articles that are using FDM, the choice for this technique is based on the high availability and favorable cost-effectiveness [57, 58, 60, 67]. However, contradicting results are reported on the favorability of FDM as a technique to print 3D printed wrist casts. For example, Górski et al. reported FDM to be a cheap and usable technique in the production of a wrist cast [55]. On the contrary, Paterson et al. compared multiple printing techniques (FDM, SLA, SLS and MJ) and marked FDM as least favorable, mainly due to the inferior surface quality [69]. Also, Chae et al. and Kim et al. described a labor-intensive post-processing process for FDM printed products, with support removal and surface smoothing [56, 64]. Articles that reported the use of MJ as the printing technology, noted that MJ is relatively expensive, while other printing techniques, such as FDM, might be evenly suitable, with similar results, but lower costs [68, 70]. The SLA process is praised for the high quality of the printed surface, which would minimize hygiene risks and for the high strength in combination with the lightness of the printed product [69, 71]. SLS is mainly favored, due to the fact that limited post-processing is required, with the self-support of the powder bed [69]. Finally, Keller et al. used DLP as a printing technique, mainly praising the high printing speed [57].

Considering materials, there is a wide variety and the choice is mainly dependent on the choice of printing technique. Most articles that used FDM as the printing technique, created the wrist cast out of either acrylonitrile butadiene styrene (ABS) or PLA. Górski et al. compared different materials for the production of a wrist cast with FDM and marked PLA as most favorable, based on strength, accuracy and favorable costs [58]. Also, PLA is praised for the high biocompatibility and the ability to recycle the product [58, 66, 67]. ABS on the other hand, is mostly praised for its mechanical properties in hardness and tensile strength, besides the higher stability compared to PLA, HIPS and nylon, causing a lower rate of production failure [58, 63]. An ABS printed cast was also lighter than the same product printed in PLA [58]. The use of thermoplastic polyurethane (TPU) for 3D printed wrist casts was praised because of the good adherence to the skin [64]. Polypropylene (PP) was complimented on adequate stability and the lightness in combination with high strength, making the product wearing friendly [57, 64].

### *Design program and pattern*

For the design of the 3D printed cast, a wide variety of design programs was used. Janzing et al. and Buonamici et al. used open source software [55, 61]. In most cases, some commercial design program was used to design the casts [17, 56, 62, 63, 64, 66, 68]. Also, a self-developed design program was used by Chen et al., Chen et al. and Lin et al. [19, 20, 71]. Uniquely, Keller et al. used a purpose built app, that automatically designs a cast around the digitized arm, based on frequently used presets [57].

For the pattern, also, a variety of designs can be observed. However, a main tendency can be found in the use of ventilation holes of organic shapes or round holes. Among organic shapes, Voronoi patterns, droplet form holes, spline-based openings and holes generated by topological optimization (TO) can be found [17, 43, 57, 60, 61, 66, 68, 69]. Round holes, varying in size, can be found evenly frequent, sometimes in combination with another geometry on a different part of the cast [59]. Some distinct patterns can also be observed. For example, Patterson et al. used a swirl pattern [69]. An orthogonal pattern was used by Kim et al., since one of their design demands was to make the geometry as simple as possible to ensure automatic generation of the cast geometry in the future and since connection bosses needed to be added to connect an outer shell to [70]. Another geometry was found in de Souza et al., namely a honeycomb pattern, that was retrieved from an open source channel, since sharing, altering and common availability was highly valued [67]. Górski et al. and Zheng et al. chose the use of diamond shaped openings as ventilation holes [58, 59]. Finally, Chae et al. and Kim et al. used solid slab, without ventilation holes, as a design [56, 64].

## Discussion

### *Digitalization technique*

It can be concluded that the use of a 3D scanner for the digitalization of the injured limb is the preferred technique. Although alternatives are available, the use of 3D scanner is favorable over the use of routine clinical imaging, because of no exposure to radiation, shorter scanning times and the ability to move the scanner to the subject, instead of bringing the subject to the scanner. For successful implementation of a workflow for 3D printed wrist casts in routine clinical practice, scanning the injured limb with a 3D scanner should be the gold standard.

### *Printing techniques and materials*

Although multiple printing techniques and materials are being deployed for the production of 3D printed wrist casts, there is no consensus about the technique and material that should be used for optimal results. Each study has its own printing characteristics and 3D printing for 3D wrist casts is overall described as a promising technique [58, 63, 64]. However, improvements are necessary, mainly in the post-processing step [64]. In the choice of printing technique, FDM is most commonly chosen, with promising results as a conclusion, but in comparison to other techniques, it proved to be the least favorable [69]. So, there is even a difference in opinion on one specific 3D printing technique. Also, some printing techniques are not yet commonly used for the purpose of 3D printing wrist casts, while these techniques could cause promising results. DLP, used by Keller et al., is one of those techniques, that might be a good alternative to FDM or SLA, but with faster printing times [57].

Material wise, there is also no consensus. Both PLA and ABS are praised for their biocompatibility [58]. ABS is then also complimented on high strength and hardness [58]. While PLA is favored because of personalization and aesthetic purposes [69]. In the comparison of multiple materials PLA was favored [58]. However, also in the choice of materials there are more choices that could have better characteristics for the production of 3D printed wrist casts. For example, tough PLA has similar biocompatible characteristics of PLA and is evenly easy and safe to use, while its toughness is closer to ABS (impact strength of PLA (3,4 $kJ/m^2$) versus tough PLA (29,8 $kJ/m^2$) versus ABS (35 $kJ/m^2$)), but with higher stiffness (Young's modulus PLA (3384 MPa) versus tough PLA (2750 MPa) versus ABS (2109 MPa)) [73, 74, 75, 76]. Finally, it is important to realize that the choice of material is nowadays also limited by the new European Medical Device Regulation (MDR), which states that particular attention should be paid to the choice of materials, regarding toxicity and biocompatibility [77]. Concluding, this means that further research is needed to form consensus about the choice of printing technique and material.

### *Design program and pattern*

For the design program, it has been proven that multiple design programs are able to design a 3D printable wrist cast successfully. Not one particular program stands out for having better or worse performance. Even self-developed design software had promising results [19, 20, 71]. In terms of clinical implementation, Keller et al. proposed the use of an integrated purpose built app, that directly designs a cast onto a scanned limb [57]. Such an integrated tool might be better accepted by clinicians, because it removes complicated design and printing steps, making it intuitive to use [57].
In terms of design pattern, also, a large variety of patterns can be distinguished, with two main groups, designing the ventilation holes either organically shaped or round. However, on this part also, often no foundation is described for the choice of ventilation pattern, so no consensus can be drawn on which patterns is best. Only one pattern had some substantiation, namely the pattern that was generated by TO [61]. This pattern ensured the desired mechanical behavior of the cast, while also minimizing the weight. However, one preset was used for multiple casts, resulting in one actual TO cast and four casts based on the preset that was calculated for the first case [61]. Nevertheless, TO might be a feasible method to take into account when determining the design pattern. Examples of different design patterns are shown in Figure 18.

***Figure 18**: Examples of different design patterns (organic shaped holes (left) [57], holes by TO (middle) [61] and round holes (right) [19]).*

Most designs were now created with limited to no input from clinicians [53]. Therefore, the designs are mostly a free interpretation of people with limited clinical knowledge and the designs require extensive digital designing expertise. Although different designs all show promising results, the implementation of 3D printed wrist casts in daily clinical routine stays out [57]. Although clinicians are often excited by the idea of AM splinting or casting, a structured design and infrastructure is needed for clinical implementation [53, 57].

*Challenges and perspectives for the use of 3D printed wrist cast for the treatment of distal radius fractures*

Clinical results are promising, mainly in the field of patient satisfaction [20, 63]. Also, comfort and even perceived function can be improved by a 3D printed cast compared to plaster casting [22]. However, most 3D printed casts nowadays are used in trials with a limited number of patients or in case studies [19, 56, 70]. For further clinical implementation, a well-founded workflow needs to be created with evidence based use of designs, materials and printing techniques. Right now, studies each show their own design, but no consensus is published around design and printing characteristics that should be met if these types of casts were to be implemented clinically in direct patient care.

If the 3D printed casts prove to be a safe alternative to traditional plaster casting, patient satisfaction will most likely increase, since the 3D printed casts will be lighter and will not have the hygiene associated problems. This will substantiate the possibility to extend 3D printed casts for other types of fractures and other body parts, improving fracture treatment and healthcare as a whole.

## Conclusion

In this systematic literature review, designs, materials, printing techniques and digitalization techniques from previous research on 3D printed wrist casts were collected to form a foundation for a 3D printable wrist cast design that is implementable clinically. For successful implementation, an evidence based workflow is necessary. The injured limb should be scanned by a 3D scanner, but for the choice of printing technique, design and material, further research is necessary. For the printing technique, FDM, SLA and possibly DLP are good options. PLA, ABS and possibly tough PLA should be tested as materials for FDM printing. Finally, the design should be created with input from clinicians, taking organic shapes and rounds into account for the ventilation holes, possibly combined with TO.

# Research goal and thesis outline

## Clinical problem

Distal radius fractures are traditionally treated with plaster casts [16]. Although this has been the gold standard for treatment for years, it also comes with disadvantages. These are the weight, not being water-resistant and a lack of ventilation, leading to skin problems, itching and compromised hygiene [17, 18, 19, 20, 21, 22]. Furthermore, plaster has no possibility for visual inspection of the skin, while up to 30% of all treatments with plaster casting lead to, mainly skin related, problems [19,23].

With 3D printing, a lightweight, waterproof, open latticed and personalized cast can be created to overcome the issues with plaster casting. Multiple start-ups, researchers and other individuals already created these 3D printed casts, however, there is no consensus about the materials and design that should be used. Also, implementation of these 3D printed wrist casts into clinical practice stays out.

## Research goal

The goal of this thesis is to investigate which steps are necessary for successful use of 3D printed wrist cast in clinical practice. The main research question is:

*"What is the feasibility of in-house design, production and implementation of 3D printed wrist casts for the treatment of distal radius fractures?"*

Accessory to the main research question, multiple sub questions were formulated.

1. Which material is most suitable for the production of 3D printed wrist casts?
2. What is a successful design (pattern) for wrist immobilization?
3. Which alterations should be made to the current workflow to implement the treatment of distal radius fractures with 3D printed wrist casts?

## Thesis outline

To answer the main research question, multiple sub studies were performed. First, design requirements were formulated in consultation with clinicians. Then, material tests were performed, followed by the design step. Subsequently, the optimal design pattern and validation of the stabilization requirements were investigated during a mechanical phantom study. Also, to affirm adequate ease of use and comfort, a comfort study was carried out. The next step was a pilot study, in which the necessary alterations in the workflow were investigated, as well as clinical outcomes and patient experiences. Finally, an individual patient case was added. The thesis outline is thus as follows:

**1. Design requirements**

**2. Printing technique and material selection**

**3. Design**

**4. Mechanical phantom study**

**5. Comfort study**

**6. Pilot study**

**7. Patient case**

# Design requirements

## Requirements with clinical input

To determine the design of the 3D printed wrist casts, first, design requirements need to be formulated. This was done in consultation with some members of the clinical staff, both (trauma) surgeons and plaster technicians. Taking their expertise into account is of paramount importance, since in the end, clinicians will be the prescribers of the product, so their standards should be met for successful clinical implementation. Below, the design requirements for the 3D printed wrist casts are formulated.

### Stabilization abilities similar to plaster casting

The most important design requirement is that the 3D printed cast should have similar stabilization abilities as traditional plaster or better. Immobilization was named by the clinicians as the most important requirement for the 3D printed wrist casts. Stabilization of the fractured arm is the primary goal of treatment and even if the fracture is stable, in case of a greenstick or buckle/torus fracture, it is not only the most important factor for healing, but also for pain relief [78].

### Solid design

Apart from immobilization, rigidity and solidity were also named as important design requirements. Especially, when the design is fenestrated for ventilation, it is important that the material is stiff and sturdy. Also, it should be able to take a beating, making sure the cast does not fail with the slightest bump.

### Personalized fit

According to the plaster technicians, the complaints they come across most often when treating patients with plaster casting are excessive tightness and overcompression of the limb, leading to swollen fingers and pain. Also, in literature, pressure sores due to inadequate fit are described frequently during treatment with plaster casting [21, 23]. With the use of 3D scanning, the precise anatomy can be recorded and a cast can be made precisely in accordance to the patient's' anatomy, also taking into account any protruding bumps. However, during the first days after the trauma, swelling increases. To prevent excessive tightness, the 3D printed cast should be able to give room for this by having the ability to be loosened up.

### Open-latticed pattern for ventilation and visual inspection

Plaster casting lacks ventilation abilities and possibilities for visual inspection. As a result, treatment with plaster complicates hygiene, due to increased sweating. As mentioned before, around 30% of the cases where plaster casting is used as treatment leads to, mainly skin related, complications [19, 23]. For the 3D printed wrist casts it is thus important to create ventilation holes. This will increase hygiene and comfort and will also allow for visual inspection.

### Water resistance

Plaster casts are not water-resistant. Therefore, one of the issues that is mostly limiting daily life and complicates good hygiene during treatment with a plaster cast, is the disability to take a shower without special measures in place [17]. Most 3D printed materials are water-resistant, so only these materials should be taken into account for the production of the 3D printed casts.

### Lightweight

Another issue with plaster, which is often disliked by patients and mainly by children, is the weight of the casts, which is around 500 grams for a traditional plaster forearm cast [63]. This is mostly an issue with lime plaster casts, however, also polyester casts, which are a little less heavy, still contribute to pain, stiffness and discomfort, with a weight of around 350 grams [17, 18, 22, 63]. The 3D printed cast should thus be as lightweight as possible, preferably made out of plastic-like material.

### Closing system

A plaster cast is created circularly around the forearm. Since the 3D printed cast should be applied to the forearm after it is printed in the desired shape, the printed cast should either consist of two parts or one part with an open slit. If the cast consists of two parts, when put together, should fully enclose the arm. With the other option, the slit should be wide enough to put the arm through. This would either require a certain flexibility of the material, to be able to fold open the cast during application, or a wide slit. Furthermore, there is no support of the wrist at the slit area, creating a higher risk of displacement or misalignment of the bone. In consultancy with the clinicians, the best option should be to create a cast with two parts.

The two cast parts should be held together by a closing system. Multiple options are available for this, such as clamps, elastic bands, Velcro straps and tie wraps. In consultancy with the clinicians, for practical reasons, attachment with Velcro straps should be the best option. This is because the Velcro straps can be set at different lengths, which also complies with the requirements of being able to loosen up the cast in case of excessive tightness, caused by swelling. Also, Velcro straps dry quickly after contact with water and are lightweight.

### Smooth surface finish

3D printing of free form objects often require support during printing. When printing is finished, this support needs to be removed. Some support materials, such as polyvinyl alcohol (PVA) are soluble in water, while other supports need to be removed by hand with a support removal tool. The attachment points of the support can leave small and sharp tips that, if not removed, could cause damage to the skin. Therefore, the prints should be oriented onto the build plate so that the support only touches the outside of the cast as much as possible. Also, the support tips should be removed and smoothed out as much as possible after the print is finished.

### Biocompatibility

The cast will come into contact with intact skin. The International Organization for Standardization (ISO) set requirements for materials that can be used for the production of medical devices. According to ISO 10993-1, for medical devices that come into contact with intact skin, the materials may not by cytotoxic, sensitizing or irritating. The cast should thus be made of materials that comply with ISO 10993-1 [79].

### Semi-automated design

Lastly, to implement the 3D printed casts into the current workflow of the hospital, the manual steps need to be minimized as much as possible. Roughly, this means the workflow should consist of three major steps: digitalization of the forearm (1), a design algorithm that creates the cast (2) and the printing, including post-processing (3). Based on the literature study, the digitalization of the arm should be done with a 3D scanner and the design of the casts should be carried out by the use of a (semi-)automated design algorithm, to minimize manual labor during this process step. Post-processing steps after 3D printing should also be minimized to prevent excessive manual labor.

# Printing technique and material selection

## Introduction

As can be seen from the literature study, there is no consensus on the choice of printing technique and material for 3D printed wrist casts. FDM, SLA and possibly DLP are promising printing techniques, which should be investigated further. Considering materials, the most frequently used materials in literature for FDM printing are PLA and ABS, with tough PLA as a promising alternative that has not yet been described to be used for wrist splinting purposes.

At the 3D lab of the ETZ, two types of printers are available: FDM printers and SLA printers respectively. Since both printer types might be suitable for the production of 3D printed wrist casts, materials for both printers should be tested.

The arm casts mainly need to be stiff, meaning that the used material should have a high flexural (Young's) modulus [80]. Also, the 0.2% yield strength should be as high as possible. This is important to take into account, since from this point on, unwanted plastic deformation will occur [81], which influences the shape and fit of the cast and that might induce displacement or misalignment of the broken bone. Additionally, the ultimate strength, mainly when flexural forces are applied, needs to be as high as possible, to prevent the patient from breaking the cast from the inside out by wrist force generation. Furthermore, mapping the failure mechanisms of the materials under flexural and tensile forces is important, since fragmentation with generation of sharp edges is unfavorable. The used materials should not be too brittle, namely, sharp edges and fragments might cause harm to the patient when the cast accidentally fails or is damaged by external forces. Because multiple factors can influence the material properties, such as print orientation and layer thickness, mechanical tests with the intended material settings are necessary to determine the mechanical properties. Both flexural and tensile properties need to be evaluated for a complete overview and to make a well-founded material choice. Finally, also other material characteristics might play a role in making a printing technique and material more or less suitable for the production of 3D printed wrist casts. These characteristics include costs, color choice, printability, adhesion between layers, surface finish and printing time.

The goal of this material study is to find the most suitable material and printing technique for the production of 3D printed wrist casts, taking both flexural and tensile parameters into account, as well as the failure mechanism and additional material characteristics, such as costs, color choice and printing time.

## Materials and methods

### Materials

Six different materials were selected for material testing. For the FDM printing technique, the materials are based on the literature study. These materials are ABS filament, PLA filament and tough PLA filament (Ultimaker B.V., Utrecht, Netherlands). For the SLA printing technique, the materials are selected based on the manufacturer's information. The selected materials are standard color resin, draft resin, which is recommended for rapid printing, and tough 2000 resin, which is recommended for strong and stiff prints (Formlabs Inc., Somerville, MA, USA) [82, 83, 84]. The flexural and tensile properties provided by the manufacturers are presented in Table 5. All materials (once processed) are not cytotoxic, not a sensitizer and not an irritant, which make them suitable for the production of medical devices that come into contact with intact skin, according to ISO 10993-1 [79]. Also, all materials were suitable for contact with water [82, 83, 84, 85, 86, 87].

*Table 5: Material properties provided by the manufacturers [82, 83, 84, 85, 86, 87].*

| Material | Printing technique | Flexural modulus (MPa) | Tensile modulus (MPa) | Ultimate flexural strength (MPa) | Ultimate tensile strength (MPa) |
|---|---|---|---|---|---|
| ABS | FDM | 2070 | 1618.5 | 70.5 | 33.9 |
| PLA | FDM | 3150 | 2346.5 | 103 | 45.6 |
| Tough PLA | FDM | 2490 | 1820 | 78 | 37 |
| Color | SLA | 2200 | 2800 | N/A* | 65 |
| Draft | SLA | 2300 | 2300 | N/A* | 52 |
| Tough 2000 | SLA | 2200 | 1900 | 65 | 46 |

*N/A = not available

## Test samples

Test samples for both the flexural tests and tensile tests were designed according to the corresponding ISO standards, ISO 178 and ISO 527 respectively [88, 89]. The computer aided design (CAD) was performed in SolidWorks (Dassault Systèmes SolidWorks Corporation, Waltham, MA, USA). The dimensions for the flexural test samples and tensile test samples are presented in Table 6. After the CAD, the designed test samples were exported as a standard tessellation language (STL) file.

*Table 6: Test sample dimensions.*

| | | Dimension (mm) | |
|---|---|---|---|
| | | *Flexural test sample* | *Tensile test sample* |
| **Length** | *Overall* | 80.0 | 170.0 |
| | *Narrow portion* | | 80.0 |
| **Width** | *Overall* | 10.0 | 20.0 |
| | *Narrow portion* | | 10.0 |
| **Thickness** | | 4.0 | 4.0 |
| **Distance between broad portions** | | | 109.3 |
| **Radius** | | | 24.0 |

The STL files were imported in Ultimaker Cura (Ultimaker B.V., Utrecht, Netherlands) for the FDM materials and in PreForm (Formlabs Inc., Somerville, MA, USA) for the SLA materials to prepare for printing. All samples were oriented vertically onto the build platform, since the final casts will also be oriented (mainly) upright. Infill density was set to 100% and layer thickness to 0.1 mm. For the FDM samples, an adhesion brim was added for stability during printing. Further settings were set to default. For the SLA flexural samples, support was automatically generated with default settings and for the SLA tensile samples the height above the raft was set to 2.00 mm to fit into the build volume, while all other settings were left at default. Support points generated elsewhere then at the bottom of the samples were removed manually for both the tensile and flexural samples.

For both the flexural and tensile tests, six samples were printed per material. Five of the samples were used for testing and one was used as a back-up, in case a test would fail. ABS, PLA and tough PLA samples were printed with an Ultimaker S5 printer (Ultimaker B.V., Utrecht, Netherlands). Color, draft and tough 2000 samples were printed with a Form 2 printer (Formlabs Inc., Somerville, MA, USA). In total, 36 samples were printed for flexural testing and 36 samples were printed for tensile testing.

Post-processing for the FDM samples was the removal of the adhesion brim, while for the SLA samples, a wash and a cure step were also required. After printing, the SLA samples were washed in isopropyl alcohol (IPA) >99,85% to remove access resin. Subsequently, the samples were cured by ultraviolet (UV) light with a set temperature. Wash and cure settings for the SLA materials are described in Table 7 [90, 91]. Finally, the support was removed with a support removal tool.

***Table 7**: Wash and cure settings for SLA materials [90, 91].*

| Resin | Wash time (min) | Cure time (min) | Cure temperature (°C) |
|---|---|---|---|
| Color | 10 | 60 | 60 |
| Draft | 10 | 5 | 60 |
| Tough 2000 | 10 + 10 | 60 | 70 |

Before testing, the sample width and thickness were checked at mid-length of the specimen with a caliper (Mitutoyo, Kawasaki, Japan) for compliance with the design dimensions. If the deviation was more than 2% of the objected dimensions stated in Table 6, the samples were excluded for testing.

## Data collection

### *Flexural testing (ISO 178)*

Flexural testing was performed with an ElectroPuls E1000 testing system (Instron, Norwood, MA, USA). The test set-up is shown in Figure 19.Test samples were placed on two supports with a radius of 5.0 mm and the span between these support was set to 64 mm according to Formula 1. To prevent a curved region at the start of the stress/strain diagram, a prestrain of 0.05%, which corresponds to 0.085333 mm, was applied as a preload. Preloading was performed with a test speed of 1 mm/min. The radius of the loading edge was 5.0 mm and loading was applied at mid-span. After the preloading was finished, the test was started. The test speed was set to a constant rate of 2 mm/min, corresponding to a flexural strain rate of 1%/min according to Formula 2. During testing, the applied force (N) was measured, as well as the deflection at mid-span (mm), with a sampling rate of 20 Hz. The test ended when the sample broke or a deflection of 20 mm was reached, since then the outcomes are not representative anymore for flexural modulus and strength calculations, because of the inlfuence of shear forces, according to Timoschenko's beam theory [92]. The failure mechanism of each sample was noted.


***Figure 19**: Test set-up with ElectroPuls E1000 for flexural testing.*

*__Formula 1__: Span for flexural testing.*

$$L = (16 \pm 1)h$$

L = span (mm)
h = test sample thickness (mm)

*__Formula 2__: Test speed for flexural testing.*

$$v = \frac{rL^2}{600h}$$

v = test speed (mm/min)
r = flexural strain rate (%/min)
L = span (mm)
h = test sample thickness (mm)

### *Tensile testing (ISO 527)*

Tensile testing was performed with an ElectroPuls E1000 testing system (Instron, Norwood, MA, USA). The test set-up is shown in Figure 20. Test samples were clamped into the grips that were spaced 115 mm apart. To prevent a curved region at the start of the stress/strain diagram, a pretension was applied, which is calculated based on the theoretical tensile modulus, according to Formula 3. Pretension values per material are stated in Table 8. After pretensioning was finished, the test was started. The test speed was set to a constant rate of 1 mm/min. During testing, the applied force (N) was measured, as well as the displacement between the grips (mm), with a sampling rate of 10 Hz. The test ended when the sample broke. The failure mechanism of each sample was noted.

*__Figure 20__: Test set-up with ElectroPuls E1000 for tensile testing.*

*__Formula 3__: Determination of pretension values.*

$$p = \frac{E_t}{2000} \times A$$

p = pretension (N)
$E_t$ = theoretical tensile modulus (MPa)
A = test sample cross-sectional area (mm$^2$)

*Table 8: Pretension values per material for tensile testing.*

| Material | Pretension (N) |
|---|---|
| ABS | 32.37 |
| PLA | 46.93 |
| Tough PLA | 36.40 |
| Color | 46.00 |
| Draft | 44.00 |
| Tough 2000 | 56.00 |

## Calculations

From the collected force and deflection/displacement data, the corresponding flexural and tensile stress and strain values can be calculated, according to Formula 4 and Formula 5 respectively.

*Formula 4: Flexural (left) and tensile (right) stress calculation.*

$$\sigma_f = \frac{3FL}{2bh^2}$$

$\sigma_f$ = flexural stress (MPa)
F = applied force (N)
L = span (mm)
b = test sample width (mm)
h = thickness of the test sample (mm)

$$\sigma_t = \frac{F}{A}$$

$\sigma_t$ = tensile stress (MPa)
F = applied force (N)
A = test sample cross-sectional area ($mm^2$)

*Formula 5: Flexural (left) and tensile (right) strain calculation.*

$$\varepsilon_f = \frac{600sh}{L^2}\%$$

$\varepsilon_f$ = flexural strain (%)
s = deflection (mm)
h = test sample thickness (mm)
L = span (mm)

$$\varepsilon_t = \frac{\Delta L}{L_0}\%$$

$\varepsilon_t$ = tensile strain (%)
L = increase of gripping distance (mm)
$L_o$ = initial gripping distance (mm)

The modulus values are calculated from the stress values ($\sigma_1$ and $\sigma_2$) corresponding to two strains, $\varepsilon_1$ = 0.05% and $\varepsilon_2$ = 0.25 %. Formula 6 shows the calculation of the moduli.

*Formula 6: Flexural (left) and tensile (right) modulus calculation.*

$$E_f = \frac{\sigma_{f2} - \sigma_{f1}}{\varepsilon_{f2} - \varepsilon_{f1}}$$

$E_f$ = flexural modulus (MPa)
$\sigma_{f1}$ = flexural stress corresponding to $\varepsilon_{f1}$ (MPa)
$\sigma_{f2}$ = flexural stress corresponding to $\varepsilon_{f2}$ (MPa)
$\varepsilon_{f1}$ = flexural strain 1 (%)
$\varepsilon_{f2}$ = flexural strain 2 (%)

$$E_t = \frac{\sigma_{t2} - \sigma_{t1}}{\varepsilon_{t2} - \varepsilon_{t1}}$$

$E_t$ = tensile modulus (MPa)
$\sigma_{t1}$ = tensile stress corresponding to $\varepsilon_{t1}$ (MPa)
$\sigma_{t2}$ = tensile stress corresponding to $\varepsilon_{t2}$ (MPa)
$\varepsilon_{t1}$ = tensile strain 1 (%)
$\varepsilon_{t2}$ = tensile strain 2 (%)

Furthermore, the 0.2% yield strength for each sample was determined by finding the intersection between the stress-strain curve and the flexural modulus slope with a 0.2% offset. Additionally, the ultimate flexural and tensile strengths were determined by finding the maximum stress values. Data calculations were performed in Microsoft Excel (Microsoft, Redmond, WA, USA) and MATLAB R2020a (The MathWorks Inc., Natick, MA, USA).

### Statistical analysis

For each parameter, per material, the mean value was calculated with its 95% confidence interval (95%-CI). To determine if the mean values differed significantly, a one-way Analysis of Variance (ANOVA) was performed. A Tukey post hoc test was performed as well to determine which materials differed significantly. During statistical analysis, a significance level of $\alpha = 0.05$ was used. Statistical analysis was performed with SPSS Statistics Version 25 (IBM, Armonk, NY, USA).

Lastly, the material parameters were ranked from 1 to 6, corresponding to from least favorable to most favorable value for use of the material for 3D printed wrist casts. For the calculated parameters, the highest value was always the most favorable. When no significant difference could be found between materials, the ranking was adjusted to 1 to 5, 1 to 4 and so on. An additional point was added when a material has favorable material characteristics, such as color choices, printability, surface finish, adhesion between layers, failure mechanism, printing time and costs. When a material characteristic would be unfavorable, one point was subtracted. If a parameter was not applicable, not available or impartial, a score of 0 was granted. The highest scoring material was chosen to use as the material for the 3D printed wrist casts.

## Results

### Test samples

The SolidWorks sample designs with the specific dimensions for the flexural tests and tensile tests are shown in Figure 21 and Figure 22 respectively.

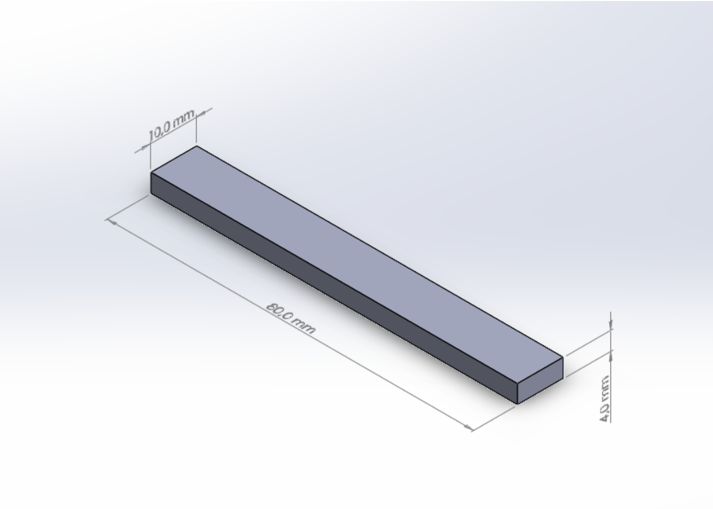


***Figure 21***: *Flexural test sample design and dimensions.*

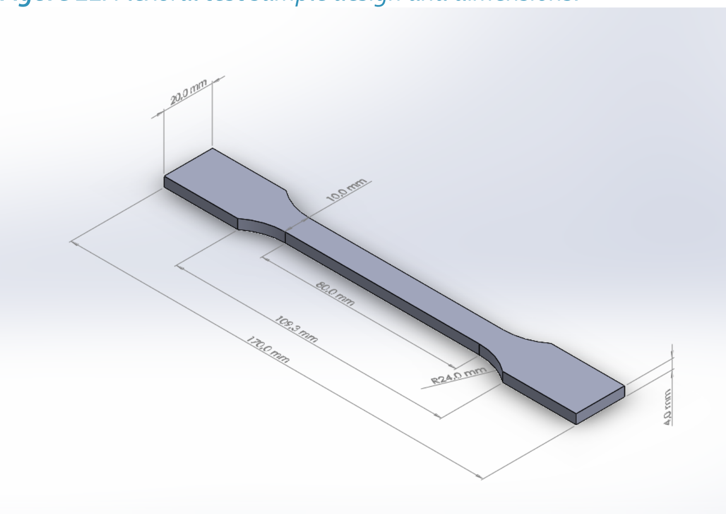


***Figure 22***: *Tensile test sample design and dimensions.*

Figure 23 and Figure 24 show the orientation of the samples on the build platform for the FDM and SLA samples respectively.

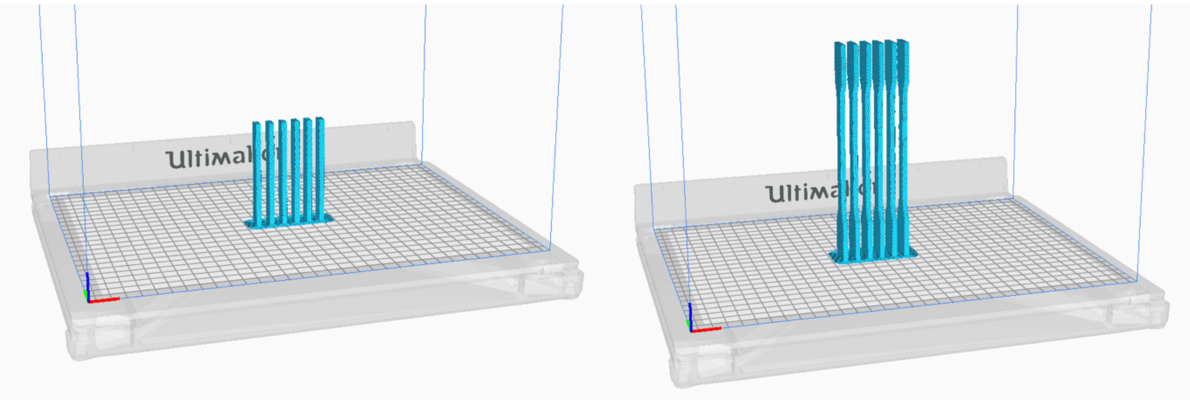

***Figure 23***: *Flexural (left) and tensile (right) test samples prepared for printing in Ultimaker Cura.*

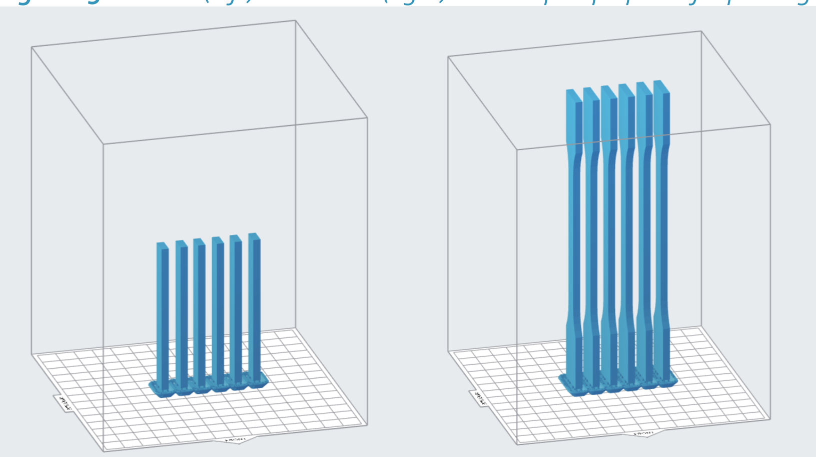

***Figure 24***: *Flexural (left) and tensile (right) test samples prepared for printing in PreForm.*

The final samples, after printing and post-processing, are shown in Figure 25. All printed samples were in compliance with the dimensional requirements.

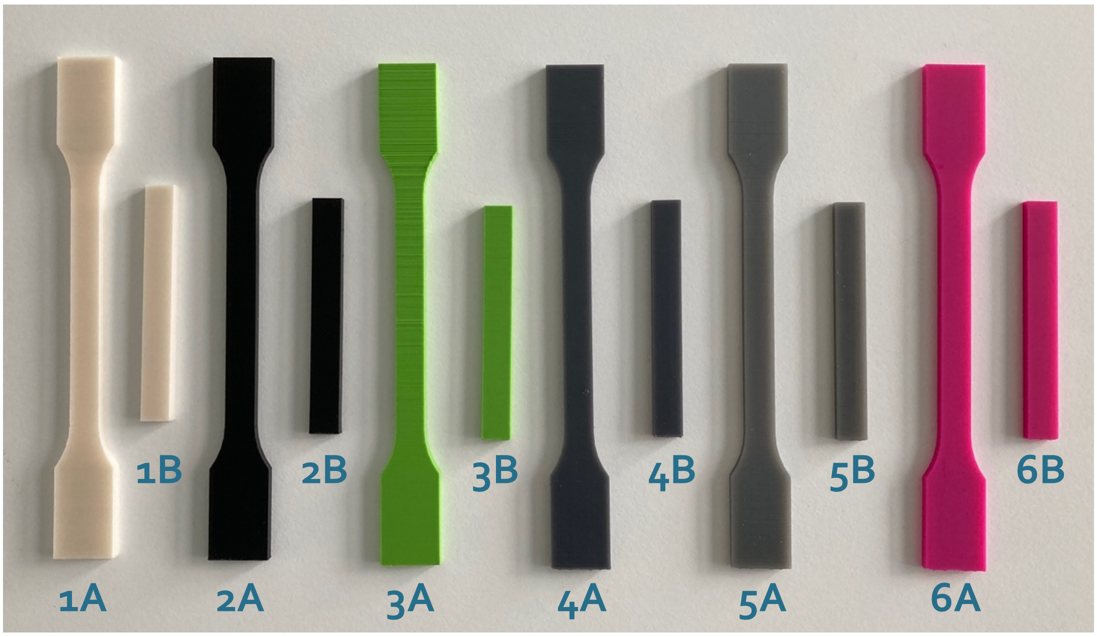


***Figure 25***: *Test samples (1 = PLA, 2 = Tough PLA, 3 = ABS, 4 = Tough 2000, 5 = Draft, 6 = Color, A = tensile samples, B = flexural samples).*

## Data collection

The fracture patterns of the samples differed between the FDM samples and the SLA samples. FDM samples showed delamination for both tests for all samples. The SLA tensile samples all showed shattering, as well as the color and draft flexural samples. However, the tough 2000 flexural samples did not break and only showed permanent bending as a deformation result. The samples after testing are shown in Figure 26.


***Figure 26**: Test samples after testing (1 = PLA, 2 = Tough PLA, 3 = ABS, 4 = Tough 2000, 5 = Draft, 6 = Color, A = tensile samples, B = flexural samples).*

The stress-strain curves are presented in Appendix I and Appendix II for the flexural and tensile testing respectively. The mean values for the moduli, ultimate strengths and 0.2% yield strengths, with the 95%-CI's are presented in Table. For ABS (both flexural and tensile), PLA (both flexural and tensile) and tough PLA (tensile), the 0.2% yield point could not be determined, since the tests failed before reaching the 0.2% yield point.

## Statistical analysis

For the moduli and ultimate strengths, the one-way ANOVA showed a significant difference between the material groups (p = 0.000). Post hoc testing showed that no significant difference was present between ABS and tough 2000 (p = 0.762), as well as between color and draft (p = 0.248) for the flexural modulus. ABS, draft and tough 2000 did not differ significantly for the tensile modulus (p = 0.325). For the ultimate flexural strength, only no significant difference was observed between tough 2000 and tough PLA (p = 0.901). Tough PLA and PLA were the only materials that did not differ significantly from each other based on the ultimate tensile strength (p = 0.458). All materials that were not mentioned above, differed significantly from each other for all parameters.

One-way ANOVA with the materials, for which the 0.2% yield flexural strength could be determined (i.e. tough PLA, color, draft and tough 2000) , showed a significant difference between the material groups (p = 0.000). Only draft and tough PLA did not differ significantly from each other (p =0.233). For the 0.2% yield tensile strength, the one-way ANOVA was performed for color, draft and tough 2000, however, no significant difference was found between the groups (p =0.051).

***Table 9**: Mean modulus, ultimate strength and 0.2% yield strength for flexural and tensile testing.*

| Material | | Flexural modulus (MPa) | Tensile (Young's) modulus (MPa) | Ultimate flexural strength (MPa) | Ultimate tensile strength (MPa) | 0.2% Yield flexural strength (MPa) | 0.2% Yield tensile strength (MPa) |
|---|---|---|---|---|---|---|---|
| ABS | *Mean* | 1961.6 | 1961.7 | 28.6 | 14.1 | N/A* | N/A* |
| | *[95%-CI]* | [1875.6 – 2047.7] | [1875.6 – 2047.8] | [24.3 – 32.8] | [12.9 – 15.3] | | |
| PLA | *Mean* | 3636.2 | 3378.7 | 72.6 | 34.1 | N/A* | N/A* |
| | *[95%-CI]* | [3597.3 – 3675.2] | [3360.6 – 3396.7] | [68.0 – 77.1] | [33.4 – 34.9] | | |
| Tough PLA | *Mean* | 2802.6 | 2705.4 | 67.0 | 32.9 | 61.1 | N/A* |
| | *[95%-CI]* | [2721.4 – 2883.9] | [2683.5 – 2727.3] | [61.9 – 72.1] | 30.5 – 35.4] | [59.1 – 63.1] | |
| Color | *Mean* | 2390.9 | 2468.7 | 82.4 | 49.3 | 50.8 | 26.4 |
| | *[95%-CI]* | [2327.3 – 2454.6] | [2454.2 – 2483.2] | [81.9 – 82.9] | [48.5 – 50.1] | [49.3 – 52.3] | [25.8 – 26.9] |
| Draft | *Mean* | 2488.1 | 2015.2 | 88.9 | 44.2 | 57.5 | 20.7 |
| | *[95%-CI]* | [2404.0 – 2572.2] | [1886.6 – 2143.8] | [86.3 – 91.6] | [43.0 – 45.3] | [52.0 – 62.9] | [13.6 – 27.9] |
| Tough 2000 | *Mean* | 1904.2 | 2031.6 | 65.1 | 27.1 | 37.1 | 22.2 |
| | *[95%-CI]* | [1777.3 – 2031.1] | [2001.7 – 2061.5] | [64.4 – 65.9] | [26.8 – 27.5] | [33.1 – 41.2] | [21.5 – 22.9] |

*N/A = not available, because test failed before 0.2% yield point.

The ranking of the material parameters is shown in Table 10. Color resin for the Formlabs SLA printers achieved the highest score and was therefore selected to be the material for production of the 3D printed wrist casts.

***Table 10**: Ranking of the material parameters and characteristics.*

| Parameter/Characteristic | ABS | PLA | Tough PLA | Color | Draft | Tough 2000 |
|---|---|---|---|---|---|---|
| Flexural modulus | 1 | 4 | 3 | 2 | 2 | 1 |
| Tensile modulus | 1 | 4 | 3 | 2 | 1 | 1 |
| Ultimate flexural strength | 1 | 3 | 3 | 5 | 4 | 2 |
| Ultimate tensile strength | 1 | 3 | 2 | 4 | 5 | 2 |
| 0.2% Yield flexural strength | 0 | 0 | 3 | 2 | 3 | 1 |
| 0.2% Yield tensile strength | 0 | 0 | 0 | 1 | 1 | 1 |
| Printability | -1 | 0 | 0 | +1 | -1 | +1 |
| Color choices | +1 | +1 | +1 | +1 | 0 | 0 |
| Surface finish | 0 | 0 | 0 | +1 | -1 | +1 |
| Adhesion between layers | -1 | 0 | 0 | +1 | +1 | +1 |
| Failure mechanism | 0 | 0 | 0 | -1 | -1 | +1 |
| Printing time | 0 | 0 | 0 | 0 | +1 | 0 |
| Costs | +1 | +1 | +1 | -1 | -1 | -1 |
| **Total** | **4** | **16** | **16** | **18** | **14** | **11** |

## Conclusion

Based on flexural and tensile material parameters, failure mechanism and additional material characteristics, such as costs, color choice and printing time, color resin for the Formlabs SLA printers is the most suitable material for the production of 3D printed wrist casts. The optimal printing technique is SLA, since the FDM printed materials failed before the 0.2%yield point was reached, making the behavior of the FDM printed materials too unpredictable.

# Design

## 3D scanning of the limb

The literature study concluded that 3D scanning should be the gold standard for digitalization of the injured limb, because of the lack of radiation, the portable character of the devices and short scanning times. Multiple 3D scanners are available, each with their own accuracy. For example, the SENSE scanner (3D SYSTEMS, Rock Hill, SC, USA) has an accuracy of 2.5 mm, while the EinScan H (SHINING 3D® Tech. Co., Hangzhou, China) has an accuracy of 0.05 mm. To ensure adequate fit and proportions of the casts, the basis, namely the 3D scan, should be as accurate as possible. A high quality 3D scanner is therefore required.

At the ETZ, an EinScan H 3D scanner was available for digitalization of the limb. The EinScan H is a handheld and lightweight 3D scanner, based on hybrid light emitting diode (LED) and infrared structured light, which is especially suitable for body scanning, since it has the ability to correct for small movements of the limb during scanning [93]. Scanning was performed in Body Scan mode, with the High Detail resolution setting. A scan of the forearm was made with the forearm positioned horizontally in the air, with the thumb pointing upward. The fingers were not spread and the wrist was positioned neutrally (slight dorsiflexion and no sideward deviation). A scan could then be made in appoxiamtely 30 seconds by moving the scanner around the arm at a working distance between 37 and 57 cm [94]. After the scan was completed, excess scanning areas, such as the shoulder and upper arm were removed from the point cloud. The collected point cloud was subsequently meshed as an unwatertight model. Finally, the mesh was exported as an STL. An example of a 3D scan of the forearm is shown in Figure 27.

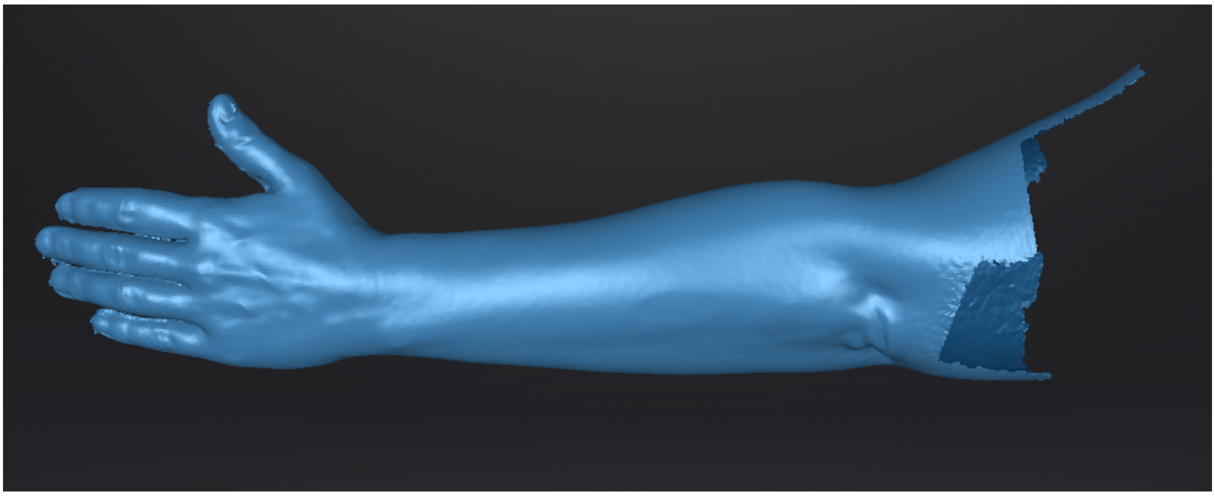

***Figure 27**: 3D model (STL) of a forearm, scanned with the EinScan H.*

## Design algorithm

Based on the 3D model of the arm, casts could be created. The steps of the semi-automated design algorithm are described below.

### Preparation of the arm model

Before a cast could be created, the 3D scan of the arm needed to be edited in Meshmixer® (AutoDesk, Inc., San Rafael, USA) to obtain the desired base surface for the cast. Firstly, the 3D model was loaded into Meshmixer and the fingers and thumb were cut off using the *Plane Cut* function with the *No Fill* option. Also, the arm was trimmed to the desired length of the cast using the same function. To allow for some swelling and prevent excessive tightness of the cast, a small offset of 0.5 mm in the normal direction was put in place, by selecting the trimmed surface and using the *Offset* function. Finally, the remaining surface was split into two parts, a radial and an ulnar part respectively, using the *Split* function. Both parts were saved separately as a STL file. The steps in Meshmixer are visualized in Figure 28.

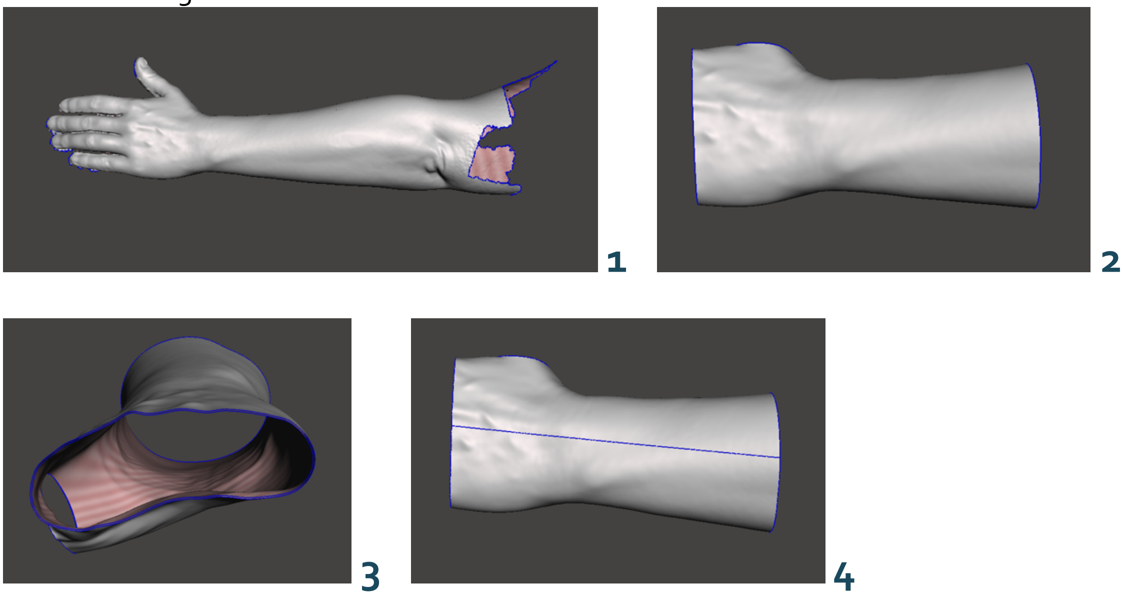


*Figure 28: Meshmixer design steps (1 = loaded 3D scan of the arm, 2 = trimmed surface, 3 = offset surface, 4 = split surface).*

## Cast creation algorithm

A semi-automated algorithm for the creation of the cast was designed in Rhino 6 (Rhinoceros, Seattle, WA, USA) with addition of the the RhinoResurf (Trunhoo Network Technology, Nanjing, Jiangsu, China), Grasshopper and Grasshopper LunchBox plugins.

The scanned data is a point cloud, which is a collection of points in space, where each point has its own X, Y and Z coordinate and the collection of points represent a 3D model. A mesh is a surface representation where each three close points form a triangle with a normal direction. A mesh is thus composed of points/vertices, lines/edges and polygons/faces as represented in Figure 29 [95]. Both point clouds and meshes are simply a representation of a model in space. However, to create a pattern onto the base surface, the surface needs to be represented mathematically as a non-uniform rational basis spline (B-spline) (NURBS) model [96].

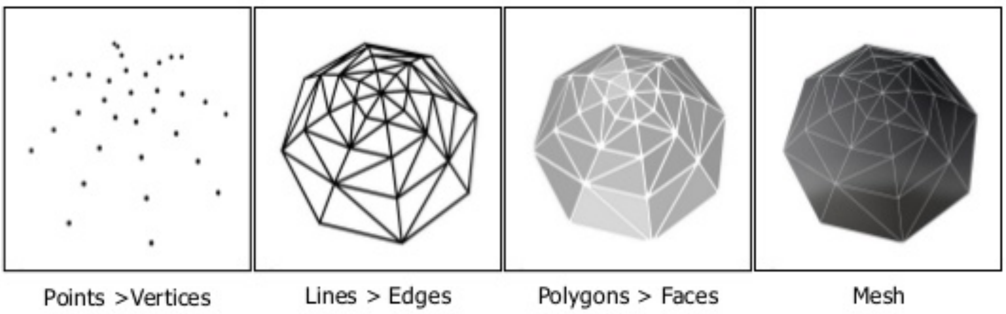


*Figure 29: Mesh elements [95].*

The first step in the semi-automated algorithm, after importing both parts into Rhino, was thus to convert the meshes into single NURBS surfaces. The *RsMesh2Surf* function from the RhinoResurf plugin was used for this. *Shape* was set to 4 corner and the corners of the mesh parts were selected. To prevent big deviations from the original mesh, *Max Tol* was set to 0.01 and *Trim* was enabled. The second step was to create a UV curve that shows the dimensions of the NURBS surfaces, that can be used for the pattern generation. For this, the *CreateUVCrv* function was used. The length and width of the UV curves were measured with the *Distance* command and the area was calculated using the *Area* command. The NURBS surfaces and the UV curves were used as input for the cast algorithm. An algorithm was created to design casts with round holes and a second algorithm was created for Voronoi pattern casts. These patterns were most frequently used in literature and were therefore selected as patterns. Mathematically, Voronoi patterns are considered to be stable patterns, because edges of the Voronoi cells are always placed exactly in the middle between two center points [96]. The algorithms were created in Grasshopper and are shown in Figure 30.

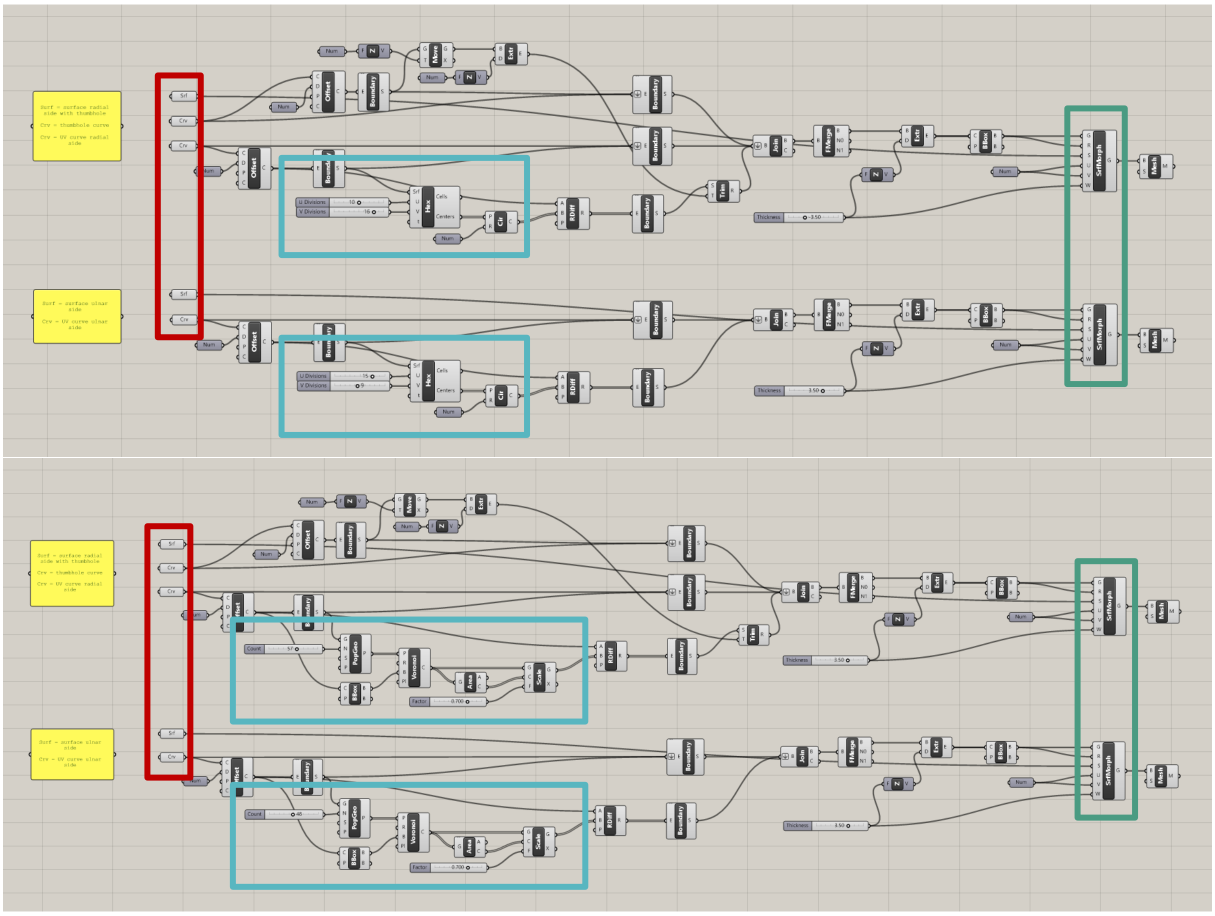

***Figure 30**: Grasshopper cast algorithm for casts with round holes (upper) and Voronoi casts (lower), the red frameworks indicate the inputs, the blue frameworks indicate the pattern creation and the green frameworks indicate the surface morphing.*

The Grasshopper algorithm works as follows. On the left side, the radial and ulnar NURBS surfaces, together with the UV curves and the curve for the thumbhole are set as inputs. The algorithm then populates the UV curves with either a hexagonal grid (circles) or randomly generated points (Voronoi). For the circular pattern, the number of grid cells is determined by the length and width of the UV curve. Per 12 mm a grid cell is added. The centers of the grid cells are used as the center for the circles, that have a set a radius of 6 mm. The random points are used as midpoints for the Voronoi cells, which are scaled with a factor 0.70 to ensure the ribs between the cells have a width of around 5 mm. The number of Voronoi cells is determined based on the area of the UV curve. For every 400 mm$^2$, a cell is added. Also, an offset of 5 mm is created at the border of the UV curve and around the thumbhole for extra solidity. The offset borders and patterns are then combined, so a 2D pattern is created with the correct dimensions. Next, this 2D pattern is morphed to the 3D NURBS surface with a thickness of 3.50 mm, which is similar to the thickness of a plaster cast. Finally, the patterned cast parts are converted into meshes again. The algorithm steps are visualized in Figure 31.

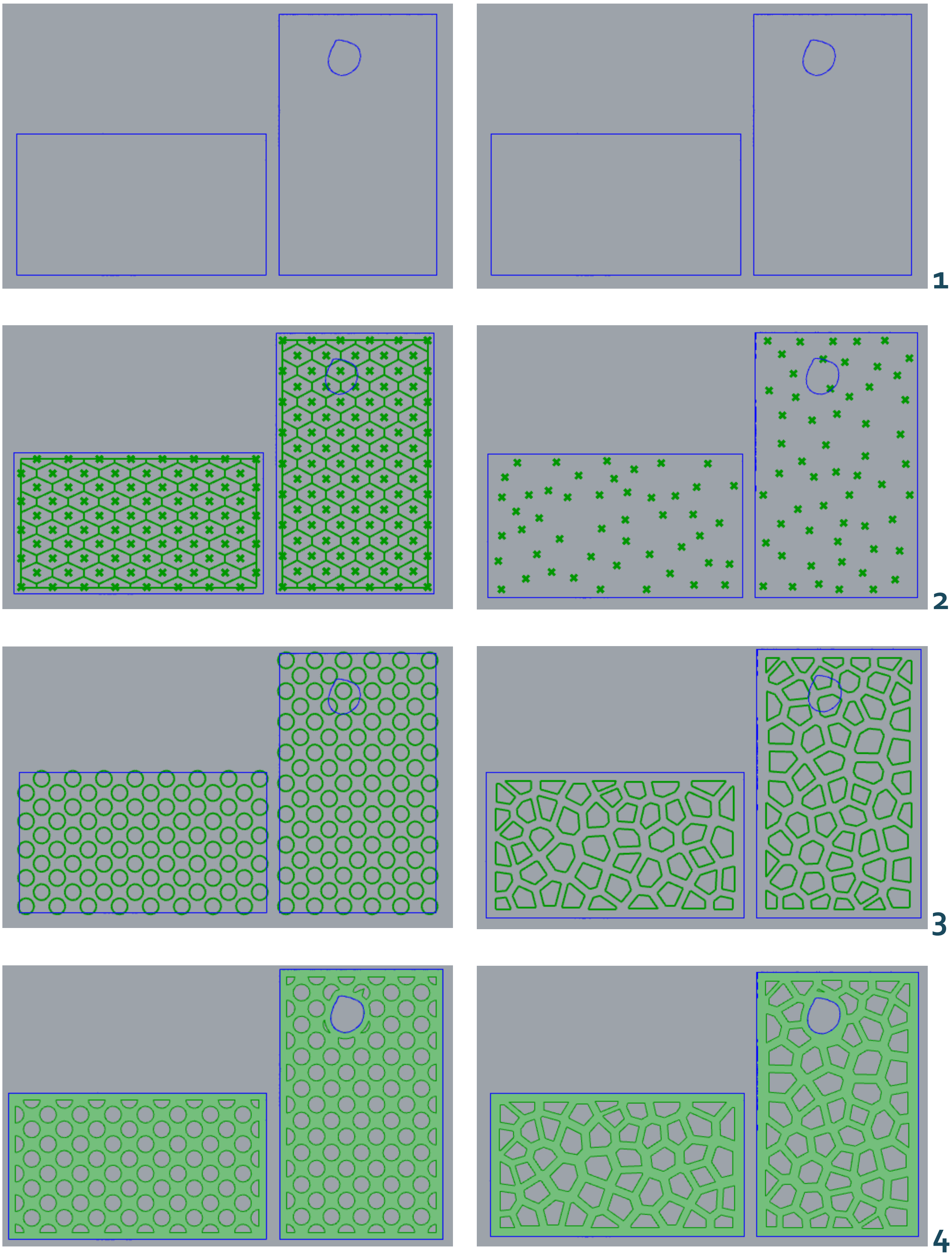
1
2
3
4

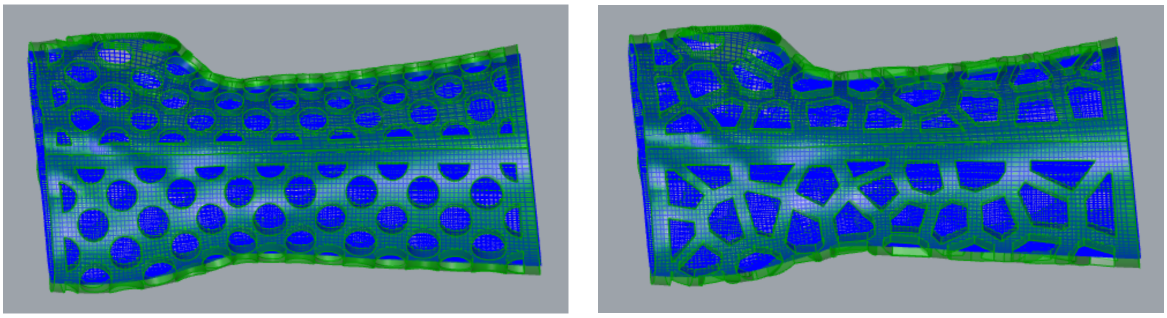

5

*Figure 31: Algorithm steps for the circular cast (left) and Voronoi cast (right) (1 = input UV curves, 2 = population of UV area, 3 = pattern generation, 4 = 2D surface pattern with offset borders, 5 = 3D surface morphing).*

Manually, only the inputs needed to be set and after the algorithm finished calculating, the meshes needed to be baked with the *Bake* function. Lastly, the cast parts were exported as STL files.

### Addition of the closing mechanism

The two cast parts should be held together with Velcro straps. However, to ensure these straps stay in place, arcs needed to be added to the cast parts. Arcs were designed in TINKERCAD® (AutoDesk, Inc., San Rafael, USA). The dimensions of the arcs are 3.0×32.0×4.5 mm and the slit for the Velcro straps is 20.0×2.5 mm. The design is shown in Figure 32. The arcs were place manually onto the casts in Meshmixer at the proximal end of the cast and at the wrist area. In total, eight arcs were placed on the cast and a single mesh was created for the ulnar part and the radial by using the *Combine* function. Figure 33 shows the arcs combined with the cast. The ulnar cast part and the radial cast part were then exported as STL files for printing.

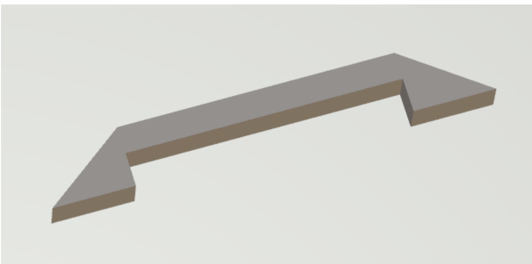

*Figure 32: Arcs for the closing system.*

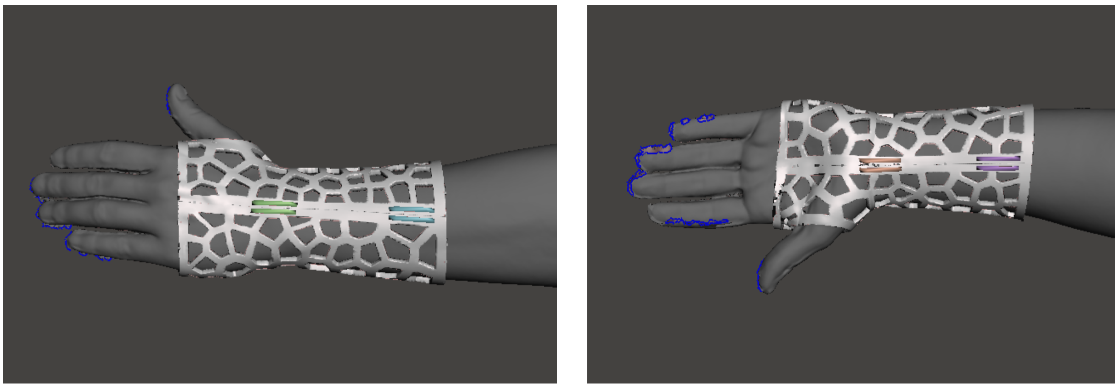

*Figure 33: Arcs attached to a Voronoi cast in Meshmixer.*

## 3D printing

For printing, the two cast parts were loaded into PreForm for support addition and slicing. The cast parts were oriented with the distal part upward and with a slight tilt so the inner surface was facing upward as well. This was done, so no support needed to be placed at the distal border, creating a smooth surface inside the palm of the hand and at the inside of the cast. Support was automatically generated with default PreForm settings. The layer thickness was set to 100 microns and the material was set to color resin. Finally, the print was uploaded to the printer and 3D printed in around 12 to 20 hours. After printing, the cast was washed in IPA for 10 min and then cured for 60 min at 60°C. Subsequently, the support was removed with a support removal tool and the remaining support tips were smoothed with fine sandpaper (3M P320 Wetordry Tri-M-ite, 3M, Delft, Nederland). Also the edges and corners of the cast were sanded for a smooth surface finish. Lastly, the Velcro straps (GM902, GeniMedical, Houten, Netherlands) were added. The orientation of the cast parts inside the build volume in PreForm and the final post-processed print with the attaches Velcro straps are shown in Figure 34. The final weight of a 3D printed cast, that was made according to this algorithm is approximately 100 grams.

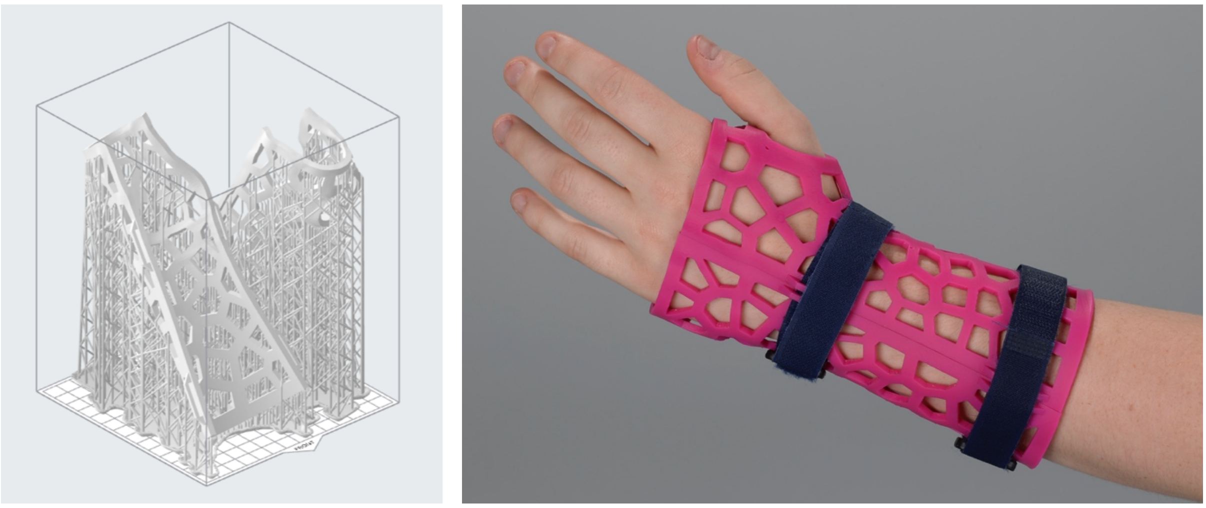

***Figure 34**: Cast orientation in PreForm (left) and final 3D printed wrist cast (right).*

## Workflow

The total workflow, from 3D scanning to the final print that is ready to be fit to the patient, can be performed within 24 hours. The workflow, with time costs per step, is shown in Figure 35.

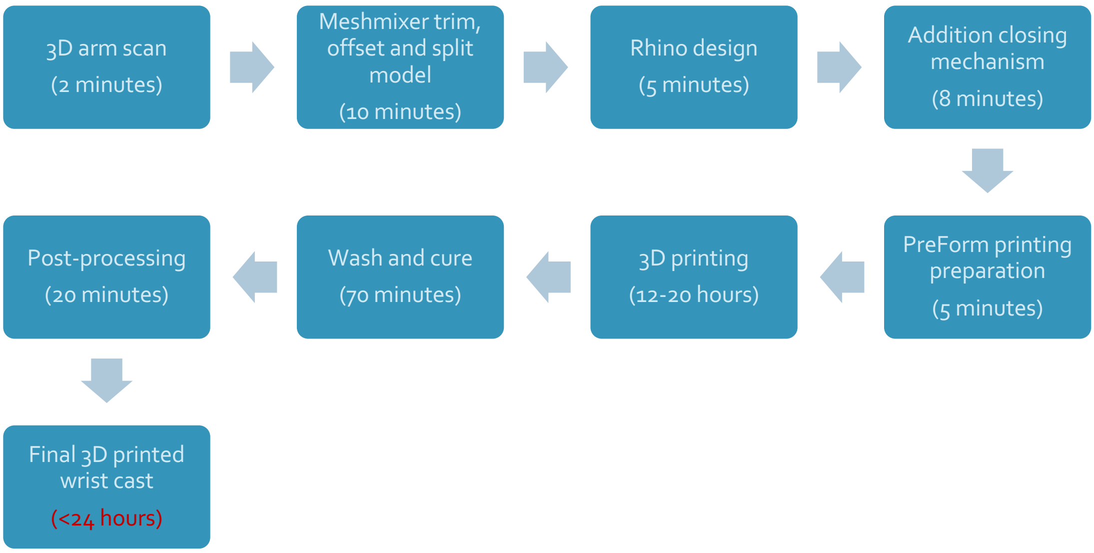


***Figure 35**:Workflow for the creation of 3D printed wrist casts with time cost per step.*

# Mechanical phantom study

## Introduction

To prove that the designed cast can be implemented clinically, it is important to demonstrate that the 3D printed wrist cast has similar stabilization abilities as traditional plaster casting. Therefore, the casts need to be able to withstand forces generated by the wrist from the inside, without major displacement or deformation of the cast. Standard mechanical testing, using a 3-point bending set-up for example, does not take the soft tissue displacement into account. To determine the stabilization abilities, a simulation should be performed which approaches the reality as close as possible. A phantom study is therefore implied.

Also, the literature study indicated that there is no consensus on the ventilation holes design pattern. The two patterns that are mostly described in literature are round holes and organic shaped/Voronoi holes. Both patterns need to be compared to determine which pattern is most suitable for the use in 3d printed wrist casts.

The goal of this mechanical phantom study is to prove noninferiority for the stabilization abilities of the 3D printed wrist cast compared to traditional plaster casting. Furthermore, the goal is to determine the optimal design pattern, by comparing casts with either round holes or a Voronoi pattern as ventilation holes design.

## Materials and methods

### Phantom design

A phantom arm was created to simulate the movements of a real life wrist. The phantom was created out of silicone with a universal joint placed inside, acting as the wrist joint.

First, a mold of a forearm was made by mixing 1 kg of alginate powder (Resion Resin Technology SR-AG1, Polyestershoppen BV, Moordrecht, Netherlands) with 3 L of water with a concrete mixing tool. This mixture was poured into a tall glass vase and the hand was placed inside the alginate mixture in a neutral position. After 10 minutes, the alginate was set and the hand was removed from the mold. This process was performed at room temperature (20°C).

Secondly, the coupling was created by fixating both a 150 mm lengthening piece and a 250 mm lengthening piece in the universal joint with bolts. The longest rod was tunneled and tapped twice, with the two tunnels perpendicular to each other. Two small threaded rods were placed inside these tunnels, sticking out at both ends to prevent the coupling from rotating inside the silicone. The 150 mm rod was cut to a length of 90 mm to fit into the hand part of the mold, so the coupling could be placed at the wrist joint position. The remaining part was tunneled and tapped 20 mm and 30 mm from the distal end, with the two tunnels perpendicular to each other again. A 20 mm threaded rod was placed in the distal tunnel and a 40 mm threaded rod was placed in the proximal tunnel. 10 mm nuts were connected to the ends of the rods. At the open sides of the nuts, hooks could be attached, so forces could be applied as if they were generated by the wrist. The coupling is shown in Figure 36.

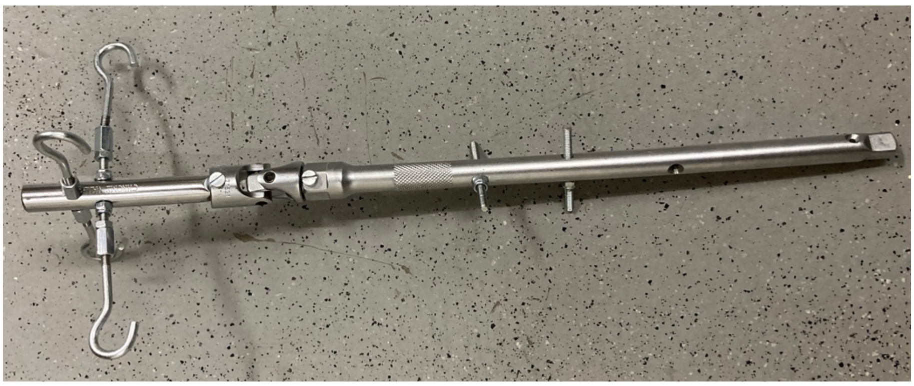

***Figure 36**: The coupling for the phantom arm.*

Finally, the coupling was positioned at the correct position into the mold and hung from a wire. From both silicone components (Resion Resin Technology silicone cast rubber 1:1 (shore 10), Polyestershoppen BV, Moordrecht, Netherland) A and B, 600 gr was weighed and mixed together with a spatula for 5 minutes, to ensure proper mixing. The mold, with the coupling placed in the correct position, was then filled with the silicone mixture. This process was also performed at room temperature (20°C). The filled mold was set overnight, for a duration of 12 hours. Subsequently, the alginate mold was removed from around the silicone phantom and the hooks were attached to the phantom. The phantom is shown in Figure 37.

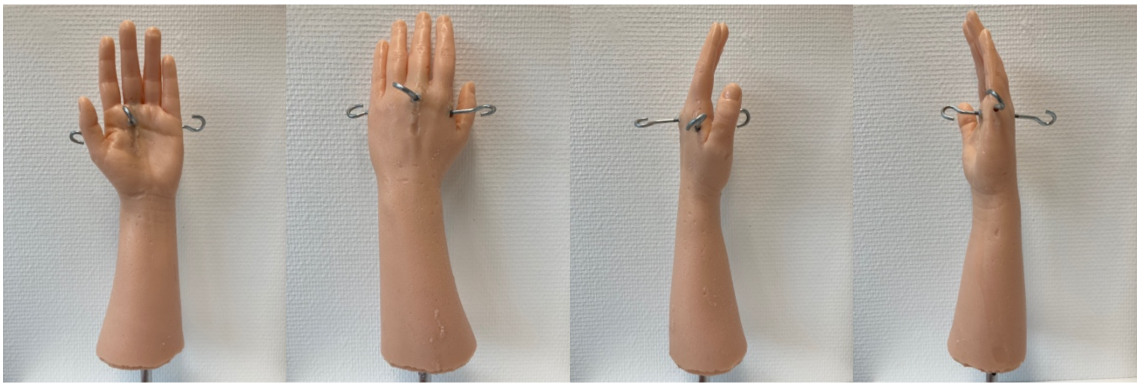

***Figure 37***: *The phantom arm.*

### Wrist casts printing and plastering

The phantom arm was first scanned with the EinScan H 3D scanner. Based on the 3D scan, one cast was designed, according to the workflow described in the previous section, with a circular ventilation pattern (UV dimensions radius: 11×15, UV dimensions ulna: 15×10) and one cast was designed with a Voronoi ventilation pattern (60 holes radius, 48 holes ulna). A small extra recess was trimmed to fit the loading hook at the radial side of the cast.

Both designs were printed thrice. The circular pattern casts were printed with the Form 3 (Formlabs Inc., Somerville, MA, USA) with color resin (cyan colored) and the Voronoi casts were printed with the Form 2 with color resin (lime colored).

For the tests with plaster casting, a plaster cast was created around the phantom arm. The cast was 3 layers thick and made from polyester cast tape with a width of 5 cm (BSN medical Inc., Charlotte, NC, USA). The plaster dried for at least 12 hours between application and testing. An elastic bandage (DIN 61632, BSN medical GmbH, Hamburg, Germany) was placed underneath the plaster for protection of the phantom. In total, three plaster casts were formed around the phantom arm.

To be able to measure the deformation of the casts and plaster under loading, Kirschner wires (k-wires) with a cross-section of 1.6 mm and a length of 150 mm (DePuy Synthes GmbH, Oberdorf, Switzerland) were cut to a length of 45 mm and attached to the palmar side, dorsal side, radial side and ulnar side of the casts/plaster with superglue.

### Test set-up

A test set-up was built at the operation room. On a weighed down table, a vise was placed and secured with a belt. Two arm holders were 3D printed to make sure the phantom arm was supported sufficiently, once it was placed horizontally in the vise. One arm holder was suitable for flexion and extension loading, while the other holder was suitable for radial and ulnar loading. The table was placed between a horizontally oriented Philips Pulsera NZS 60 C-arc (Philips Medical Systems International BV, Best, Netherlands) for X-ray screening of the coupling in the phantom arm under loading. The height of the C-arc was set to 27 cm for flexion and extension tests. For radial deviation tests, the height was set to 25.5 cm and for ulnar deviation to 27.5 cm. The test set-up is demonstrated in Figure 38.


***Figure 38**: Test set-up for the mechanical phantom loading tests.*

### Data collection

To make sure the cast is suitable for clinical use, a safety margin should be put in place with consideration of the forces the cast should be able to withstand. Delp et al. investigated the isometric moments that healthy males can generate with their dominant wrist in the four main directions: flexion, extension, radial deviation and ulnar deviation [97]. Application of loading forces, corresponding with the maximum moments in Delp et al. should provide the requested safety margin for the use in unhealthy (and pediatric) patients. Loading masses were calculated according to Formula 7 and were rounded up to whole kilograms. For flexion and extension, the moment arm was 0.08 m. For radial and ulnar deviation, the moment arm was 0.07 m.

***Formula 7**: Calculation of loading mass from isometric moment.*

$$m = \frac{M}{9.81r}$$

m = loading mass (kg)
M = isometric moment (Nm)
r = moment arm (m)

Loading weights of 1.0, 2.0, 3.0, 4.0 and 10.0 kg were created to be able to create all necessary loading masses. Per cast, an X-ray was made before loading. Subsequently, the casts were loaded in the four directions (flexion, extension, radial deviation and ulnar deviation), by hanging weights onto the hook that was pointing to the ground. Loading was done in steps of 1.0 kg until the mean loading mass was reached. For each loading step, an X-ray was made. Additionally, one X-ray was made when the maximum loading mass was hung from the hook. A final X-ray was made after unloading of the arm, to check for any plastic deformation of the cast. This process was done for every cast, so it was performed nine times in total (three plaster casts, three circular pattern casts and three Voronoi pattern casts). Also, loading was performed in steps of 1.0 kg up to 10.0 kg for the arm without any cast. Here also, an X-ray was made prior to loading and after loading.

For every X-ray the angle was measured with a goniometer (BASELINE ™, Fabrication Enterprises Inc, White Plains, NY, USA) and angular displacement compared to the X-ray before loading was determined. Also the distance between the k-wires perpendicular to the X-ray direction was determined for the unloaded, mean loading, maximum loading and after loading situation. The increase in distance compared to the unloaded situation was determined for the mean loading, maximum loading and after loading situation.

### Statistical analysis

For the mean loading, maximum loading and after loading situation the mean values for the angular displacement and displacement of the k-wires were calculated with the corresponding 95%-CI's for each loading direction. A one-way ANOVA was performed to determine if the angular displacements differed significantly between the cast types. In case of a significant difference, post hoc testing with a Tukey test was performed as well to determine which cast types differed significantly. During statistical analysis, a significance level of $\alpha = 0.01$ was used. Statistical analysis was performed with SPSS.

## Results

### Wrist casts printing and plastering

The printed wrist casts and the created plaster cast with the attached k-wires are shown in Figure 39.

*Figure 39: Circular pattern 3D printed cast (left), Voronoi pattern 3D printed cast (middle) and plaster cast (right) with k-wires.*

### Data collection

The maximum moments from Delp et al. [97] with the corresponding loading masses during the phantom study are shown in Table 11.

*Table 11: Wrist moments (Nm) and corresponding loading weights (kg) for testing.*

| Movement | Mean wrist moment (Nm) [range] | Mean loading mass (kg) | Maximum loading mass (kg) |
|---|---|---|---|
| Flexion | 12.2 [5.2 – 18.7] | 16 | 24 |
| Extension | 7.1 [3.9 – 9.4] | 10 | 12 |
| Radial deviation | 11.0 [7.9 – 15.3] | 17 | 23 |
| Ulnar deviation | 9.5 [5.9 – 11.9] | 14 | 18 |

### Statistical analysis

In total, 669 X-rays were made. For all X-rays the angle and angular displacement compared to the unloaded situation were determined. The graphs that show angular displacement under loading for the four different loading directions (flexion, extension , radial deviation and ulnar deviation) are presented in Appendix III. The mean angular displacements within the different cast types (with 95%-CI) under several loading conditions, compared to the unloaded situation, are shown in Table 12.

*Table 12: Mean angular displacement in different cast types under mean loading, maximum loading and after loading for flexion, extension, radial deviation and ulnar deviation.*

| Movement | | Angular deviation mean loading mass (°) [95%-CI] | Angular deviation maximum loading mass (°)[95%-CI] | Angular deviation after loading (°) [95%-CI] |
|---|---|---|---|---|
| Flexion | *Plaster* | 12.5 [9.2 – 15.7] | 15.3 [13.9 – 16.8] | 2.3 [0.9 – 3.8] |
| | *Circles* | 11.3 [10.6 – 12.1] | 14.8 [14.1 – 15.6] | 0.5 [0.5 – 0.5] |
| | *Voronoi* | 10.5 [10.5 – 10.5] | 14.7 [13.2 – 16.1] | 0.8 [0.1 – 1.6] |
| Extension | *Plaster* | 8.7 [6.7 – 10.6] | 10.0 [8.8 – 11.2] | 2.2 [0.3 –4.1] |
| | *Circles* | 10.3 [9.6 – 11.1] | 11.3 [10.6 –12.1] | 0.5 [-0.7 – 1.7] |
| | *Voronoi* | 10.5 [10.5 – 10.5] | 11.5 [10.3 – 12.7] | 0.7 [-0.1 – 1.4] |
| Radial deviation | *Plaster* | 8.0 [5.8 – 10.2] | 9.3 [6.7 – 11.9] | 2.3 [-0.3 – 4.9] |
| | *Circles* | 8.8 [6.9 – 10.7] | 10.5 [9.3 – 11.7] | 0.3 [-0.4 – 1.1] |
| | *Voronoi* | 9.3 [7.9 – 10.8] | 10.7 [10.0 -11.2] | 0.7 [-0.1 – 1.4] |
| Ulnar deviation | *Plaster* | 8.2 [7.5 – 8.9] | 9.7 [8.2 – 11.1] | 1.5 [0.3 – 2.7] |
| | *Circles* | 9.0 [7.7 – 10.2] | 10.7 [10.0 – 11.3] | 0.2 [-0.6 – 0.9] |
| | *Voronoi* | 9.8 [9.1 – 10.6] | 11.0 [9.8 – 12.2] | 0.3 [-0.4 – 1.1] |

The one-way ANOVA showed no significant differences for angular displacement with the maximum loading masses. For the mean loading masses a significant difference was found between the plaster cast and Voronoi cast (p = 0.002 and p = 0.007) for flexion and ulnar deviation. For flexion, the angular displacement was significantly less than the plaster cast, while for ulnar deviation the displacement was larger. For flexion under mean loading mass, a significant difference was also shown between the Voronoi cast and the cast with circular ventilation holes (p = 0.002). The Voronoi cast is more stable than the plaster and circularly patterned cast in flexion. However, compared to plaster it is slightly less stable in ulnar deviation. Furthermore, no other significant differences were found.

The one-way ANOVA showed significant differences for flexion and ulnar deviation between the plaster cast and the 3D printed casts for the angular deviation after loading. This might indicate that the plaster is plastically deformed after loading.

For flexion, a significant difference was also found between the displacement of the k-wires, before and after loading masses were applied (p = 0.000). This contributes to the validity of the hypothesis that plaster is deformed plastically after heavy loading.

## Conclusion

The stabilization abilities of the 3D printed casts are non-inferior to plaster casting, with a better performance for Voronoi casts in flexion and slightly worse performance for ulnar deviation under mean loading conditions. Since flexion is however the main movement of force generation because of grasping and gripping, the better performance of Voronoi casts for this direction is decisive. The stabilizing abilities of Voronoi casts are significantly better than the circular casts in flexion as well. 3D printed casts should therefore preferably be designed with a Voronoi pattern for the ventilation holes.

# Comfort study

## Introduction

Now that the desired stabilization abilities are met, the next step is to gather information on wear comfort and ease of use during daily activities, such as sleeping, taking a shower and buttoning a shirt. Also, possible complications should be clarified.

The theoretical advantages of 3D printed casts over plaster casting are lightness, being waterproof, ventilation abilities and personalization, but these have not yet proven to be beneficial in practice. Before clinical implementation is proceeded to, these advantages should be affirmed.

The goal of this comfort study is to gather information on the possible advantages and complications for wearing a 3D printed wrist cast in daily life. The most important parameter is the comfort of the cast.

## Methods

### Protocol

Ten volunteers were asked to wear a 3D printed wrist cast for the duration of 48 hours. They were requested to bathe or shower at least once with the cast in place and to sleep with the cast. After bathing, the cast was allowed to be taken off to dry the skin and the inside of the cast. Another option was to use a cold blow-dryer to dry the skin and cast. While driving a car, the cast was allowed to be taken off, due to insurance reasons. Also, when heavy duty or sports were performed, the volunteers were allowed to take off the cast. Volunteers were reminded that the device is intended for immobilization purposes, thus being able to perform burdensome activities with the cast in place was not the intention of the experiment. If the volunteers experienced any skin irritation, pressure sores or blisters, they were advised to take off the cast and stop the experiment. After 48 hours, the volunteers were asked to fill in a questionnaire about their experiences and recommendations. The information letter that was sent to the volunteers is added in Appendix IV. This letter was in Dutch.

The casts were created with a Voronoi pattern, according to the design workflow that was stated earlier. The casts were printed with either the Form 2 or Form 3 printer. Five of the volunteers received a 3D printed cast for their dominant hand and five volunteers received a cast for their non-dominant hand. Volunteers could give up a preference for the color of their cast, based on availability of tanks and resins.

### Questionnaire

A questionnaire was designed to map experiences on comfort and ease of use during daily activities. The questionnaire consisted of 13 questions that had to be scored according to a visual analog scale (VAS) score, 4 open questions and 1 multiple choice question. The VAS scored questions were about comfort, fit, sweating, itching, smell, pressure sores, skin irritation (swelling, discoloration, redness, blisters), maceration of the skin due to water contact, trouble with sleeping, ease of putting the cast on and off, immobilization qualities, ease of use during daily activities and looks. The open questions asked about advantages, disadvantages, possible improvements and other recommendations. The questionnaire was concluded with a multiple choice question where the preference for future treatment needed to be indicated between a 3D printed cast and a plaster cast. Also, general information was gathered, such as age, sex, dominant hand, the side where the cast was worn and if the person had ever been treated with traditional plaster before. The questionnaire was in Dutch and is presented in Appendix V.

### Analysis of the results

Descriptive statistics were performed with the use of SPSS Statistics Version 25, meaning that the population characteristics were determined, as well as the mean scores per VAS question, with the 95%-CI. The distribution of the scores was analyzed for notable data points. Also, independent T-tests were performed in SPSS to see if the scores were significantly different for people who wore the cast on their dominant hand versus people who wore the cast at their non-dominant hand. Finally, the results of the open questions were summarized and the scores of the multiple choice question was added to the population characteristics.

## Results

### Produced wrist casts

Figure 40 gives and overview of the wrist casts that were produced for this comfort study and their fit around the volunteers' arms. All volunteers had right-sided dominance, so five left-sided casts were produced and five right-sided casts were produced. All volunteers made it through the 48 hours, while no major complications were observed.

### Questionnaire

The population characteristics for this comfort study are presented in Table 13. Figure 41 shows the distribution of the scores per question and the mean scores per question are stated in Table 14, together with the 95%-CI and the range of scores.

***Table 13**: Population characteristics.*

| Population characteristics | | Mean | Range | Number (n) |
|---|---|---|---|---|
| Age (years) | | 34 | 23 to 58 | |
| Sex | *Male* | | | 5 |
| | *Female* | | | 5 |
| Dominant side | *Left* | | | 0 |
| | *Right* | | | 10 |
| Side of cast | *Left* | | | 5 |
| | *Right* | | | 5 |
| Earlier treatment with plaster | *Yes* | | | 3 |
| | *No* | | | 7 |
| Future desired treatment | *Plaster* | | | 0 |
| | *3D printed cast* | | | 9 |
| | *No choice* | | | 1 |

Overall, the scores for the VAS questions are satisfactory, with an ample sufficient score for the overall comfort of 8.1. Also, ease of putting the cast on and off, the fit, immobilization, itching, look, maceration of the skin after bathing, skin irritation, smell and sweating had favorable scores, with a maximum score difference of 1.9 from the perfect score. Most of these scores were distributed somewhat normally as well and ranged either within the under half of possible scores or within the upper half of possible scores.

One outstanding result was the trouble with sleeping, which was highly impacted by one score of 10. Furthermore, pressure sores were named more towards sometimes than never, with a score of 3.5 and widely varying scores were found for the possibility of performing daily activities, with a mean score of 7.2, meaning some people felt more limited by the cast then others.

The scores did not differ significantly for most questions between persons who wore the cast at the dominant hand and persons who wore the cast at the nondominant hand. Only, significant differences were found in itching, smell and maceration, with less optimal scoring for the left-bearing volunteers.

***Figure 40**: 3D printed wrist casts around the forearm of the ten volunteers, all volunteers had right-sided dominance.*

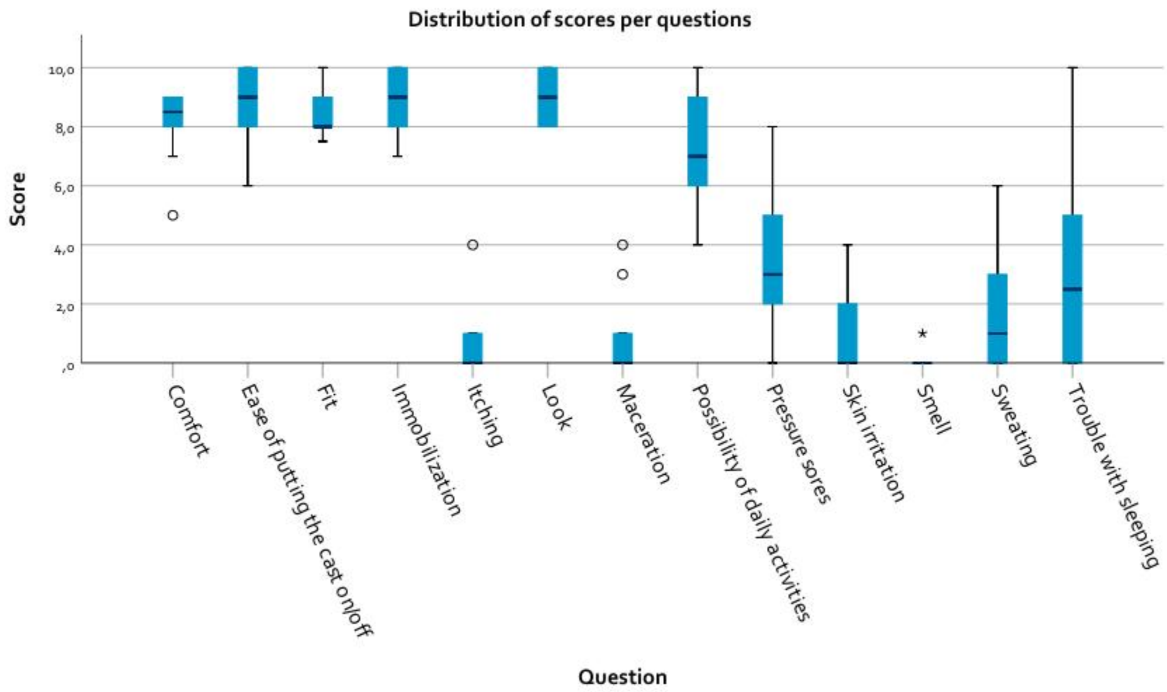


***Figure 41**: Distribution of scores per question.*

***Table 14**: Mean score, 95%-CI and range per VAS question.*

| Question | Mean score | 95%-CI | Range |
|---|---|---|---|
| Comfort | 8.1 | 7.2 – 9.0 | 5.0 – 9.0 |
| Ease of putting the cast on/off | 8.8 | 7.8 – 9.7 | 6.0 – 10.0 |
| Fit | 8.6 | 7.9 – 9.2 | 7.5 – 10.0 |
| Immobilization | 8.8 | 8.1 – 9.5 | 7.0 – 10.0 |
| Itching | 0.6 | 0.0 – 1.5 | 0.0 – 4.0 |
| Look | 9.0 | 8.3 – 9.7 | 8.0 – 10.0 |
| Maceration | 0.8 | 0.0 – 1.9 | 0.0 -4.0 |
| Possibility of daily activities | 7.2 | 5.7 – 8.5 | 4.0 – 10.0 |
| Pressure sores | 3.5 | 1.7 – 5.3 | 0.0 – 8.0 |
| Skin irritation | 1.1 | 0.0 – 2.2 | 0.0 – 4.0 |
| Smell | 0.1 | 0.0 – 0.3 | 0.0 – 1.0 |
| Sweating | 1.9 | 0.4 – 3.4 | 0.0 – 6.0 |
| Trouble with sleeping | 3.0 | 0.7 – 5.3 | 0.0 – 10.0 |

The named advantages, disadvantages and recommendations are summarized in Table 15, together with the number of mentions.

*Table 15: Advantages and disadvantages for 3D printed wrist casts (number of mentions).*

| Advantages | Disadvantages | Recommendations/ Improvements |
|---|---|---|
| Ventilation/Airy/Skin is able to breath (6) | Velcro straps get stuck in clothes/hair sometimes (5) | Change closing mechanism/Closing mechanism without Velcro straps (2) |
| Waterproof/Bathing possible (6) | Pressure sore at head of ulna (with activities) (3) | Prevent pressure sores at the head of the ulna/Improve fit at ulna head (2) |
| Hygienic feel (no sweat/heat/smell) (4) | Hard material (2) | Neutral colors |
| Lightweight (4) | Arm hair gets stuck between cast parts (2) | Recyclable material |
| Less itching than plaster/No itching (3) | Pressure points (at edges) (2) | Create possibility to adjust pressure points |
| Possibility to scratch through the holes (2) | Skin irritation at knuckles/thumb (1) | Smoother edges |
| Easy to use during daily activities (2) | Difficulty with grabbing small items (1) | Leave more room at the thumb base and around the thumb |
| Easy to put on/off (2) | Uneasy with sleeping (1) | |
| Self-removable(2) | Doesn't fit through sleeve of coat (1) | |
| Less maceration of the skin (1) | Production time (1) | |
| Look (1) | | |
| Nice to sleep with (2) | | |
| Comfortable (1) | | |
| Easy to clean (1) | | |
| Dressing still possible (1) | | |
| Less hot than plaster (1) | | |

The most comments for future improvements were made about the Velcro straps, that could sometimes stick to clothes or hair and to prevent pressure points, mainly at the head of the ulna. The Velcro straps can be cut to a shorter length, so no excess Velcro can stick to clothes or hair. The head of the ulna should be given special attention during the design of the wrist casts. Furthermore, the 3D printed wrist cast was described as a nice/top product, which is a real addition to current treatment possibilities.

An important final note is that all volunteers (apart from one, who stated that it was undecidable, since he had no experience with plaster) preferred the 3D printed wrist cast for possible future treatment. However, since most volunteers were never treated with a plaster cast, only the responses of the people who did, should be taken into account. Then still, a 3D cast is preferred.

## Conclusion

Overall, the comfort was ample sufficient with a score of 8.1. No major complications were reported, but improvements could be made to prevent pressure points. Also, by cutting the Velcro straps to the appropriate length, most problems with the straps getting stuck in clothes and hair should be resolved. All volunteers would prefer treatment with a 3D printed cast over plaster in case of a future wrist fracture.

# Pilot study

## Introduction

A 3D printed wrist cast, made from color resin with SLA 3D printing, with a Voronoi patterned design, has proven to feature adequate stabilization abilities and sufficient comfort and ease of use. To make sure the casts can be implemented for the treatment of distal radius fractures, the necessary workflow alterations need to be investigated, together with clinical outcomes and patient experiences. Therefore, a pilot study needs to be conducted.

Usually, a pilot study is performed with patients that are well instructable. This is to minimize the risk of complications, which means, often adults without co-morbidity are chosen as a research group. However, in the case of distal radius fractures, there is one group of fractures that is stable and is therefore a very suitable group for the first clinical implementation step, namely children with greenstick or buckle/torus fractures. A previous study showed that immobilization of these fractures is not always necessary and a pressure bandage is already sufficient for pain relief [29]. The stable character of these fractures minimizes risks of misalignment. Additionally, children also usually suffer less from swelling, which is described to be a challenge in previous studies [63].

Currently, the clinical workflow for the treatment of a child with a greenstick or buckle/torus fracture is as follows. A child comes to the ER, with suspicion of a distal radius fracture. An X-ray is made to rule out or confirm a fracture. When a greenstick or buckle/torus fracture is affirmed, depending on the time of arrival, the child receives some sort of cast. During working hours, a polyester cast is directly created by the plaster technicians, while during weekends and evening hours, an emergency lime plaster cast is formed around the wrist by the ER nurses. In this case, the child comes back the next working day to change to a polyester cast. This cast remains in place for 2 to 3 weeks, depending on the fracture type (2 weeks for buckle/torus fractures and 3 weeks for greenstick fractures). After this period, the child comes back to the hospital once more, to cleave the plaster. The current workflow is visualized in Figure 42.

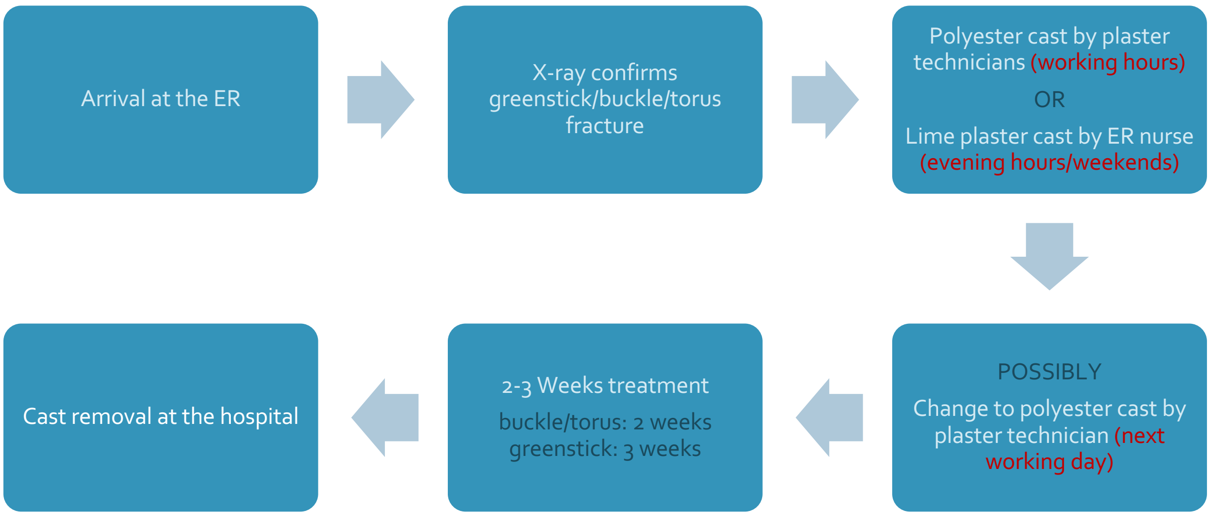


***Figure 42**: Current workflow for treatment of greenstick and buckle/torus fractures.*

This pilot study aims to formulate the necessary alterations that need to be made in the current workflow, as well as clinical outcomes and patient experiences. The goals is to prove feasibility of successful implementation of treatment of a pediatric wrist fracture with a personalized 3D printed wrist cast.

## Methods

### Inclusion

For this pilot study, a nonscientific medical research (non-WMO) statement was obtained from the medical ethics review committee (METC).

Pediatric patients of 4 to 15 years that presented themselves between the 26th of April 2021 and 7th of May 2021 at the ER of the ETZ with a greenstick or buckle/torus fracture were eligible for inclusion. Patients that were not able to communicate properly (address pain or discomfort) and patients with comorbidities were excluded for eligibility. The same goes for children and parents that did not master the Dutch language.

### Workflow

Patients that were eligible for inclusion presented themselves at the ER. After a greenstick or buckle/torus fracture was affirmed by an X-ray, informed consent was obtained from the child's parents and the forearm of the patients was scanned according to the design workflow. Subsequently, the patients received a lime plaster cast from the ER nurse and were sent home for two days. As soon as the scan was completed, a cast was designed according to the design algorithm. After two days, the patients came back to the hospital where the plaster was removed and changed for the 3D printed wrist cast. The patients received instructions for use (see Appendix VI) and were sent home for treatment with the 3D printed casts for two weeks. After two weeks, patients came back to the hospital and an evaluation of the wrist function was carried out. Also, both the parents and the child received a questionnaire on the experience during treatment. In case of adequate recovery, the patient was set free form the cast. In case of pain or reduced function of the wrist, the treatment was continued for another week. If, during treatment, any complications occurred, parents were instructed to contact the hospital and then another suitable form of treatment was offered. The new workflow is visualized in Figure 43.

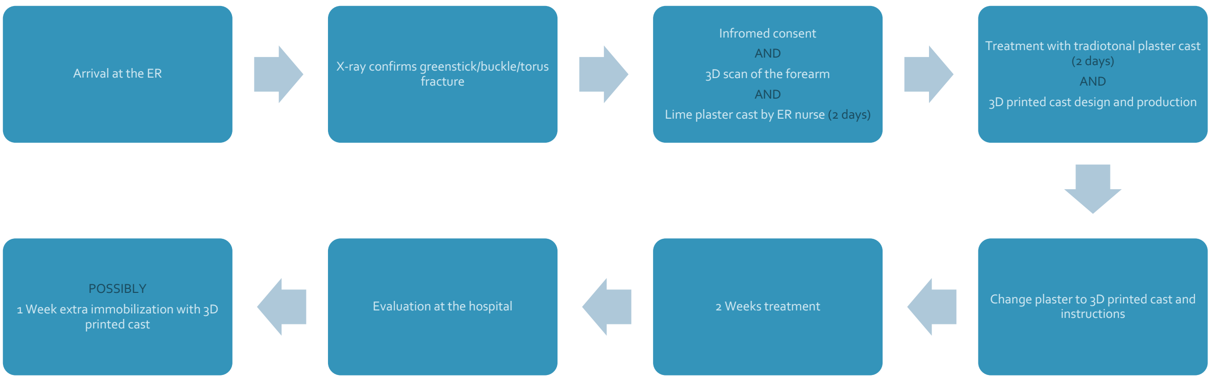


***Figure 43**: New workflow for treatment of greenstick and buckle/torus fractures.*

### Questionnaire

The questionnaires, for both the parents and children, covered the same topics as the questionnaire from the comfort study. The children's questionnaire was adjusted to fit the language level and visual needs of children, by creating a VAS score based on smileys, ranging from 1 (never/great) to 5 (often/bad). The children's questionnaire is presented in Appendix VII and the parent's questionnaire is presented in Appendix VIII. Both questionnaires were in Dutch.

Apart from the questionnaires, the total time of the design and production workflow was measured and the number of hospital visits was registered.

## Results

### Included patients

Eventually, 2 patients were included in this pilot study. One boy (7 years) and one girl (10 years). The patient characteristics are shown in Table 16, together with the questionnaire scores of both the child and the parents. Figure 44 shows the casts that were created with the Form 3 printer, fitted around the patients' arms. The blue boxes are to cover the patients' names, that were modeled into the cast.

***Table 16**: Patient characteristics and questionnaire scoring.*

| **Question/Patient characteristic** | **Score** | | | |
|---|---|---|---|---|
| | *Patient 1* | *Parents 1* | *Patient 2* | *Parents 2* |
| Age (years) | 7 | | 10 | |
| Sex | Male | | Female | |
| Fracture type | Greenstick | | Torus | |
| Laterality fracture | Right | | Left | |
| Number of hospital visits | 3 | | 3 | |
| Design and production time (hours) | 19 (30) | | 23 | |
| Pain | 1.0 | 0.0 | 1.0 | 0.0 |
| Itching | 1.0 | 0.0 | 2.0 | 0.0 |
| Sweating | 2.0 | | 2.5 | |
| Smell | 1.0 | 0.0 | 1.0 | 0.0 |
| Skin irritation | 1.0 | 0.0 | 1.0 | 1.0 |
| Weight | 1.0 | 0.0 | 1.0 | 0.0 |
| Bathing | 1.0 | 0.0 | 1.0 | 0.0 |
| Look | 1.0 | 10.0 | 1.0 | 8.0 |
| Daily activities | 1.0 | 1.0 | 2.0 | 1.0 |
| Sleeping | | 0.0 | | 0.0 |
| Treatment score | | 9.0 | | 9.0 |
| Preferred future treatment | 3D printed cast | 3D printed cast | 3D printed cast | 3D printed cast |

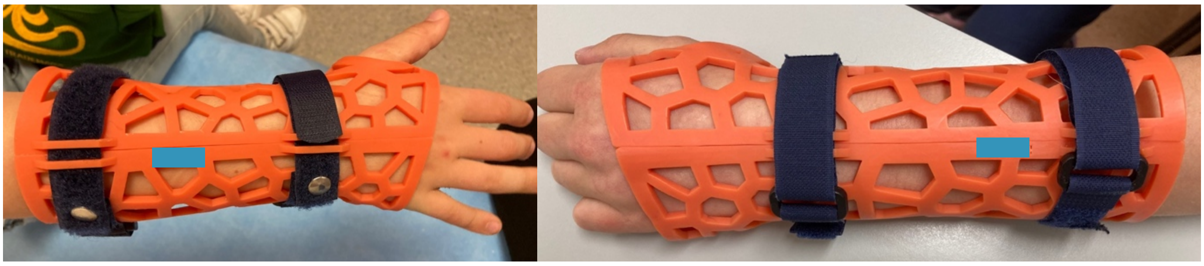

***Figure 44**: 3D printed wrist casts around the forearm of the patients.*

As can be seen from Table 15, both the children and parents were more than satisfied with the new treatment, scoring the treatment with a 9.0 out of 10.0 and preferring this treatment over traditional plaster casting in case of a future fracture. All parameters were scored more than satisfactory. Only sweating was slightly more a burden with the second patient.

The number of hospital visits was similar for the patient as when they would have come in during the evening or weekend. So, no extra burden was put on the patient in that respect. Eventually, the evaluation visit can even be skipped, since no plaster technician is necessary to remove the cast. Both casts were created within 24 hours. Although, due to a printer error (power failure), one misprint was made for patient 1, increasing the total production time.

Advantages that were listed by the parents were furthermore that the cast was lightweight, caused no itching, no smells and no sweating and was easy to sleep with. Moreover, the water resistance and improved hygiene were praised, causing the child to be more independent.

Disadvantages were that the child forgets that the wrist needs rest, because of all the advantages. The first patient eventually even broke one part of the cast (radial side, at the palm of the hand as shown in Figure 45), by hitting someone on the head with it. After contact with the hospital, the patient came back to the ER. Because clinical recovery was achieved, the patient was set free from the cast and no further treatment was indicated. Also for patient 2, one of the Velcro arcs was damaged.

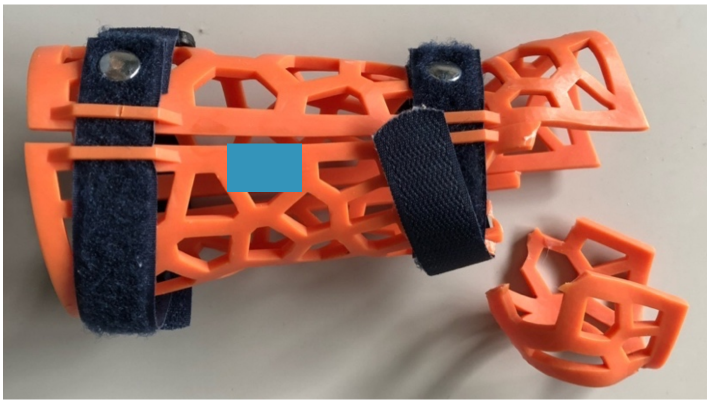

***Figure 45**: Broken 3D printed wrist cast of patient 1.*

Improvements, according to these experiences, are to use a less brittle material and reinforcement of the Velcro arcs.

Both patient regained full function of the wrist and swelling was minimized after two weeks of treatment. Patient 2 was still slightly painful at the position of the fracture, so she was sent home with the advice to wear the cast for a week longer during, after which she was set free from the cast as well.

## Conclusion

The new workflow is feasible for implementation into clinical practice, because no extra visits are required and a cast can be created within 24 hours after presentation at the ER. Clinically, full function was recovered by both patients and swelling and pain were drastically reduced. Both patients and parents were extremely enthusiastic about the treatment with the 3D printed cast, scoring the treatment with a 9.0 out of 10.0. In the future, both included patients and parents would choose treatment with a 3D printed cast over traditional plaster casting, because the advantages outweigh the disadvantages by a lot.

# Patient case: orthosis for wrist arthrosis

## Patient case

During the course of this thesis, a patient came across the plaster room with severe arthrosis of the hands (mainly right) and carpal tunnel syndrome (female, 75 years old). The plaster technicians already made a splinted brace, in which a stiff plate was encased in soft casting materials. Although this brace was comfortable, in daily use, the patient was unable to perform simple daily tasks with it, such as vacuum cleaning and turning a key. Moreover, especially in summer, the brace was really warm, which caused poor hygiene and bad smells inside the cast. To overcome these issues, it was requested to try to create a semi-flexible wrist orthosis using 3d printing.

## Prototypes

Multiple prototypes were created based on the design algorithm that was created during this thesis. However, since in this case the material needed to be somewhat flexible, because it was used as support and not as an immobilization device, tough 2000 resin was chosen as the preferred material. Also, a lower thickness than the thickness of the immobilization casts was chosen, since a thinner layer would be more flexible. The main purpose of the orthosis was to provide support at the thumb base.

Firstly, a scan was made of the hand in relaxed position and a cast was created around that. The first cast was 1.75 mm thick and consisted of one piece with a slit, where the cast could be folded open for application. An offset border of 10 mm was used. The first prototype is visualized in Figure 46. The prototype was fitted to the patient and appeared to be suboptimal. The thumb hole was too small, since the knuckle of the thumb was wider than the cut-off point that was set during the design phase, and the edges were too sharp. Also, the general fit was too tight.

***Figure 46**: First prototype of the orthosis.*

A second cast was then created, based on the same 3D scan. The edges and corners were smoothed, the offset was increased to 0.75 mm and the sharp point at the palm of the hand was lowered. Also, the edge of the slit was moved away from the head of the ulna. The thumb hole was designed to be a sort of gutter to fit the thumb. Finally, an arc was added to fixate the thumb into the gutter with a felt Velcro strap. The second prototype is shown in Figure 47, while it was fitted to the patient. This prototype still had some pressure points, causing worsening of the already present pain. The main complaints were still the hard edges and the notch into the palm of the hand. Also, too little movement of the thumb was allowed, making it impractical for daily activities.

***Figure 47**: Second prototype of the orthosis.*

Three new scans were then made to improve the designed orthosis further. One scan was made with the hand in a relaxed position, the second scan was made with the hand in full extension and finally, a last scan was made while the patient was holding a bottle. The scans are shown in Figure 48.

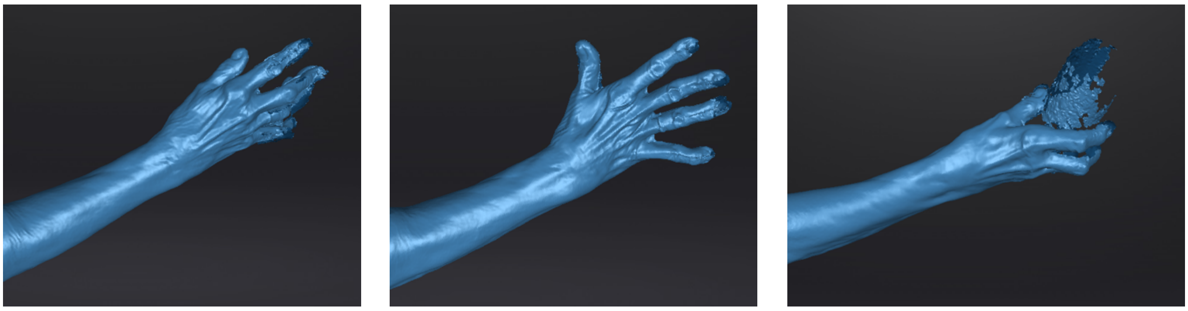

***Figure 48**: Relaxed scan (left), extension scan (middle) and bottle holding scan (right).*

A cast was then formed based on the combination of these scans. The palmar part was determined by the extension scan and the width of the thumb gutter was determined by both the relaxed and bottle holding scan. To create some extra flexibility, moreover, the thickness of the cast was reduced to 1.50 mm. After printing, the orthosis was fitted onto the patient again. The present pressure points were removed by heating the cast with a strong blow-dryer and deforming the cast slightly at these points. Moreover, the distal edge of the orthosis was layered with felt to create smooth and soft edges. The final design, fitted around the arm, is presented in Figure 49.

***Figure 49**: Final prototype of the orthosis.*

The fit of the final orthosis was perceived as a lot better than the first two prototypes. Also, daily activities could be performed more effortlessly than with the splinted brace. However, due to varying degrees of inflammation, pain and swelling, that are changing day by day, an optimal fit has not yet been found. Still, the abilities to create custom, open-latticed and semi-flexible casts open new doors for implementation of 3D technologies into the orthotics workflow. According to the plaster technicians, 3D technologies will start to play a larger role within their profession during the upcoming years. They expect that 3D technologies will be deployed mainly in the field of orthotics for chronic pain and for long-term upper extremity treatments.

## Conclusion

3D printing can be a solution for designing personalized orthosis for patients with arthrosis. However, due to the varying character of the illness, with changing inflammation, pain and swelling day by day, an optimal fit is difficult to find.

# Discussion

## Limitations

Although all steps taken in this thesis were substantiated and thought of, every sub study has its own limitations and possible (necessary) improvements. Limitations are elaborated below.

### Printing technique and material selection

*Print orientation samples*

For the material testing, samples were printed vertically oriented, since it was expected that this would also be the main printing direction for the 3D printed casts. This orientation, however, ensured that the testing direction was perpendicular to the printing direction, which is theoretically the weakest orientation, since that is also the direction in which the layers are built. Especially for the FDM samples, theoretical strength values were not met. A different printing direction could have influenced the results of the material selecting study significantly.

To obtain a more complete overview of the material behavior, actually, samples should have been tested in multiple printing directions. Then, the strength values could not only have been determined more adequately, but also a conclusion could have been drawn on the most optimal printing orientation for the 3D printing of the wrist casts.

*Failure mechanism and fracture patterns*

Delamination was observed as the typical failure mechanism for the FDM samples, which is caused by weak links in a construct, for example via small air pockets between the layers that are influenced by temperature differences while printing [98]. With SLA, this does not occur, since the binding between two layers is created in a homogeneous resin bath by a laser and therefore the binding between the layers is better.

Coherent to the print orientation of the samples is the failure mechanism of the samples. As stated earlier, fragmentation of the cast is undesirable in case of failure of the construct. However, all SLA materials showed shattering upon failure, while all FDM materials delaminated. Based on the fracture pattern, FDM materials should thus be preferred. However, during testing, the FDM samples did not reach the 0.2% yield point, which normally indicates the point where plastic deformation starts to occur. Therefore, the FDM materials' failure mechanisms were unpredictable and the SLA materials were favored, even though a shattering pattern was observed as a fracture pattern.

*Material ranking*

The materials were ranked during the materials study and the highest ranked material was selected for the design. However, although the way of ranking was clearly stated in advance and carried out accordingly, it is still arbitrarily chosen. Another way of ranking could have led to different results.

### Design

*Design parameters*

In the creation of the design algorithm, some arbitrary choices were made considering design parameters, such as the cast thickness and the ventilation to material ratio. Although the thickness, for example, was based on the current thickness of plaster casting, no study was carried out in which the optimal thickness value was determined. The same goes for the ventilation to material ratio, that was set to be around 60%. Also for this, a separate study should be carried out to find the optimal value, without giving in on stabilization abilities.

## Mechanical phantom study

### *Underestimation of the moment by loading masses on set hooks*

During the mechanical phantom study, loads where hung from hooks perpendicular to the forearm to create a predefined moment with respect to the pivot axis. However, with increasing loading masses, the angle of the wrist coupling changed and therefore, also, the positions of the hooks and thus the moment arm changed. The moment arm was overestimated, mainly when the maximum loading masses were applied. However, the loading masses that were applied exceeded realistic clinical values and were moreover equal for both 3D printed cast groups and the plaster cast group.

### *Simulation of external forces*

Another limitation for the mechanical phantom study, is that no external forces were tested. Especially, when looking back on the pilot study, where one patient achieved to break the cast on the head of another person, the assumption is raised that external force impact should also be investigated.

## Comfort study

### *Immobilization of a healthy person*

Pressure points were named as one of the disadvantages of the 3D printed wrist casts during the comfort study. Volunteers scored the burden of pressure points with a score of 3.5 out of 10, which leans towards a mean value where most people sometimes suffered from pressure points. However, it is striking that during the pilot study pressure points were never an issue with the patients. This might be caused by the fact that patients actually experience pain and are more conscious of the need of resting the arm. When using healthy volunteers, it might be that they do not comply as much with the resting advice, making them perform more activities than a patient would, which can create a false image of the investigated parameters.

## Pilot study

One major limitation of the pilot study, is that it was performed with only two patients. The initial goal was to include five to ten patients, since a larger amount of patients would create more power for the conclusions. However, the results are in accordance with each other and clinical implementation was shown to be feasible.

## General limitations

### *Printing time*

Although a workflow was created in which a cast could be produced within 24 hours, printing time is still one of the most limiting factors for clinical implementation of 3D printed wrist casts in practice. Especially when patients come in during working hours, one of the plaster technicians can create a polyester cast on the spot, while a bridging treatment is necessary between admission at the hospital and eventually fitting the 3D printed cast.

Quicker printing techniques exist, such as DLP, which could create a wrist print in only a few hours, however, these techniques are often still expensive and not widely available, thus not suitable for in-house production of 3d printed wrist casts.

### *Limited build volume*

During this study, prints were made using a Form 2 and a Form 3 SLA printer from Formlabs. The size of the possible prints was limited by the build volumes of the printers, which are 14.5 × 14.5 × 17.5 cm and 14.5 × 14.5 × 18.5 cm respectively [99]. Since the arms of the children in the pilot study were a lot smaller than the arms of the volunteers during the comfort study, arm casts with an adequate length could be created for the children. For adults, the printing volume is actually slightly too small to produce a cast with an adequate length. For the phantom study and comfort study, now, shorter arms casts were designed than what would be clinically required, which was suboptimal. If, in the future, casts would be needed for adults, a printer with a bigger build volume will be necessary.

### *Swelling*

One of the design requirements is adequate fit and the possibility to loosen up the cast in case of excessive swelling. However, since in clinical practice the cast is always created during the first days after injury, swelling will be in place. Thus, the swelling will be scanned and it will codetermine the fit of the cast. Therefore, at the end of treatment, when the swelling is diminished, the fit will most probably be (too) loose. This effect can also be observed for healthy subjects, as a result of temperature changes for example. To improve the fit, a predictive model should be made that can estimate the amount and the progress of swelling during injury. However, even if swelling can be modelled accurately, a cast needs to be created that fits with both excessive swelling and without any swelling. Therefore a cast should most probably be somewhat flexible, which will most likely be at the expense of some of the stabilization abilities.

### *Cost-effectiveness*

Right now, only the material costs of one 3D printed cast are around €25, while the costs of a circular forearm plaster cast are only a few euros [6]. Although a workflow can be created with the same amount of hospital visits as traditional treatment, the manual labor for the design and production of the casts, together with the material costs, up until now, cause unfavorable cost-effectiveness. With the emerge of more and faster printing techniques, materials will become cheaper, however the manual labor remains an issue.

## Future perspectives

3D printed wrist casts are a promising solution for the treatment of distal radius fractures. Future perspectives are listed below.

### Extrapolation to unstable fracture

During this research, tests and a pilot were performed based on stable fractures. However, the majority of the fractures is not stable. So to use 3D printed wrist cast as a treatment, also for these fractures, proof is needed that the 3D printed wrist cast has the right stabilization abilities to treat unstable fractures as well.

### Clinical implementation

Because of the higher costs of 3D printed casts and the printing times, the first steps of clinical implementation will most likely be for patients that need long-term treatment with plaster. Usually, these patients need one or more cast changes, for which a detachable and cleanable 3D printed wrist cast could be a solution.

Also, a randomized controlled trial RCT should be conducted, in which one group of patients is treated traditionally with a plaster cast and the other group is treated with the new 3D printed casts, to show the possible beneficial aspects and outcomes of the 3D printed casts in comparison to plaster systematically. In this way, complication rates, patient experiences and clinical outcomes can be compared between the two groups.

### Extrapolation to other body parts

The 3D printed wrist casts in this study were only used for the treatment of distal radius fractures. However, with the same design algorithm, an ankle cast can be created or a helmet for skull protection after surgery can be produced. The extrapolation of the use of 3D printed casting to other body parts is therefore a logical follow-up step.

### Orthotics

As shown in the patient case that was added, another possible application of 3D printed casting lies with orthotics. According to the plaster technicians of the ETZ, 3D printing will play a bigger role in this field during the upcoming years, since here, devices are made for longer use and prefabricated solutions that are used, are often not the right fit for specific patients. The use of 3D printing could therefore be a useful addition.

## Medical Device Regulation (MDR)

As of the 26th of May 2021 the new MDR is in place. Since the 3D printed casts are non-invasive devices, they fall under Class I (low risk) medical devices [77]. However, with the new MDR in place, the definition of custom-made devices has changed. A custom made device is *any device specifically made in accordance with a duly qualified medical practitioner's written prescription which gives, under his responsibility, specific design characteristics and is intended for the sole use of a particular patient. The abovementioned prescription may also be made out by any other person authorized by virtue of his professional qualifications to do so. However, mass-produced devices which need to be adapted to meet the specific requirements of any professional user and devices which are mass-produced by means of industrial manufacturing processes in accordance with the written prescriptions of any authorized person shall not be considered to be custom-made devices*. Although 3D printing is considered to be an industrial manufacturing technique, in-house 3D printing of individual wrist casts is not considered as mass-production, since every device is tailor-made, so the 3D printed wrist casts are classified as Class I custom-made medical devices [100]. Therefore, 3D printed wrist casts are exempt from the MDR requirements, except for the general safety and performance requirements in Annex I of the MDR [77, 100]. A quality management system (QMS) should however be put into place, as well as documentation on the manufacturing process, design and performance evaluations and review experiences from clinical use to comply with the MDR [77, 100]. As long as the use of these medical devices is limited to in-house use, no additional certifications are necessary [77].

# Conclusion

*"What is the feasibility of in-house design, production and implementation of 3D printed wrist casts for the treatment of distal radius fractures?"*

The answers to the sub questions are as follows.

1. Color resin, printed with an SLA printer is most suitable for the production of 3D printed wrist casts.
2. A 3D printed cast with a Voronoi design pattern is most successful for adequate wrist immobilization, achieving similar stabilization abilities as a plaster cast.
3. To implement the treatment of distal radius fractures with 3D printed wrist casts into the current workflow, a workflow as used for traditional treatment during the evenings and weekends is required.

The answers from the sub questions, combined with the conclusions from each individual sub study, lead to the following answer of the main research question:

*"A customized, lightweight, water-resistant and ventilated wrist cast can successfully be designed, with adequate stabilization abilities. This cast can be produced within 24 hours, with the use of a semi-automated design algorithm that creates a wrist cast with ventilation holes based on a Voronoi pattern. The 3D printing should be performed with an SLA printer, with the use of color resin. The produced wrist casts ensure adequate comfort and ease of use and can be implemented clinically for successful treatment of children with greenstick and buckle/torus fractures. Only small alterations are necessary in the current workflow to allow for the production of the 3D printed wrist casts. No extra hospital visits are required and the new workflow is comparable to the weekend workflow. Further research is necessary to tackle the unfavorable cost-effectiveness and the adaption of the casts to swelling. For the future, treatment with 3D printed casts should be extrapolated to unstable fractures, other body parts and the field of orthotics."*

## References

[1] Ayhan Ç, Ayhan E. Kinesiology of the wrist and the hand. Comparative Kinesiology of the Human Body – Chapter 13 (Academic Press). 2020; 211-282.
[2] Berger RA. The anatomy and basic biomechanics of the wrist joint. J Hand Ther. 1996; 9 (2): 84-93.
[3] Iftikhar N, Gossett T. Important Joints: Hand and Wrist Bones. 2019. [Cited 16-10-2020] Available from: https://www.healthline.com/health/wrist-pain#_noHeaderPrefixedContent.
[4] Verhaar JAN, van Mourik JBA. Het lichamelijk onderzoek. Leerboek Orthopedie – Hoofdstuk 1 (Bohn Stafleu van Loghum). 2013; 3-20.
[5] Dutton M. BIOMECHANICS. Dutton's ORTHOPAEDIC Examination, Evaluation, and Intervention – SECTION IV – THE EXTREMITIES – The Forearm, Wrist and Hand (The McGraw-Hill Companies, Inc.). 2012; 688-689.
[6] Brink PRG, Bransz N, Deijkers RLM, van Eerten PV, Kolkman S, van Loon J, Poolman, RW, Segers MJM. Distale radius fracturen – Bijlage: Algemene inleiding. Richtlijnendatabase Federatie Medisch Specialisten. 2010; 1-73.
[7] Reed MH. Fractures and dislocations of the extremities in children. J Trauma. 1977; 17 (5): 351-354.
[8] Sinikumpu JJ, Nietosvaara Y. Treatment of Distal Forearm Fractures in Children. Scand J Surg. 2020; 1-5.
[9] Atanelov Z, Bentley TP. Greenstick Fractures. StatPearls (StatPearls Publishing). 2020.
[10] Corsino CB, Reeves RA, Sieg RN. Distal Radius Fractures. StatPearls (StatPearls Publishing). 2020.
[11] Oakley EA, Ooi KS, Barnett PL. A randomized controlled trial of 2 methods of immobilizing torus fractures of the distal forearm. Pediatr Emerg Care. 2008; 24 (2): 65-70.
[12] Sprakel J. Distale radiusfractuur. 2015. [Cited 13-11-2020] Available from: http://www.surgeryassistant.nl/artikel.php?actie=17&Anumberid=264&language=NL#up.
[13] Activate Physiotherapy. Greenstick & Buckle Fracture. 2019. [Cited 13-11-2020] Available from: https://activatephysiotherapy.com.au/greenstick-buckle-fracture/.
[14] Traumaprotocol. Pols en Onderarm fractuur bij kinderen. 2020. [Cited 02-07-2020] Available from: http://traumaprotocol.nl/index.php/bovenste-extr/pols-en-onderarmfractuur-bij-kinderen.
[15] Sintenie JB, Allema JH, Ivanyi B, Kempink DRJ, van de Kerkhof-Bon B, Oostenbroek H, de Ridder VA, van Rijn R, Rövekamp M, Schuuring M. Fracturen bij kinderen – Polsfracturen bij kinderen. Richtlijnendatabase Federatie Medisch Specialisten. 2019; 87-109.
[16] Plint AC, Perry JJ, Correll R, Gaboury I, Lawton L. A randomized, controlled trial of removable splinting versus casting for wrist buckle fractures in children. Pediatrics. 2006; 117 (3): 691-697.
[17] Blaya F, Pedro PS, Silva JL, D'Amato R, Heras ES, Juanes JA. Design of an Orthopedic Product by Using Additive Manufacturing Technology: The Arm Splint. J Med Syst. 2018; 42 (3): 54.
[18] Boutis K, Willan A, Babyn P, Goeree R, Howard A. Cast versus splint in children with minimally angulated fractures of the distal radius: a randomized controlled trial. CMAJ. 2010; 182 (14): 1507-1512.
[19] Chen YJ, Lin H, Zhang X, Huang W, Shi L, Wang D. Application of 3D-printed and patient-specific cast for the treatment of distal radius fractures: initial experience. 3D Print Med. 2017; 3 (1): 11.
[20] Chen Y, Lin H, Yu Q, et al. Application of 3D-Printed Orthopedic Cast for the Treatment of Forearm Fractures: Finite Element Analysis and Comparative Clinical Assessment. Biomed Res Int. 2020; 2020: 9569530.
[21] Shirley ED, Maguire KJ, Mantica AL, Kruse RW. Alternatives to Traditional Cast Immobilization in Pediatric Patients. J Am Acad Orthop Surg. 2020; 28 (1): e20-e27.
[22] Graham J, Wang M, Frizzell K, Watkins C, Beredjiklian P, Rivlin M. Conventional vs 3-Dimensional Printed Cast Wear Comfort. Hand (N Y). 2020; 15 (3): 388-392.
[23] Halanski M, Noonan KJ. Cast and splint immobilization: complications. J Am Acad Orthop Surg. 2008; 16 (1): 30-40.

[24] Kropman RH, Bemelman M, Segers MJ, Hammacher ER. Treatment of impacted greenstick forearm fractures in children using bandage or cast therapy: a prospective randomized trial. J Trauma. 2010; 68 (2): 425-428.
[25] Hill CE, Masters JP, Perry DC. A systematic review of alternative splinting versus complete plaster casts for the management of childhood buckle fractures of the wrist. J Pediatr Orthop B. 2016; 25 (2): 183-190.
[26] Price CT. A splint was not inferior to a cast for distal radial fracture in children. J Bone Joint Surg Am. 2011 May 18;93(10):970.
[27] West S, Andrews J, Bebbington A, Ennis O, Alderman P. Buckle fractures of the distal radius are safely treated in a soft bandage: a randomized prospective trial of bandage versus plaster cast. J Pediatr Orthop. 2005; 25 (3): 322-255.
[28] Firmin F, Crouch R. Splinting versus casting of "torus" fractures to the distal radius in the paediatric patient presenting at the emergency department (ED): a literature review. Int Emerg Nurs. 2009; 17 (3): 173-178.
[29] Plint A, Clifford T, Perry J, Bulloch B, Pusic M, Lalani A, Ali S, Nguyen BH, Joubert G, Millar K. Wrist buckle fractures: a survey of current practice patterns and attitudes toward immobilization. CJEM. 2003; 5 (2): 95-100.
[30] Al Khudairy A, Hirpara KM, Kelly IP, Quinlan JF. Conservative treatment of the distal radius fracture using thermoplastic splint: pilot study results. Eur J Orthop Surg Traumatol. 2013; 23 (6): 647-650.
[31] Davidson JS, Brown DJ, Barnes SN, Bruce CE. Simple treatment for torus fractures of the distal radius. J Bone Joint Surg Br. 2001; 83 (8): 1173-1175.
[32] von Keyserlingk C, Boutis K, Willan AR, Hopkins RB, Goeree R. Cost-effectiveness analysis of cast versus splint in children with acceptably angulated wrist fractures. Int J Technol Assess Health Care. 2011; 27 (2): 101-107.
[33] Taylor E, Hanna J, Belcher HJC. Splinting of the hand and wrist. Current Orthopaedics. 2003; 17 (6): 465–474.
[34] The Royal Children's Hospital, Victorian Paediatric Orthopaedic Network. Fracture care: buckle injury. 2018. [Cited 25-01-2021] Available from: https://www.rch.org.au/kidsinfo/fact_sheets/Fracture_care_buckle_injury/.
[35] Levesque JN, Shah A, Ekhtiari S, Yan JR, Thornley P, Williams DS. Three-dimensional printing in orthopaedic surgery: a scoping review. EFORT Open Rev. 2020; 5 (7): 430-444.
[36] Aimar A, Palermo A, Innocenti B. The Role of 3D Printing in Medical Applications: A State of the Art. J Healthc Eng. 2019; 2019: 5340616.
[37] GE Additive. Additive Manufacturing vs. 3D Printing. 2020. [Cited 30-10-2020] Available from: https://www.ge.com/additive/additive-manufacturing/information/3d-printing.
[38] 3D HUBS. The Complete Engineering Guide 3D Printing. 2020. [Cited 30-10-2020] Available from: https://www.3dhubs.com/guides/3d-printing/.
[39] OCEANZ. What is the difference between 3D printing and Additive Manufacturing? 2020. [Cited 06-11-2020] Available from: https://www.oceanz.eu/en/what-is-the-difference-between-3d-printing-and-additive-manufacturing/.
[40] ASTM INTERNATIONAL. ASTM F42/ISO TC 261 Develops Additive Manufacturing Standards. 2013. [Cited 30-10-2020] Available from: https://www.astm.org/COMMIT/F42_AMStandardsStructureAndPrimer.pdf.
[41] SME. Additive Manufacturing Processes. 2020. [Cited 30-10-2020] Available from: https://www.sme.org/globalassets/sme.org/technologies/medical-manufacturing/amtechnologies.pdf.
[42] Redwood B, Schöffer F, Garret B. The 3D Printing Handbook – Technologies, design and applications (3D Hubs). 2017.
[43] Hoogervorst P, Knox R, Tanaka K, et al. A Biomechanical Comparison of Fiberglass Casts and 3-Dimensional-Printed, Open-Latticed, Ventilated Casts. Hand (N Y). 2019; 1558944719831341.

[44] Formlabs. Form Wash + Form Cure. 2020. [Cited 05-11-2020] Available from: https://formlabs.com/wash-cure/.
[45] Ventola CL. Medical Applications for 3D Printing: Current and Projected Uses. P T. 2014; 39 (10): 704-711.
[46] Tack P, Victor J, Gemmel P, Annemans L. 3D-printing techniques in a medical setting: a systematic literature review. Biomed Eng Online. 2016; 15 (1): 115.
[47] Diment LE, Thompson MS, Bergmann JHM. Clinical efficacy and effectiveness of 3D printing: a systematic review. BMJ Open. 2017; 7 (12): e016891.
[48] Malik HH, Darwood AR, Shaunak S, Kulatilake P, El-Hilly AA, Mulki O, Baskaradas A. Three-dimensional printing in surgery: a review of current surgical applications. J Surg Res. 2015; 199 (2): 512-522.
[49] Levesque JN, Shah A, Ekhtiari S, Yan JR, Thornley P, Williams DS. Three-dimensional printing in orthopaedic surgery: a scoping review. EFORT Open Rev. 2020; 5 (7): 430-441.
[50] Aimar A, Palermo A, Innocenti B. The Role of 3D Printing in Medical Applications: A State of the Art. J Healthc Eng. 2019; 5340616.
[51] Rengier F, Mehndiratta A, von Tengg-Kobligk H, Zechmann CM, Unterhinninghofen R, Kauczor HU, Giesel FL. 3D printing based on imaging data: review of medical applications. Int J Comput Assist Radiol Surg. 2010; 5 (4): 335-341.
[52] Hoang D, Perrault D, Stevanovic M, Ghiassi A. Surgical applications of three-dimensional printing: a review of the current literature & how to get started. Ann Transl Med. 2016; 4 (23): 456.
[53] Kelly S, Paterson A, Bibb R. A review of wrist splint designs for additive manufacture. Rapid Design, Prototyping and Manufacture conference (RDPM 14) Loughborough (Great Britain). 2015.
[54] Mooij CDY. Design guidelines for 3D printed wrist casts for the treatment of distal radius fractures. ETZ 3D Lab. 2020; 4-12.
[55] Janzing HMJ, Bessems SAM, Ligthart MAP, Van Lieshout EMM, Theeuwes HP, Barten DG, Verhofstad MHJ. Treatment of dorsally dislocated distal radius fractures with individualized 3D printed bracing: an exploratory study. 3D Print Med. 2020; 6 (1): 22.
[56] Chae DS, Kim DH, Kang KY, Kim DY, Park SW, Park SJ, Kim JH. The functional effect of 3D-printing individualized orthosis for patients with peripheral nerve injuries: Three case reports. Medicine (Baltimore). 2020; 99 (16): e19791.
[57] Keller M, Guebeli A, Thieringer F, Honigmann P. In-hospital professional production of patient-specific 3D-printed devices for hand and wrist rehabilitation. Hand Surg Rehabil. 2020; S2468-1229 (20): 1-8.
[58] Górski F, Wichniarek R, Kuczko W, Żukowska M, Lulkiewicz M, Zawadzki P. Experimental Studies on 3D Printing of Automatically Designed Customized Wrist-Hand Orthoses. Materials (Basel). 2020; 13 (18): 4091.
[59] Zheng Y, Liu G, Yu L, Wang Y, Fang Y, Shen Y, Huang X, Qiao L, Yang J, Zhang Y, Hua Z. Effects of a 3D-printed orthosis compared to a low-temperature thermoplastic plate orthosis on wrist flexor spasticity in chronic hemiparetic stroke patients: a randomized controlled trial. Clin Rehabil. 2020; 34 (2): 194-204.
[60] Górski F, Zawadzki P,Wichniarek R, Kuczko W, Ż ukowska M, Wesołowska I, Wierzbicka N. Automated Design of Customized 3D-Printed Wrist Orthoses on the Basis of 3D Scanning. Computational and Experimental Simulations in Engineering. Proceedings of ICCES2019 – Chapter 97 (Mechanisms and Machine Science; Springer). 2016; 1133–1143.
[61] Buonamici F, Furferi R, Governi L, Lazzeri S, McGreevy KS, Servi M, Talanti E, Uccheddu MF, Volpe Y. A practical methodology for computer-aided design of custom 3D printable casts for wrist fractures. Vis Comput. 2018; 36: 375-390.
[62] Lee KH, Kim DK, Cha YH, Kwon JY, Kim DH, Kim SJ. Personalized assistive device manufactured by 3D modelling and printing techniques. Disabil Rehabil Assist Technol. 2019; 14 (5): 526-531.
[63] Guida P, Casaburi A, Busiello T, Lamberti D, Sorrentino A, Iuppariello L, D'Albore M, Colella F, Clemente F. An alternative to plaster cast treatment in a pediatric trauma center using the CAD/CAM

technology to manufacture customized three-dimensional-printed orthoses in a totally hospital context: a feasibility study. J Pediatr Orthop B. 2019; 28 (3): 248-255.
[64] Kim SJ, Kim SJ, Cha YH, Lee KH, Kwon JY. Effect of personalized wrist orthosis for wrist pain with three-dimensional scanning and printing technique: A preliminary, randomized, controlled, open-label study. Prosthet Orthot Int. 2018; 42 (6): 636-643.
[65] Buonamici F, Furferi R, Governi L, Lazzeri S, McGreevy KS, Servi M, Talanti E, Uccheddu MF, Volpe Y. A CAD-based Procedure for Designing 3D Printable Arm-Wrist-Hand Cast. Computer-aided Design and Applications. 2018; 16: 25-34.
[66] Blaya F, San Pedro P, Lopez-Silva J, D'Amato R, Juanes JA, and Lagándara JG. Study, design and prototyping of arm splint with additive manufacturing process. Proceedings of the 5th International Conference on Technological Ecosystems for Enhancing Multiculturality – Article 57 (TEEM 2017; Association for Computing Machinery). 2017; 1–7.
[67] Abreu de Souza M, Schmitz C, Marega Pinhel M, Palma Setti JA, Nohama P. Proposal of custom made wrist orthoses based on 3D modelling and 3D printing. Annu Int Conf IEEE Eng Med Biol Soc. 2017; 2017: 3789-3792.
[68] Cazon A, Kelly S, Paterson AM, Bibb RJ, Campbell RI. Analysis and comparison of wrist splint designs using the finite element method: Multi-material three-dimensional printing compared to typical existing practice with thermoplastics. Proc Inst Mech Eng H. 2017; 231 (9): 881-897.
[69] Paterson AM, Bibb R, Campbell RI, Bingham G. Comparing additive manufacturing technologies for customised wrist splints. Rapid Prototyp. J. 2015; 21 (3): 230-243.
[70] Kim H, Jeong S. Case study: Hybrid model for the customized wrist orthosis using 3D printing. J Mech Sci Technol. 2015; 29 (12): 5151-5156.
[71] Lin H, Shi L, Wang D. A rapid and intelligent designing technique for patient-specific and 3D-printed orthopedic cast. 3D Print Med. 2015; 2 (1): 4.
[72] SJR. Scimago Journal & Country Rank. 2020. [Cited 04-12-2020] Available from: https://www.scimagojr.com/journalrank.php.
[73] Ultimaker. Ultimaker Tough PLA. 2020. [Cited 14-12-2020] Available from: https://ultimaker.com/materials/tough-pla.
[74] MCPP. PLA. 2019. [Cited 02-02-2020] Available from: https://www.mcpp-3dp.com/wp-content/uploads/2018/TDS/New/PLA%20-%20UK.pdf.
[75] MCPP. TOUGH PLA. 2020. [Cited 02-02-2020] Available from: https://www.mcpp-3dp.com/wp-content/uploads/2018/TDS/TOUGH%20PLA.pdf.
[76] MCPP. ABS. 2019. [Cited 02-02-2020] Available from: https://www.mcpp-3dp.com/wp-content/uploads/2018/TDS/New/ABS%20-%20UK.pdf.
[77] REGULATION (EU) 2017/745 OF THE EUROPEAN PARLIAMENT AND OF THE COUNCIL. 2017. [Cited 02-02-2020] Available from: https://eur-lex.europa.eu/legal-content/EN/TXT/PDF/?uri=CELEX:32017R0745.
[78] Ziekenhuis St. Jansdal. Pols fractuur bij kinderen. 2021. [Cited 26-03-2021] Available from: https://www.stjansdal.nl/folders/pols-fractuur-bij-kinderen.
[79] ISO 10933-1. Use of International Standard ISO 10993-1, "Biological evaluation of medical devices - Part 1: Evaluation and testing within a risk management process". 2016.
[80] Instron. What is Tensile Testing? 2021. [Cited 23-03-2021] Available from: https://www.instron.us/en-us/our-company/library/test-types/tensile-test.
[81] Instron. Yield Point. 2021. [Cited 23-03-2020] Available from: https://www.instron.us/en-us/our-company/library/glossary/y/yield-point.
[82] Formlabs. Material data sheet STANDARD. 2017. [Cited 18-01-2021] Available from: https://formlabs-media.formlabs.com/datasheets/1801089-TDS-ENUS-0P.pdf.
[83] Formlabs. Standard resin DRAFT. 2020. [Cited 18-01-2021] Available from: https://formlabs-media.formlabs.com/datasheets/2001477-TDS-ENUS-0.pdf.
[84] Formlabs. Engineering resin TOUGH 2000. 2020. [Cited 18-01-2021] Available from: https://formlabs-media.formlabs.com/datasheets/2001340-TDS-ENUS-0P.pdf.

[85] Ultimaker. Technical data sheet ABS. 2018. [Cited 18-01-2021] Available from: https://support.ultimaker.com/hc/en-us/article_attachments/360010199279/TDS_ABS_v3.011_-en.pdf.
[86] Ultimaker. Technical data sheet PLA. 2018. [Cited 18-01-2021] Available from: https://support.ultimaker.com/hc/en-us/article_attachments/360010199879/TDS_PLA_v3.011-en.pdf.
[87] Ultimaker. Technical data sheet Tough PLA. 2018. [Cited 18-01-2021] Available from: https://support.ultimaker.com/hc/en-us/article_attachments/360010175560/TDS_Tough_PLA_RB-en.pdf.
[88] ISO 527. Plastics – Determination of tensile properties. 2019.
[89] ISO 178. Plastics – Determination of flexural properties. 2019.
[90] Formlabs. Form Wash time settings. 2021. [Cited 02-02-2021] Available from: https://support.formlabs.com/s/article/Form-Wash-Time-Settings?language=en_US.
[91] Formlabs. Form Cure time and temperature settings. 2021. [Cited 02-02-2021] Available from: https://support.formlabs.com/s/article/Form-Cure-Time-and-Temperature-Settings?language=en_US.
[92] Timoshenko SP. On the transverse vibrations of bars of uniform cross-section. Philosophical Magazine. 1992; 125.
[93] Shining 3D®. EinScan H. 2021. [Cited 04-03-2021] Available from: https://www.einscan.com/handheld-3d-scanner/einscan-h/.
[94] Shining 3D®. EinScan H. User Manual. 2020; 1-57.
[95] Nourian P. Polygon Mesh Models. TU Delft, presentation Geomatics Master, Architecture. 2016.
[96] Rhinoceros®. What are NURBS? 2021. [Cited 04-03-2021] Available from: https://www.rhino3d.com/features/nurbs/.
[96] Kang J. Voronoi Diagram. Encyclopedia of GIS (Springer). 2008.
[97] Delp SL, Grierson AE, Buchanan TS. Maximum isometric moments generated by the wrist muscles in flexion-extension and radial-ulnar deviation. J Biomech. 1996; 29 (10): 1371-1375.
[98] Simplyf y3D. Layer Separation and Splitting. 2021. [Cited 04-03-2021] Available from: https://www.simplify3d.com/support/print-quality-troubleshooting/layer-separation-and-splitting/.
[99] Formlabs. What is the build volume of the Form 2 and Form 3? 2019. [Cited 04-03-2021] Available from: https://support.formlabs.com/s/article/What-is-the-build-volume-of-the-Form-2-and-Form-3?language=en_US.
[100] Spentys. The implications of the new MDR: the three most prominent changes that will affect orthopaedic technicians. 2021. [Cited 04-03-2021] Available from: https://www.spentys.com/blog/the-implications-of-the-new-mdr-the-three-most-prominent-changes-that-will-affect-orthopaedic-technicians.

# Appendix I: Stress-Strain curves for flexural testing

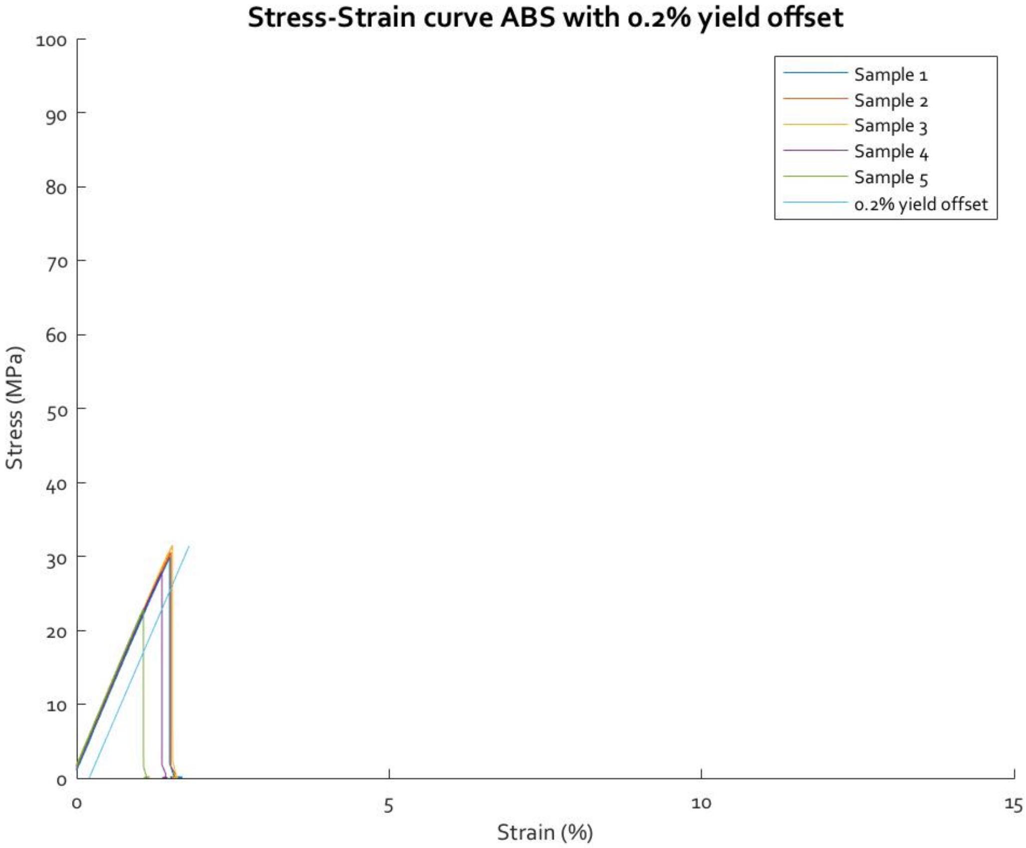


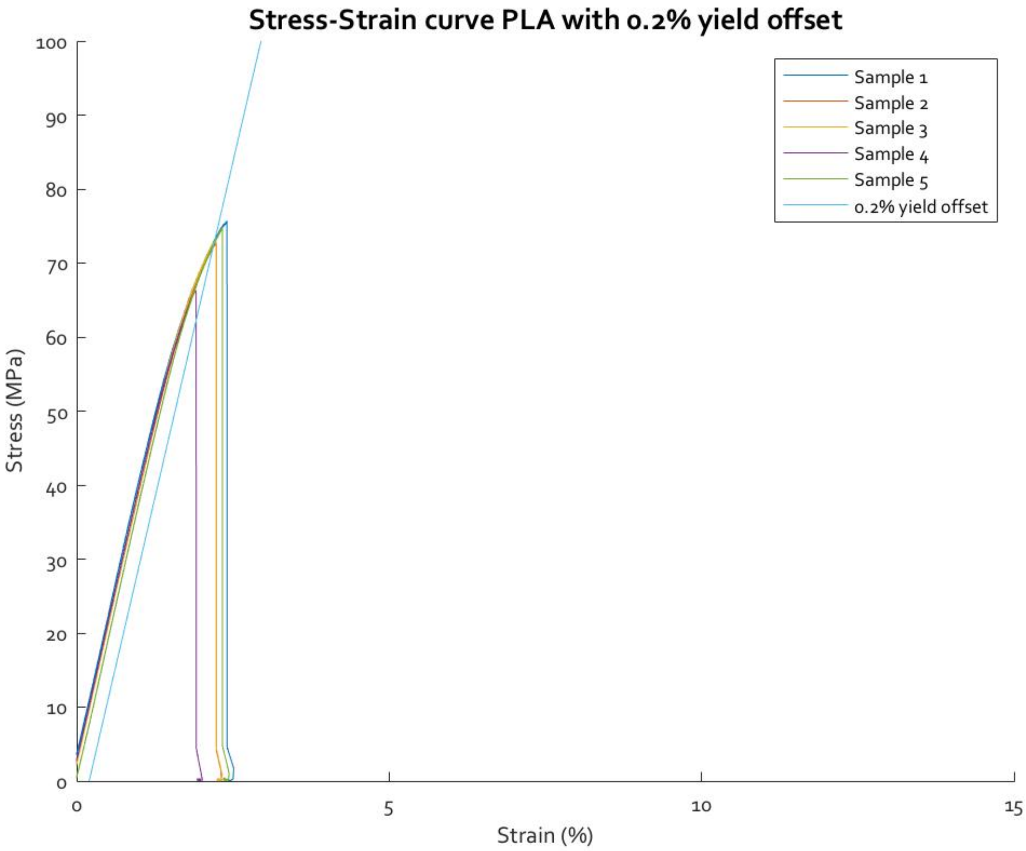

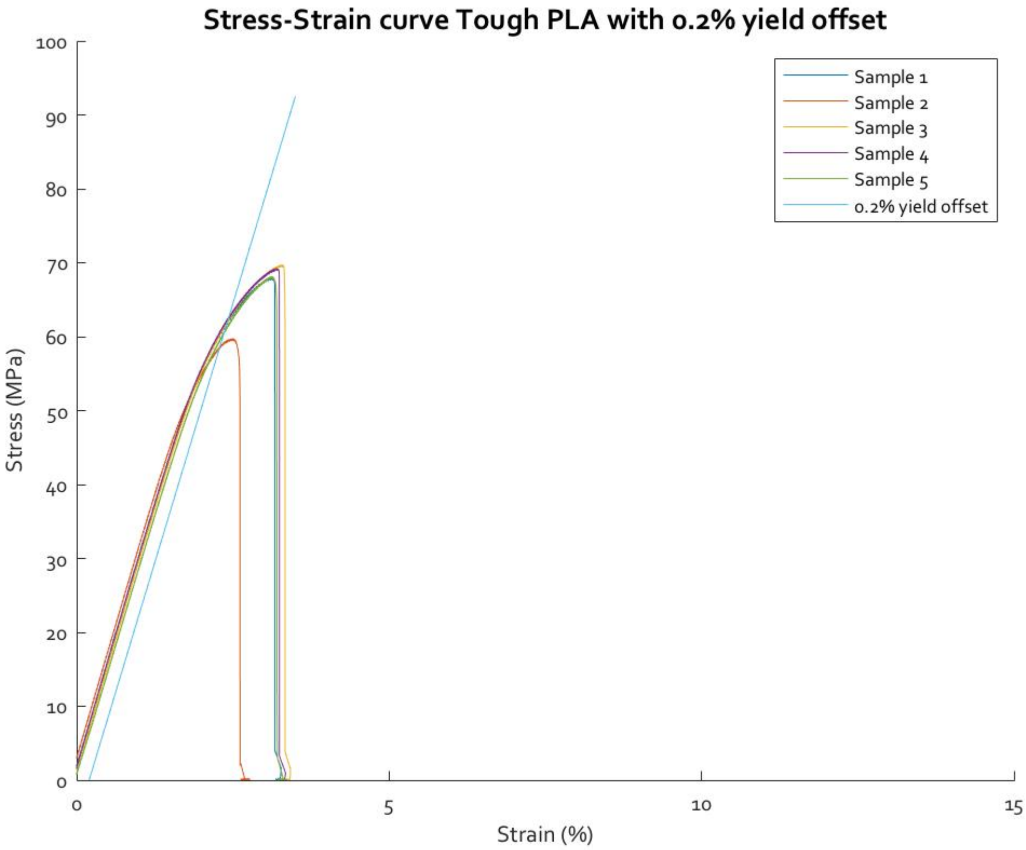
Stress-Strain curve Tough PLA with 0.2% yield offset
Stress (MPa)
Strain (%)
Sample 1
Sample 2
Sample 3
Sample 4
Sample 5
0.2% yield offset
0
10
20
30
40
50
60
70
80
90
100
0
5
10
15

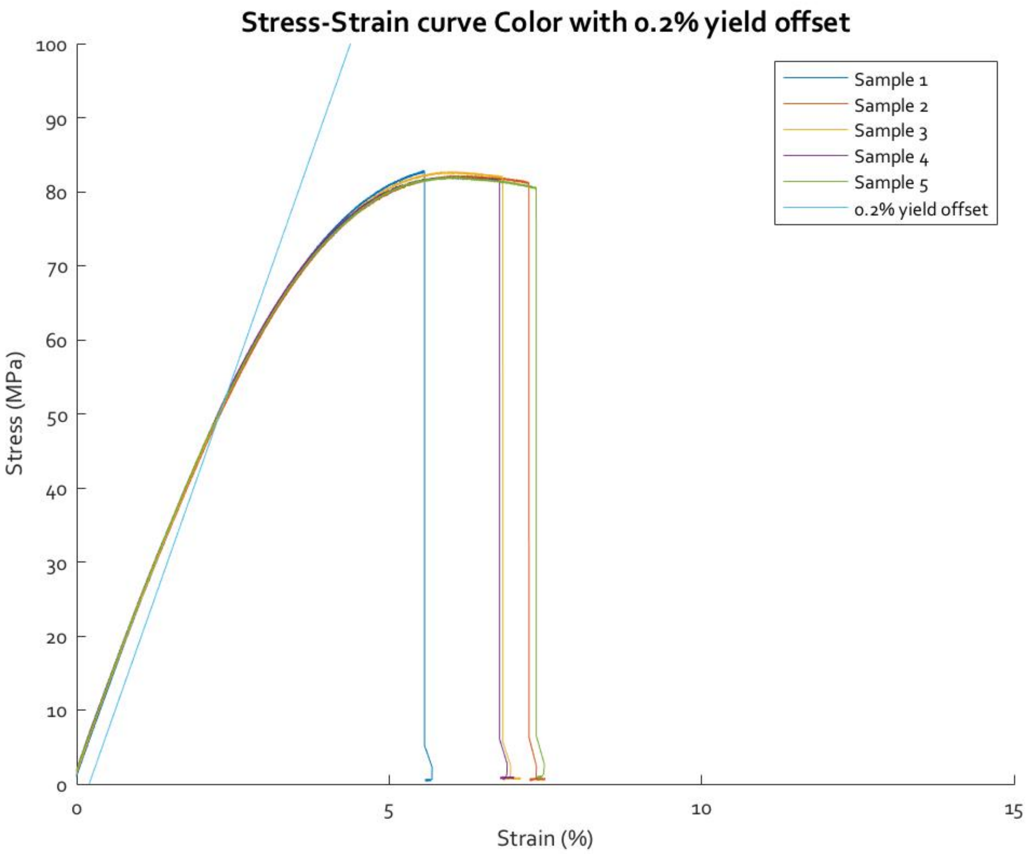
Stress-Strain curve Color with 0.2% yield offset
Stress (MPa)
Strain (%)
Sample 1
Sample 2
Sample 3
Sample 4
Sample 5
0.2% yield offset
0
10
20
30
40
50
60
70
80
90
100
0
5
10
15

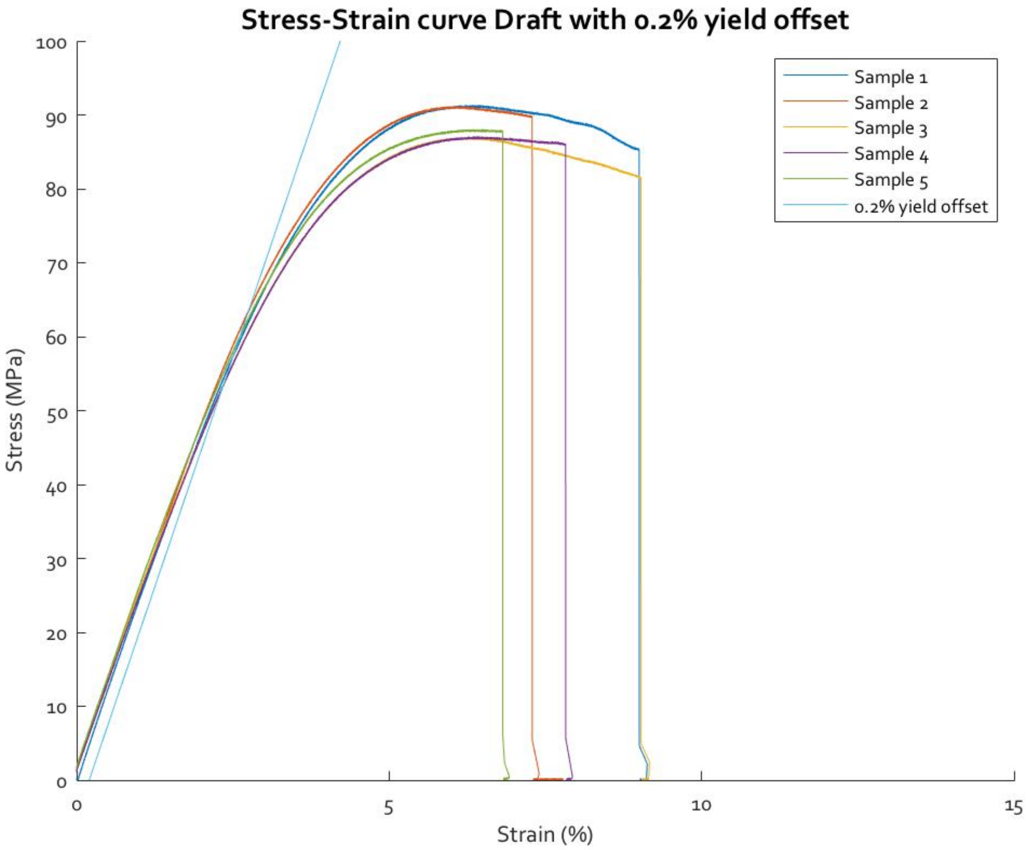
Stress-Strain curve Draft with 0.2% yield offset
Stress (MPa)
Strain (%)
0
10
20
30
40
50
60
70
80
90
100
0
5
10
15
Sample 1
Sample 2
Sample 3
Sample 4
Sample 5
0.2% yield offset

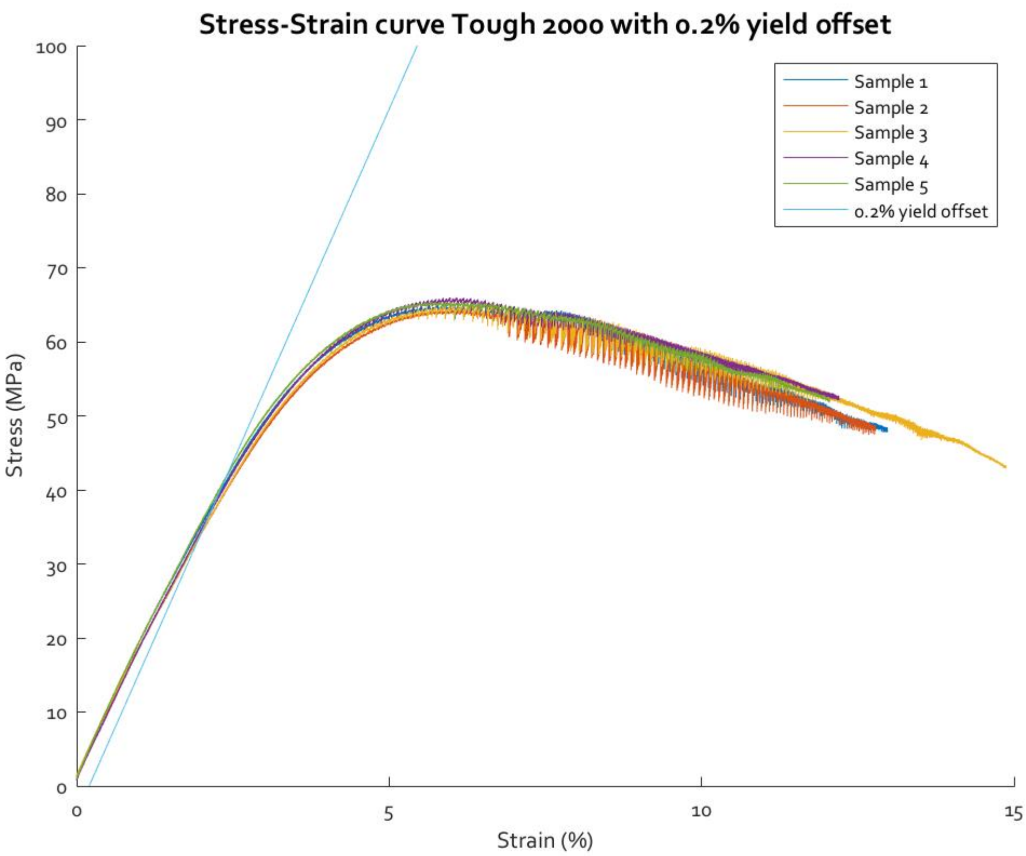
Stress-Strain curve Tough 2000 with 0.2% yield offset
Stress (MPa)
Strain (%)
0
10
20
30
40
50
60
70
80
90
100
0
5
10
15
Sample 1
Sample 2
Sample 3
Sample 4
Sample 5
0.2% yield offset

## Appendix II: Stress-Strain curves for tensile testing

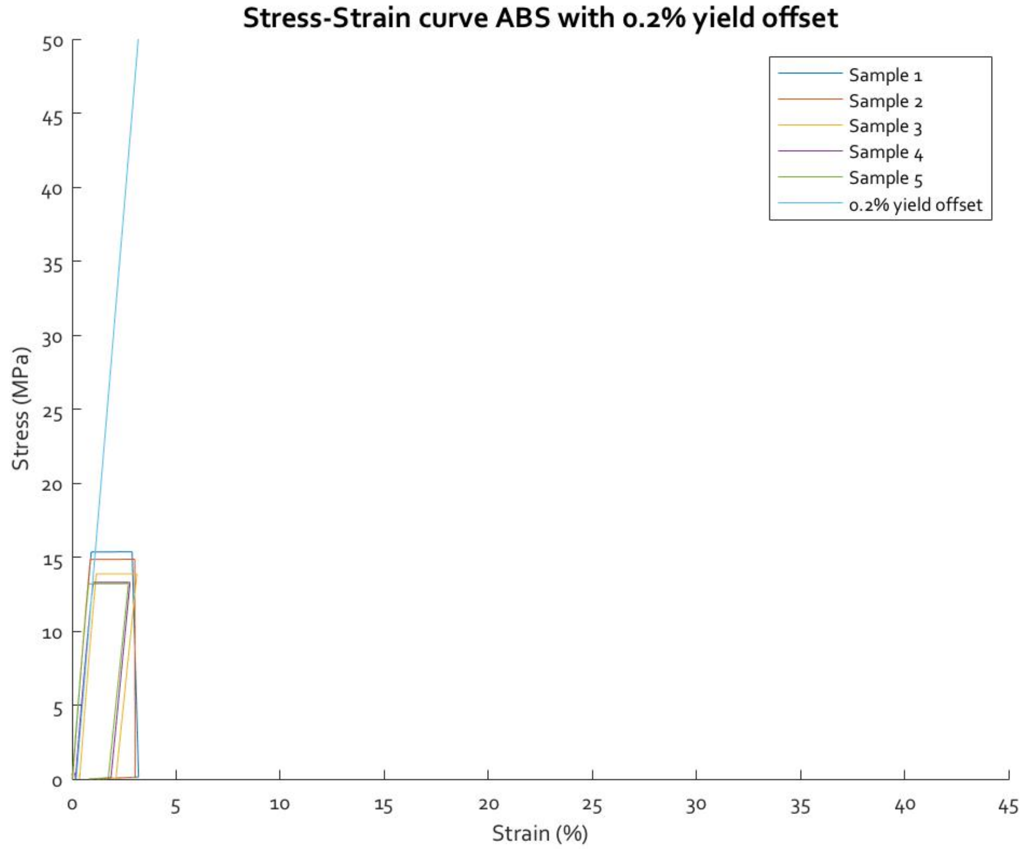


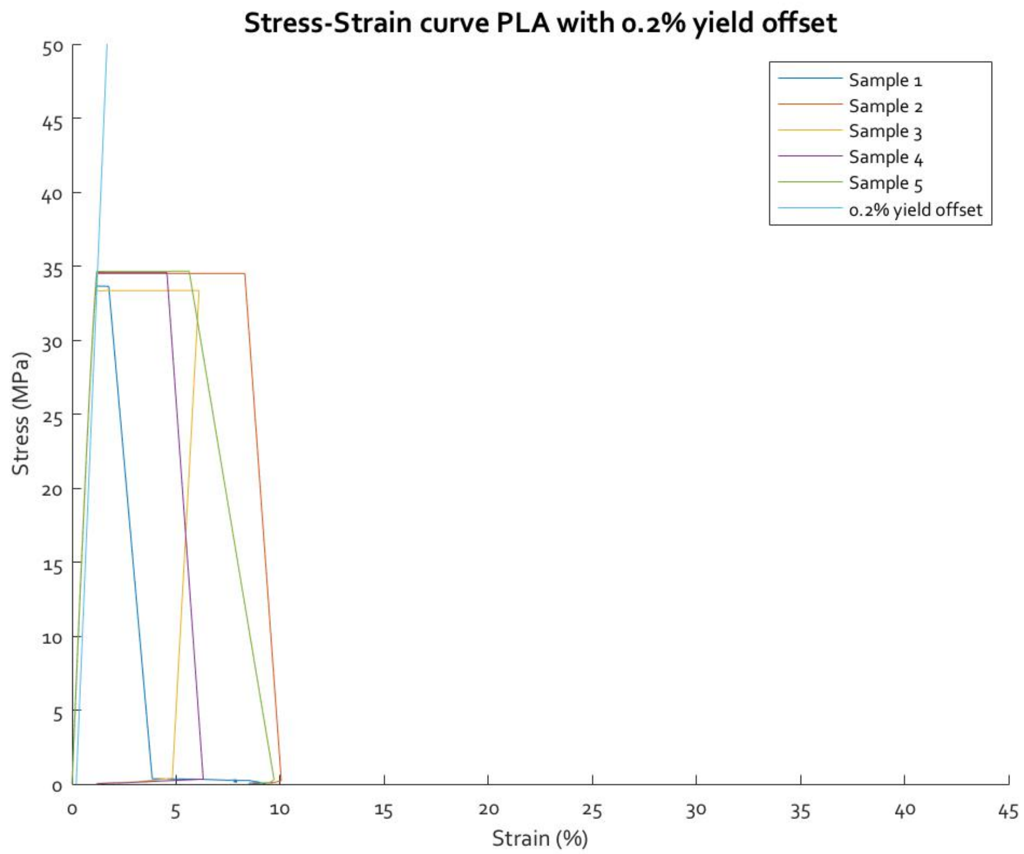

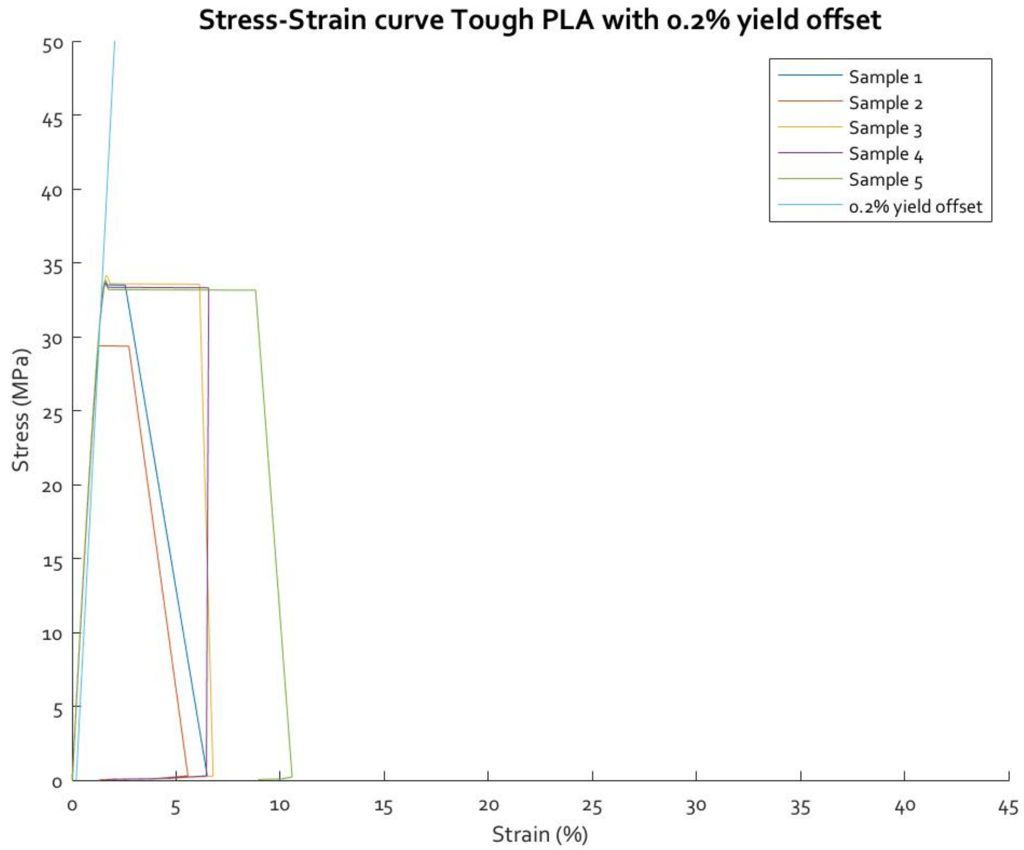
Stress-Strain curve Tough PLA with 0.2% yield offset
Sample 1
Sample 2
Sample 3
Sample 4
Sample 5
0.2% yield offset
Stress (MPa)
Strain (%)
0
5
10
15
20
25
30
35
40
45
50

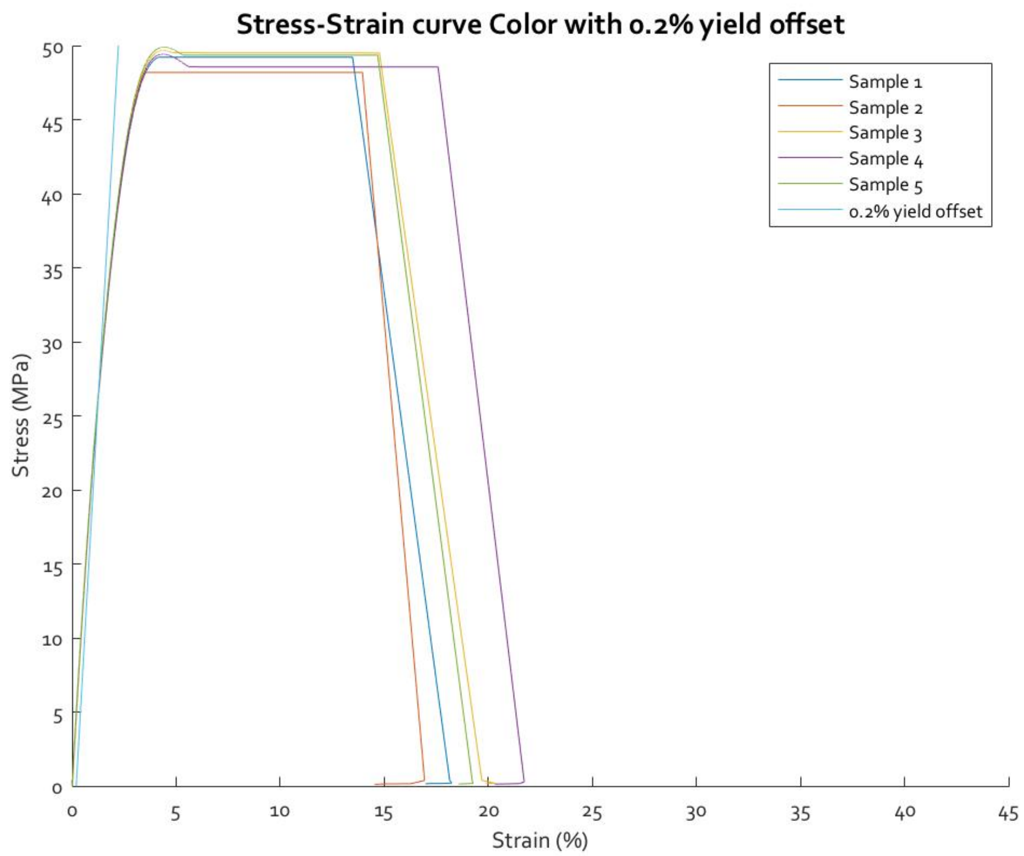
Stress-Strain curve Color with 0.2% yield offset
Sample 1
Sample 2
Sample 3
Sample 4
Sample 5
0.2% yield offset
Stress (MPa)
Strain (%)
0
5
10
15
20
25
30
35
40
45
50

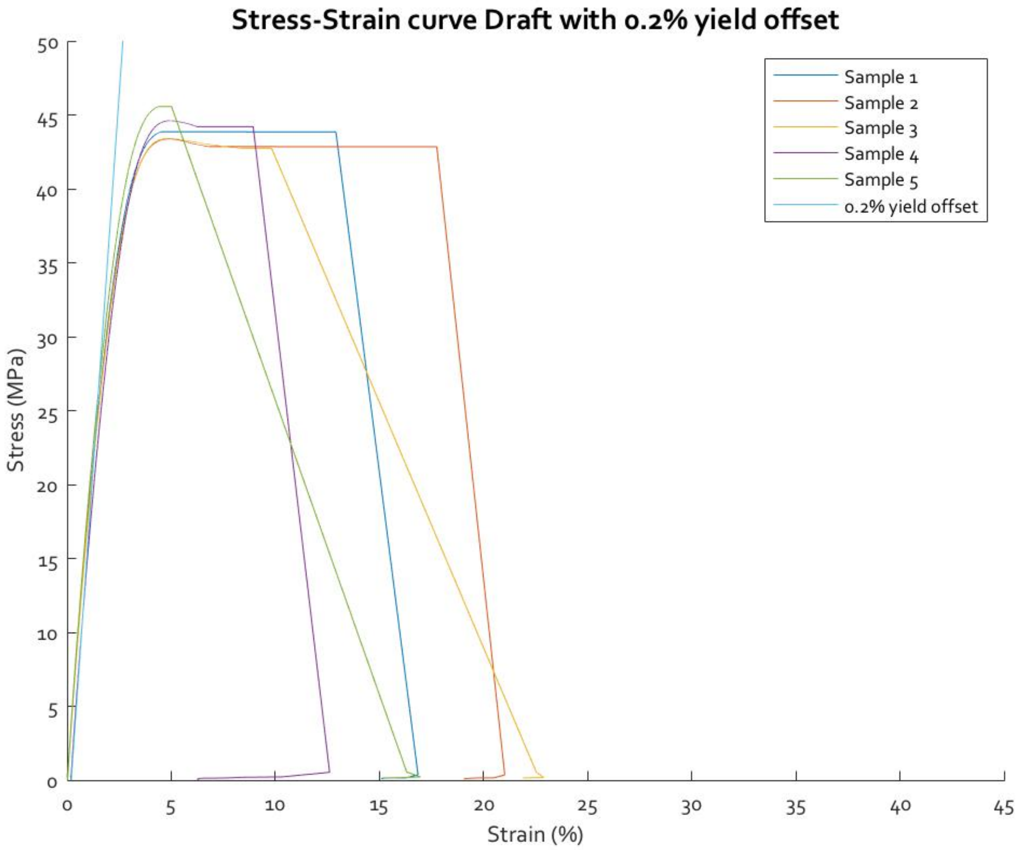

Stress-Strain curve Draft with 0.2% yield offset
Sample 1
Sample 2
Sample 3
Sample 4
Sample 5
0.2% yield offset
Stress (MPa)
Strain (%)


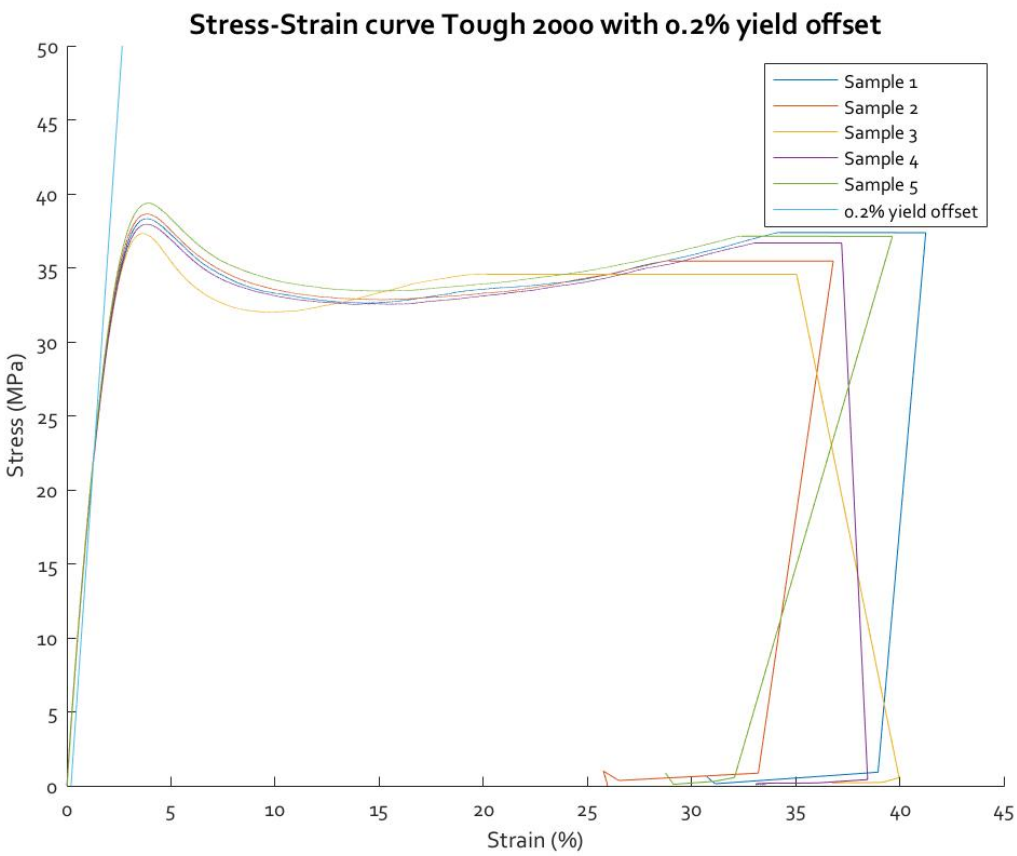

Stress-Strain curve Tough 2000 with 0.2% yield offset
Sample 1
Sample 2
Sample 3
Sample 4
Sample 5
0.2% yield offset
Stress (MPa)
Strain (%)

# Appendix III: Angular displacement under loading

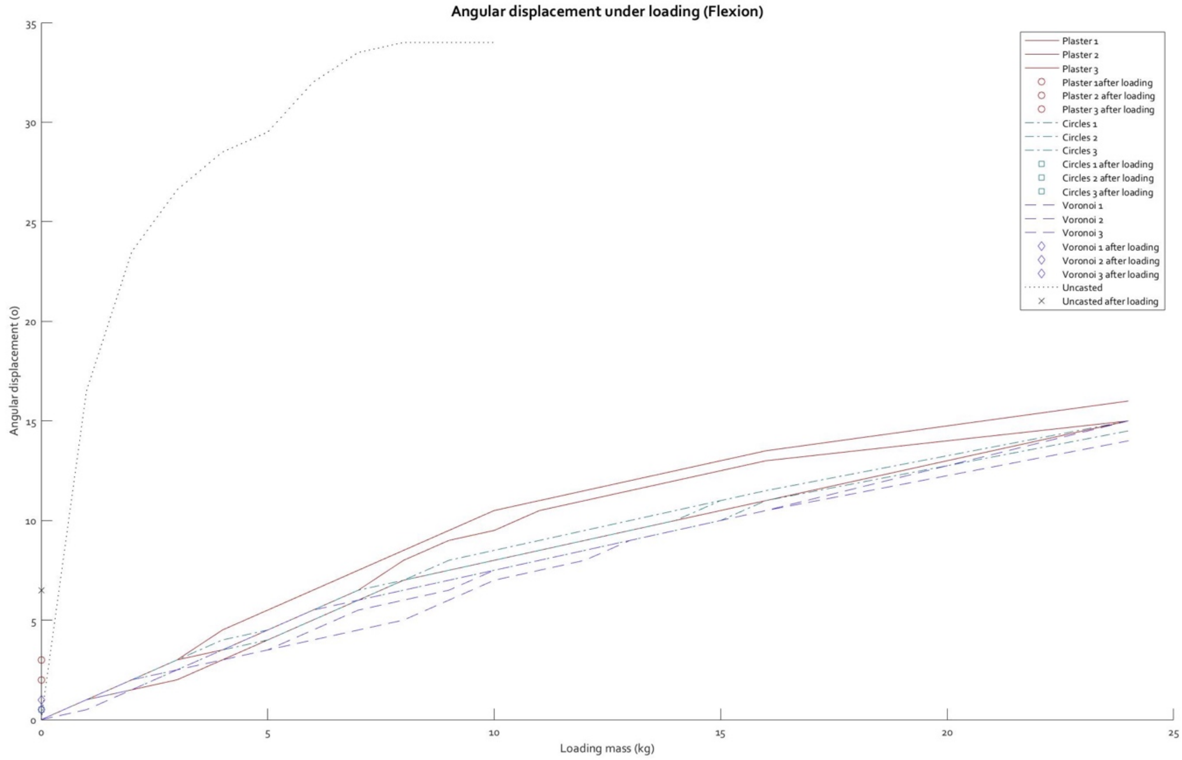


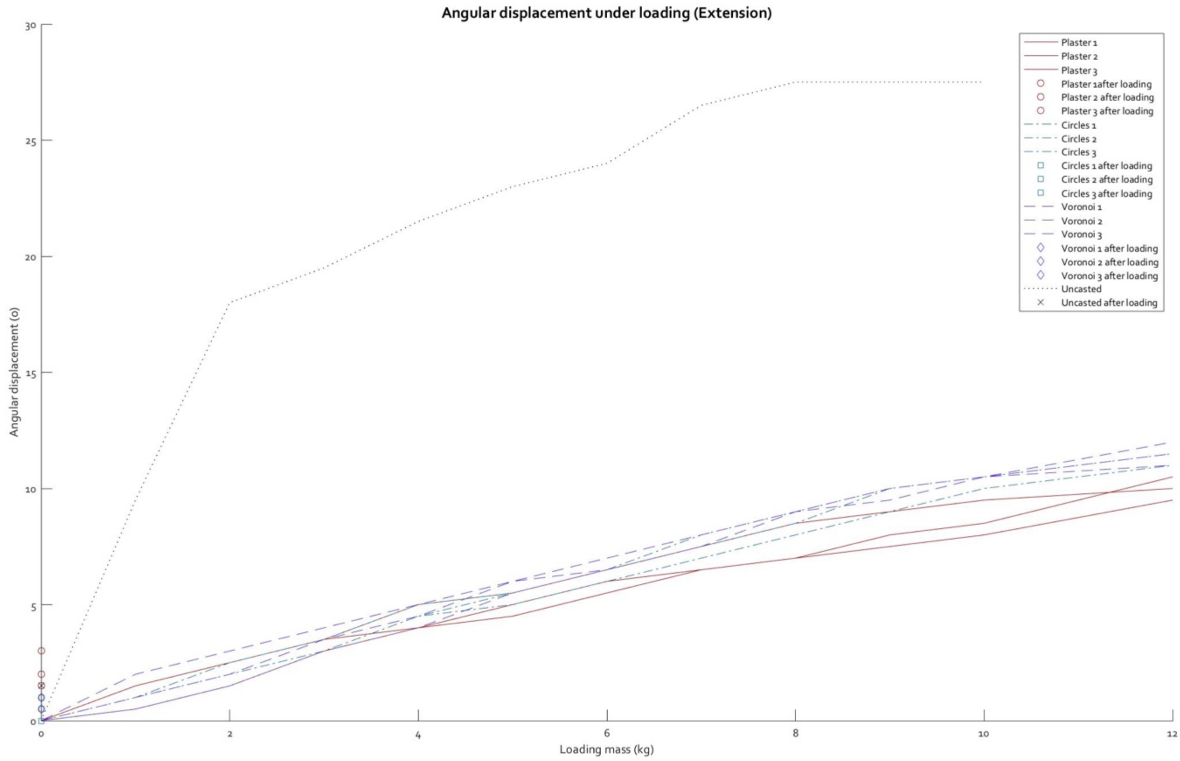

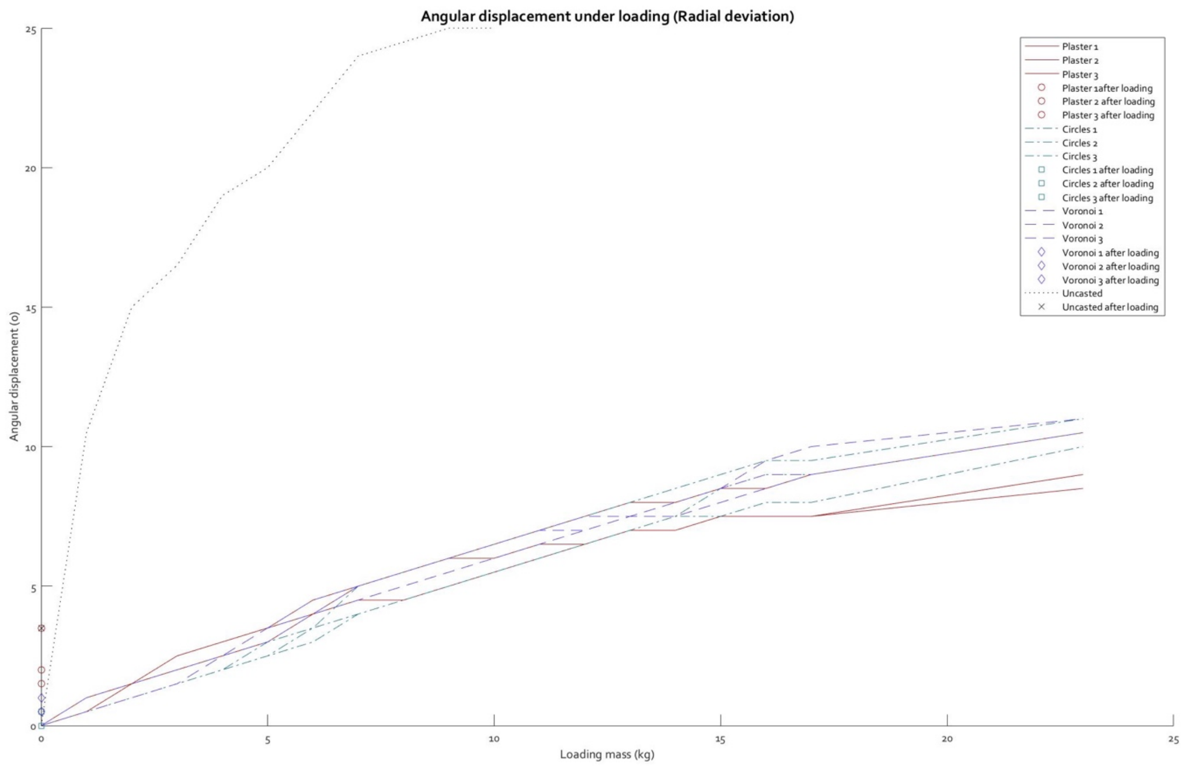
Angular displacement under loading (Radial deviation)
Angular displacement (o)
Loading mass (kg)
Plaster 1
Plaster 2
Plaster 3
Plaster 1after loading
Plaster 2 after loading
Plaster 3 after loading
Circles 1
Circles 2
Circles 3
Circles 1 after loading
Circles 2 after loading
Circles 3 after loading
Voronoi 1
Voronoi 2
Voronoi 3
Voronoi 1 after loading
Voronoi 2 after loading
Voronoi 3 after loading
Uncasted
Uncasted after loading

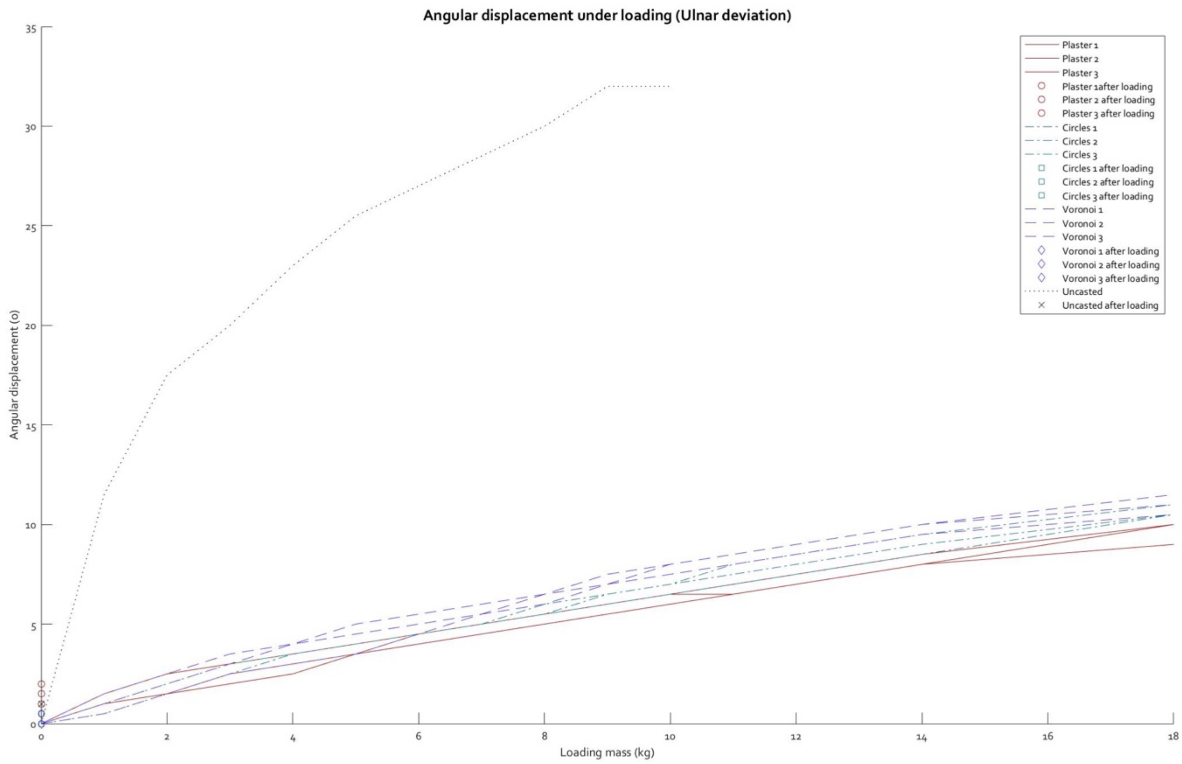
Angular displacement under loading (Ulnar deviation)
Angular displacement (o)
Loading mass (kg)
Plaster 1
Plaster 2
Plaster 3
Plaster 1after loading
Plaster 2 after loading
Plaster 3 after loading
Circles 1
Circles 2
Circles 3
Circles 1 after loading
Circles 2 after loading
Circles 3 after loading
Voronoi 1
Voronoi 2
Voronoi 3
Voronoi 1 after loading
Voronoi 2 after loading
Voronoi 3 after loading
Uncasted
Uncasted after loading

# Appendix IV: Information letter comfort study

## Informatie comfort studie 3D geprinte polsspalk

Fijn dat je mee wilt doen aan de comfort studie voor mijn afstudeerproject!

Met deze comfort studie willen we bepalen wat het draagcomfort is van de spalken die ik tijdens mijn project heb ontworpen en waar nog punten van verbetering liggen. Hieronder volgt uitleg over de spalk en een aantal instructies voor het dragen van de polsspalk tijdens deze studie.

**3D geprinte polsspalk**
Je krijgt een 3D geprinte spalk voor jouw pols. Deze spalk wordt gemaakt op basis van de 3D scan van jouw arm, waardoor de spalk precies om jouw arm/hand past. Iedere spalk is dus uniek. De spalk wordt gemaakt van lichtgevoelige hars met een (stereolithografie) 3D printer. De spalk heeft gaten voor ventilatie en is waterproof. We willen graag weten of dit ervoor zorgt dat het hygiënischer en comfortabeler is dan gips. Daarnaast zijn we benieuwd naar de pasvorm en potentiële verbeterpunten.

**Instructies**

- Draag de spalk gedurende **48 uur**.
- **Douch of baad** minstens één keer met de spalk (na het douchen/baden mag de spalk kort afgedaan worden om de huid en binnenkant van de spalk te drogen of droog de huid en spalk met een **koude** föhn .
- Houd de spalk om tijdens het **slapen**.
- Met **autorijden** mag de spalk afgedaan worden (i.v.m. verzekering).
- Bij andere activiteiten, waarbij de spalk het uitvoeren van deze activiteit belemmert, zoals **sport of zwaar tillen**, mag de spalk kort afgedaan worden (doe de spalk vervolgens zo snel mogelijk weer om).
- Houd in gedachten dat de spalk bedoeld is voor **immobilisatie** van de pols, het is dus niet de bedoeling belastende activiteiten te ondernemen met de arm/hand in de spalk (i.e. een glas drinken pakken of een knoop dichtmaken kan; tillen, koken of andere activiteiten waarbij kracht vereist is, is niet de bedoeling).
- Doe bij **klachten**, zoals huidirritatie, drukplekken of blaren, de spalk af.
- Vul na 48 uur de **vragenlijst** in en stuur deze met een foto van de spalk om de arm naar C.D.Y.Mooij@student.tudelft.nl of app de foto en foto's van de ingevulde vragenlijst naar +31(0)6 20891534.

**Vragen?**
Bij vragen of klachten ben ik op ieder moment bereikbaar via onderstaande contactgegevens.

**Contact**
Charlotte Mooij, student Technical Medicine
Mail: C.D.Y.Mooij@student.tudelft.nl
Telefoon: +31(0)6 20891534

## Appendix V: Questionnaire comfort study

## Vragenlijst comfort studie 3D geprinte polsspalk

Hieronder volgen een aantal vragen over een aantal algemene persoonlijke gegevens en vervolgens over het draagcomfort van de 3D geprinte polsspalk die u de afgelopen twee dagen hebt gedragen. Onder de meeste vragen staat een balk met een schaal van 0 tot 10. Op deze balk kunt u aangeven in hoeverre u het eens bent met de vraag (de beschrijving staat onder de scorebalk) door een cijfer te omcirkelen. Bij de overige vragen, kunt u een keuze maken tussen verschillende opties, door het vakje voor het gewenste antwoord aan te kruisen of uw antwoord op de stippellijn in te vullen.

**Algemene gegevens**

Geslacht: ☐ man ☐ vrouw

Leeftijd: ......................jaar

Dominante hand: ☐ links ☐ rechts

Zijde 3D geprinte polsspalk: ☐ links ☐ rechts

Heeft u ooit eerder gips gehad en zo ja, hoe vaak: ☐ ja, ......keer ☐ nee

---

**Vragen 3D geprinte polsspalk**

1. Wat vond u van de pasvorm van de spalk?

   0 1 2 3 4 5 6 7 8 9 10

   Slecht Matig Geweldig

2. Had u last van zweten in de spalk?

   0 1 2 3 4 5 6 7 8 9 10

   Nooit Soms Vaak

3. Had u last van jeuk in de spalk?

   0 1 2 3 4 5 6 7 8 9 10

   Nooit Soms Vaak

4. Zorgde het dragen van de spalk voor onaangename geuren?

   0 1 2 3 4 5 6 7 8 9 10

   Niet Soms Erg

5. Had u last van drukplekken in de spalk?

   0 1 2 3 4 5 6 7 8 9 10

   Niet Soms Erg

6. Had u last van huidirritatie (zwelling, verkleuring, roodheid, blaren) door de spalk?

   0 1 2 3 4 5 6 7 8 9 10

   Nooit Soms Vaak

7. Had u last van maceratie (week worden) van de huid na het douchen (of handen wassen) door het dragen van de 3D geprinte polsspalk?

0 1 2 3 4 5 6 7 8 9 10

Niet Soms Erg

8. Had u last van de 3D geprinte polsspalk met slapen?

0 1 2 3 4 5 6 7 8 9 10

Niet Soms Erg

9. Hoe gemakkelijk was de spalk om en af te doen?

0 1 2 3 4 5 6 7 8 9 10

Moeilijk Makkelijk

10. Gaf de spalk voldoende steun om de pols te immobiliseren?

0 1 2 3 4 5 6 7 8 9 10

Niet Soms Erg

11. Kon u nog dagelijkse handelingen uitvoeren met de spalk (knoop dichtmaken, glas oppakken)?

0 1 2 3 4 5 6 7 8 9 10

Moeilijk Makkelijk

12. Welk cijfer geeft u het uiterlijk van de 3D geprinte polsspalk?

0 1 2 3 4 5 6 7 8 9 10

13. Welk cijfer geeft u het algehele comfort van de 3D geprinte polsspalk?

0 1 2 3 4 5 6 7 8 9 10

14. Wat vindt u voordelen van de 3D geprinte polsspalk?

15. Wat vindt u nadelen van de 3D geprinte polsspalk?

16. Wat kan er nog verbeterd worden aan de 3D geprinte polsspalk?

.....................................................................................................................................................................................

.....................................................................................................................................................................................

17. Zou u in het geval van een polsbreuk voorkeur hebben voor behandeling met een 3D geprinte polsspalk of traditioneel gips?

☐ 3D geprinte polsspalk ☐ Gips

18. Heeft u verder nog op- of aanmerkingen?

.....................................................................................................................................................................................

.....................................................................................................................................................................................

*Bedankt voor het invullen van de vragenlijst!*

# Appendix VII: Information letter pilot study

# Patiënteninformatie 3D geprinte polsspalken bij greenstick- en torusfracturen

**Botbreuk**
Uw kind heeft een twijgbreukje (greenstickfractuur) of knikje (torusfractuur) in het spaakbeen of de ellepijp ter hoogte van de pols opgelopen. Dit is een breukje in het bot, waarbij het botvlies dat om het bot heen ligt, intact is gebleven. Het bot is meer geknikt dan gebroken, waardoor verplaatsing of losraking van de botdelen onwaarschijnlijk is.

**Genezing**
Omdat kinderen in de groei snel nieuw bot aanmaken, geneest een greenstick- of torusfractuur over het algemeen snel, in ongeveer 2 weken. In geval van een kleine knikstand, herstelt dit vanzelf, binnen enkele weken tot maanden.

**Behandeling**
Normaal gesproken wordt een greenstick- of torusfractuur behandeld met een drukverband of gips, naar voorkeur van de patiënt en ouders. U en uw kind doen nu mee aan een onderzoek waarbij een gepersonaliseerde, 3D geprinte polsspalk wordt ingezet voor de behandeling van deze fracturen. Hieronder volgen instructies voor de behandeling.

**Patiëntinstructies**
1. Uw kind krijgt een polsspalk en voor de eerste dagen een draagdoek (mitella), om de pols rust te geven. Rust is belangrijk voor goede genezing en vermindert de pijn. Bij het slapen mag de mitella af. Zodra de pijn het toelaat, hoeft de mitella ook overdag niet meer gedragen te worden.
2. Na een week, zodra de pijn het toelaat, mag uw kind weer bewegen, dit voorkomt stijfheid van de elleboog en bevordert de genezing.
3. Douchen en zwemmen kan met de polsspalk. Na het nat worden, mag de spalk kort afgedaan worden om de arm en spalk te drogen. Een andere optie is om met een koude föhn, de arm droog te föhnen.
4. We raden aan iedere dag de huid kort te inspecteren. Let hierbij op zwelling, verkleuring, drukplekken, blaren en wondjes. De spalk mag voor inspectie kort afgedaan worden.
5. Na twee weken zien we uw kind terug voor controle en mag de spalk af.

**Vragen?**
Het is belangrijk om te weten dat bij klachten of vragen op ieder moment contact opgenomen mag worden met de hoofdonderzoeker (Mike Bemelman, traumachirurg).
Op verzoek van patiënt en ouders kan op ieder moment deelname aan het onderzoek beëindigd worden. In overleg met de hoofdonderzoeker wordt de behandeling dan volgens de conventionele richtlijnen voortgezet.

**Contact**
Mike Bemelman, traumachirurg
+31(0)13 221 65 87
+31(0)6 296 261 82

## Appendix VII: Questionnaire pilot study - child

# Vragenlijst 3D geprinte polsspalk - kind

Versie 1 (23-04-2021) - Type fractuur: ☐ Greenstick ☐ Torus

**Over mij:**

Ik ben: ........................ jaar

Ik ben: ☐ een jongen ☐ een meisje

De kant waar mijn pols is gebroken: ☐ links ☐ rechts

---

1. **Had je last van jeuk in de spalk?**

Nooit | Bijna nooit | Soms | Regelmatig | Vaak

2. **Had je last van zweten in de spalk?**

Nooit | Bijna nooit | Soms | Regelmatig | Vaak

3. **Had je last van stank door de spalk?**

Nooit | Bijna nooit | Soms | Regelmatig | Vaak

4. **Had je last van pijn door de spalk?**

Nooit Bijna nooit Soms Regelmatig Vaak

5. **Had je last van huidirritatie door de spalk?**

Nooit Bijna nooit Soms Regelmatig Vaak

6. **Had je last van het gewicht van de spalk?**

Nooit Bijna nooit Soms Regelmatig Vaak

7. **Hoe ging het met douchen?**

Heel goed Goed Oké Niet goed Slecht

8. **Hoe mooi vond je de spalk?**

Heel mooi Mooi Oké Niet zo mooi Lelijk

9. **Had je last van de spalk in het dagelijks gebruik?**

Nooit Bijna nooit Soms Regelmatig Vaak

10. **Stel je breekt nog een keer je pols, zou je dan opnieuw kiezen voor een deze polsspalk of liever voor gips?**

☐ Polsspalk ☐ Gips

11. **Wat zou er nog beter kunnen aan de spalk?**

***Bedankt voor het meedoen aan dit onderzoek!***

# Appendix VIII: Questionnaire pilot study - parents

## Vragenlijst 3D geprinte polsspalk - ouder

Versie 1 (23-04-2021) - Type fractuur: ☐ Greenstick ☐ Torus

---

Hieronder begint de vragenlijst. Onder de meeste vragen staat een balk met een schaal van 0 tot 10. Op deze balk kunt u aangeven in hoeverre u het eens bent met de vraag (de beschrijving staat onder de scorebalk) door een cijfer te omcirkelen. Bij de overige vragen, kunt u een keuze maken tussen verschillende opties, door het vakje voor het gewenste antwoord aan te kruisen of uw antwoord op de stippellijn in te vullen.

1. **In hoeverre werd uw kind beperkt in dagelijkse handelingen door de 3D geprinte polsspalk?**

0 1 2 3 4 5 6 7 8 9 10

Niet Soms Vaak

2. **Zorgde de 3D geprinte polsspalk voor huidirritatie bij uw kind?**

0 1 2 3 4 5 6 7 8 9 10

Niet Gedeeltelijk Erg

3. **Heeft uw kind geklaagd over jeuk?**

0 1 2 3 4 5 6 7 8 9 10

Nooit Soms Vaak

4. **Heeft uw kind geklaagd over het gewicht van de 3D geprinte polsspalk?**

0 1 2 3 4 5 6 7 8 9 10

Nooit Soms Vaak

5. **Zorgde het dragen van de spalk voor onaangename geuren?**

0 1 2 3 4 5 6 7 8 9 10

Niet Soms Erg

6. **Heeft uw kind geklaagd over pijn, veroorzaakt door de 3D geprinte polsspalk?**

| 0 | 1 | 2 | 3 | 4 | 5 | 6 | 7 | 8 | 9 | 10 |
|---|---|---|---|---|---|---|---|---|---|---|
| Nooit | | | | | Soms | | | | | Vaak |

7. **Had uw kind last van maceratie (week worden) van de huid na het douchen (of zwemmen) door het dragen van de 3D geprinte polsspalk?**

| 0 | 1 | 2 | 3 | 4 | 5 | 6 | 7 | 8 | 9 | 10 |
|---|---|---|---|---|---|---|---|---|---|---|
| Niet | | | | | Gedeeltelijk | | | | | Erg |

8. **Had uw kind last van de 3D geprinte polsspalk met slapen?**

| 0 | 1 | 2 | 3 | 4 | 5 | 6 | 7 | 8 | 9 | 10 |
|---|---|---|---|---|---|---|---|---|---|---|
| Nooit | | | | | Soms | | | | | Vaak |

9. **Welk cijfer geeft u de behandeling van uw kind met de 3D geprinte polsspalk?**

| 0 | 1 | 2 | 3 | 4 | 5 | 6 | 7 | 8 | 9 | 10 |
|---|---|---|---|---|---|---|---|---|---|---|

10. **Welk cijfer geeft u het uiterlijk van de 3D geprinte polsspalk?**

| 0 | 1 | 2 | 3 | 4 | 5 | 6 | 7 | 8 | 9 | 10 |
|---|---|---|---|---|---|---|---|---|---|---|

11. **Wat vindt u voordelen van de 3D geprinte polsspalk?**

.................................................................................................................................

.................................................................................................................................

12. **Wat vindt u nadelen van de 3D geprinte polsspalk?**

.................................................................................................................................

13. **Wat kan er nog verbeterd worden aan de 3D geprinte polsspalk?**

14. **Zou u in het geval van een volgende breuk bij uw kind voorkeur hebben voor behandeling met een 3D geprinte polsspalk of traditioneel gips?**

    ☐ 3D geprinte polsspalk ☐ Gips

15. **Heeft u verder nog op- of aanmerkingen?**

***Bedankt voor het invullen van de vragenlijst!***